



Sustainable Development of Mega Drainage Basins of the Eastern Desert of Egypt; Halaib–Shalatin as a Case Study Area

Hossam H. Elewa, Ahmad M. Nosair, and Elsayed M. Ramadan

Abstract

This book chapter focuses on using effective tools of monitoring and management of natural resources, based on the integration of remote sensing (RS) and geographic information systems (GIS) techniques with a field survey in surface and groundwater resources evaluation. It is anticipated to provide operational and effective systems of investigation, management and protection of the available natural resources, and improve the livelihood of the surrounding population. This work depends on the previous expertise and overwhelmed researches of the National Authority for Remote Sensing and Space Sciences (NARSS) and addresses the key challenges for the sustainable development in this remote area. Sustainable water supply is vital for the development of communities in arid regions, such as that of the South Eastern Desert of Egypt. The economic importance of the area is enormous, besides the fact that it has long been a target zone for mineral resources excavation and mining. One of the challenges facing this arid area is the limited water resources needed for agricultural, industrial, mining, or domestic uses. Bedouin depend mainly on rainwater, which constitutes the main source feeding their hand-dug wells and fracture springs. Rainwater harvesting (RWH), as a historical and worldwide trend, could fulfill the gap of water scarcity in arid or semi-arid regions. This proposed work is to use the modern techniques of RS, geographic information systems

(GIS), and watershed modeling systems (WMS) to provide a plan for the RWH. RWH is the accumulation and storage of rainwater for reuse before it reaches the aquifer system (Groundwater). Multi-spectral remote sensing (MSRS) and geographic information systems (GIS) are vital tools to optimize the surface water usage of episodic rainfalls, where the concept of runoff water harvesting (RWH) in promising watersheds should be applied. (Elewa et al. in *Am J Environ Sci* 8:42–55, 2016). GIS and digital elevation models (DEM) enable the development of hydrological models to investigate every ancient terraced field in a non-invasive manner, without disturbing the archaeological remains (Bruins et al. in *J Environ* 166:91–107, 2019). The RWH could be used also for maximizing the recharge possibilities of groundwater. As a non-conventional water resource, RWH could provide water for gardens, livestock, irrigation, mining, cleaning of bathrooms as in the first flush, etc. In many places with similar climate conditions, the collected water is redirected to a deep pit with percolation to recharge the groundwater for later use and protection, especially in structurally controlled groundwater accumulations. The harvested water could be used as drinking water, if the storage is a tank that can be accessed and cleaned when needed. The work recommendations will be a good source for the up-to-date databases, which could be used effectively by the decision-makers, researchers, executive authorities, planners, and related governorates. The **objective** of this book chapter is to assess the South Eastern Desert of Egypt for the RWH capabilities, with the determination of their optimum methods and techniques. The overall **goal** is to assist in poverty alleviation, Bedouin and urban allocation, supporting animal husbandry, accelerating agricultural development, improved agricultural and food production for local inhabitants, combating desertification, resolving unemployment problems, and raising individual incomes. Bedouin and natives as the main end users will be a major target of

H. H. Elewa (✉)

Engineering Applications & Water Division (EAWD), National Authority for Remote Sensing & Space Sciences (NARSS), Cairo, Egypt
e-mail: elewa.hossam@gmail.com; ; hossam.eliewa@narss.sci.eg

A. M. Nosair

Geology Department, Faculty of Science, Zagazig University, Zagazig, Egypt

E. M. Ramadan

Water Structures Department, Faculty of Engineering, Zagazig University, Zagazig, Egypt

the work. Innovative ways to improve the capture, storage, and use of rainwater will have their own bearing on the sustainable and profitable production of dry season vegetable crops in South Eastern Desert. According to the worldwide trends and techniques in RWH, which is applied aggressively in many neighboring countries, Egypt should enter the era of catching every water droplet for domestic and agricultural development. The results of the present research work could establish a good example to be applied in other parts of the country as well as worldwide.

Keywords

Egypt • Eastern desert • Remote sensing • GIS spatial modeling • Drainage systems • Hydromorphometric analysis • Watershed modeling • Water harvesting

List of Acronyms and Abbreviations Listed in the Text

ANOVA	Analysis Of Variance
ASTER	Advanced Spaceborne Thermal Emission & Reflection Radiometer
BA	Basin Area
BL	Basin Length
BS	Basin Slope
Dd	Drainage Density
DEM	Digital Elevation Model
E	Degree of Effectiveness
EIA	Environmental Impact Assessment
ETM	Enhanced Thematic Mapper
Fm	Formation
GIS	Geographic Information System
GSA	Global Sensitivity Analysis
HS	Halaib–Shalatin region
IF	Basin Infiltration Number
masl	Meter above sea level
MCDSS	Multi-Criteria Decision Support System
MFD	Maximum Flow Distance
OFD	Overland Flow Distance
RS	Remote Sensing
RWH	Runoff Water Harvesting
SAM	Spatial Analysis Model
LMP	Land use Master Plan
ST	Total effect, Sensitivity index
VAF	Volume of Annual Flood
V_i	A partial variance
W	Wadi (dry valley)
W_c	Criterion Weight
WMS	Watershed Modeling System (WMS Software); Water Management System
WSPM	Weighted Spatial Probability Model

1 Introduction

In Halaib–Shalatin (HS) area (about 23,615 km²), the natural springs and hand-dug wells are the main dependable water resources from the native dwellers. The area is suffered for several decades from intensive aridity, overgrazing, and desertification. The rainless periods may continue for 4, 5, or even 8 years, which leads to great tragic starvation for the native people, and for the animal husbandry.

Serious strategies for water exploration and development must be established to fully utilize the surface and groundwater resources. The success of these strategies is dependent on the availability and reliability of basic hydrogeologic and hydrologic information and related subjects.

Recently, the area has got more attention as a promising region for different developmental activities as tourism, fishery, animal husbandry, and mining and for its importance as a trading route between Egypt and Sudan. The growth of such activities requires a simultaneous strategy for using and development of the available water resources of the study area to meet the water demands.

Remote sensing (RS) techniques were used as an important tool, among others, for investigation of surface geological, structural, and hydrological (drainage systems) features. These surface features were used, with ground investigations to study the surface and groundwater resources.

1.1 Aim and Scope of the Present Work

The objectives of the present work are to evaluate HS area for the runoff water harvesting (RWH) and groundwater recharge possibilities. It also include determining the suitable sites for control works implementation either for RWH and/or groundwater recharge using optimum methods and techniques. The overall goal is to construct a developmental and management system for water resources in this important area to increase and improve agricultural activity, food production, and improve the standard of living for natives. Additionally, the present work includes construction of RWH system helps in the mitigation of flood hazards that are frequently threatening the different developmental activities. The specific objectives of the present work include drainage mapping of main wadies, construction of a digital database for runoff volumes, delineation of watersheds, determining the suitable sites for implementing water harvesting control works.

1.2 Location

HS area is a strategic region located at the far southeastern (SE) corner of Egypt and lies between longitudes 34°30′–37°00′ E and latitudes 22°00′–23°30′ N (Fig. 1). The study area

Fig. 1 Location map of the study area

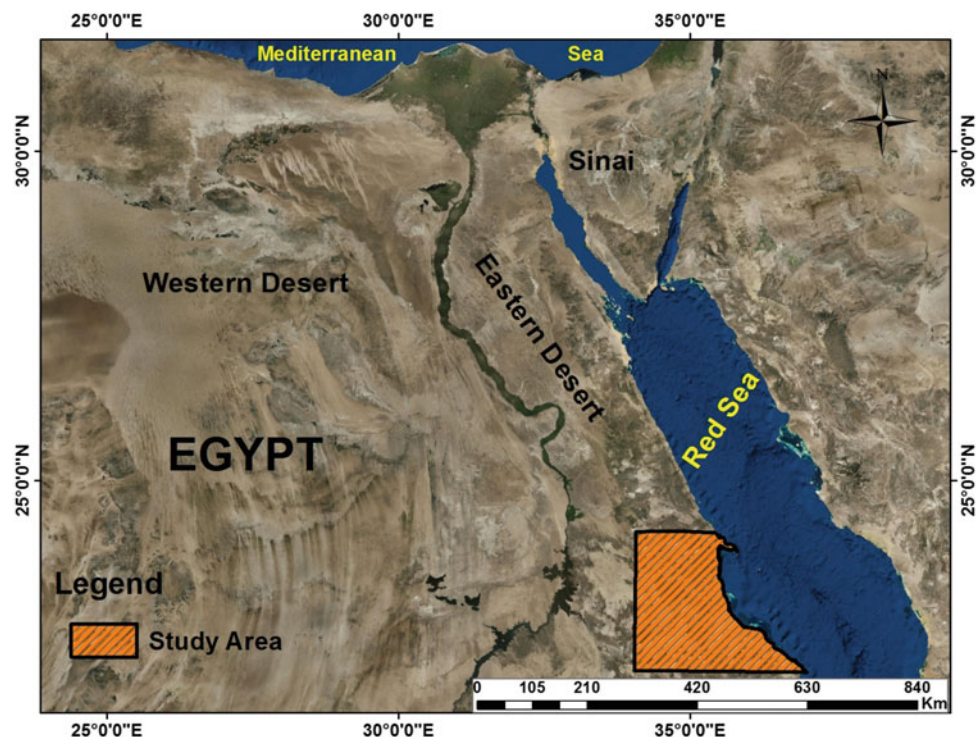
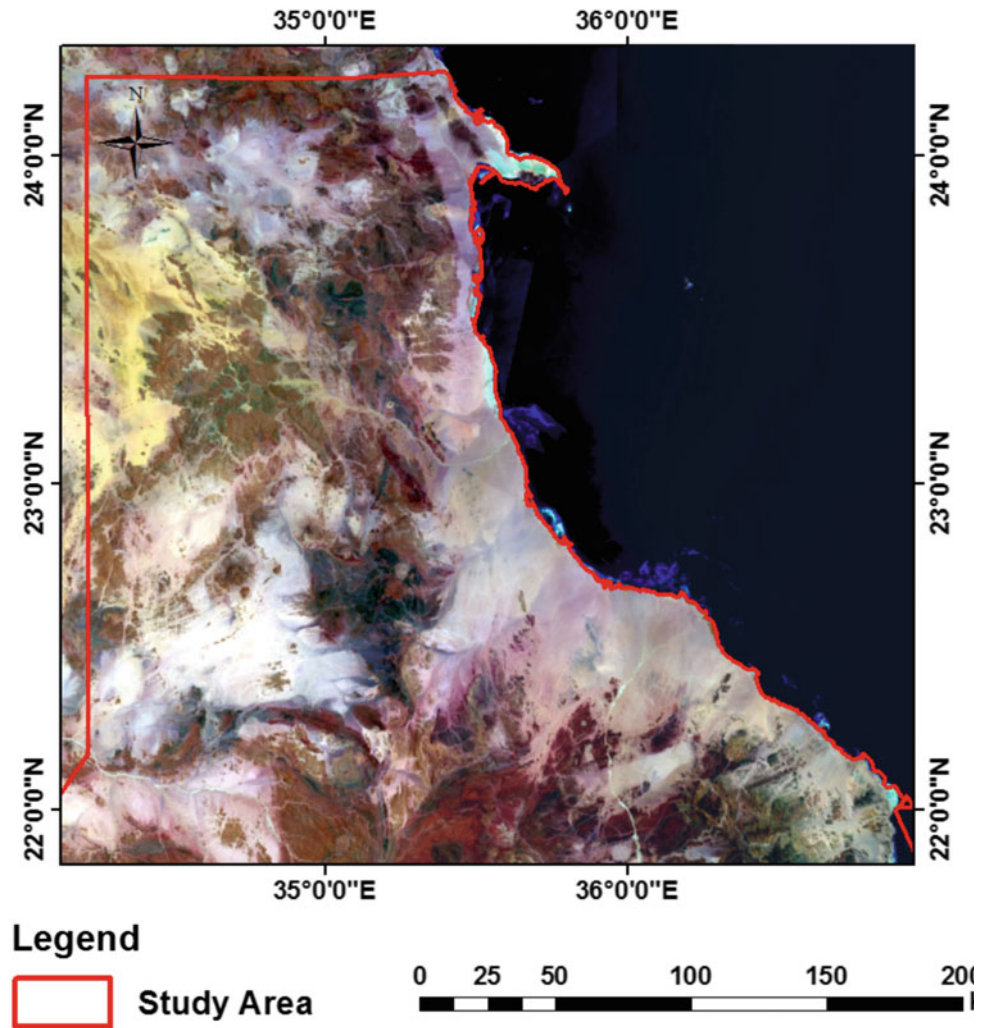


Fig. 2 A satellite ETM + 8 image showing the study area



is bounded by the Red Sea coast to the east, the Nile Valley hydrographic basin to the west, and the Egyptian–Sudanese border to the south (lat. 22°00' N). This area is accessible and traversed by a number of paved roads and desert tracks. The area is covered by Landsat (ETM + 8) image scenes (see Fig. 2).

1.3 Climatic Conditions

The study area is situated within the arid belt where sporadic rainfall may occur from time to time and accompanied by some flash floods. Sometimes an extremely rainless or shortage in rainfall may continue for years, reaching 6 or 8 years, this is impressed through the desert varnish phenomena formed in many places of the study area and indicating the hot arid climate of the area, (Fig. 3). The

inhabitants depend on their own ways of storing rainwater and drill hand-dug wells for their domestic use and for animal drinking (Figs. 4 and 5).

The climatic parameters include temperature, solar radiation, rainfall precipitation, and wind velocity. The Desert Research Institute constructed a complete meteorological station in the study area (in Wadi (W.) Rahaba)(Desert Research Institute 1998) (Table 1).

1.3.1 Temperature

The study area is characterized by a hot summer with an average temperature of about 32 °C, and cool winter with an average temperature of about 19 °C.

1.3.2 Humidity

The net humidity is about 43–49%, while the evaporation rate is about 16.8 mm/day.

Fig. 3 Field photo showing the desert varnish phenomena in W. Hodein indicating the arid climate of the study area



Fig. 4 A field photo showing a hand-dug well with hoisting via robes (Bir Iqet)



1.3.3 Rainfall

The rainfall is scarce over most of the year. The average rainfall precipitation is about 2.35 mm/year. The maximum rainfall precipitation is about 24.8 mm (recorded in October 1997), while the minimum rainfall precipitation is about 0.76 mm (recorded in April 1998).

1.3.4 Wind Velocities

The minimum average wind velocity is about 30.39 km/h (recorded in November 1997) and the maximum average wind velocity is about 38.93 km/h (recorded in June 1997). The maximum wind velocity is about 41.30 km/h (recorded in February 1997), which represents the beginning of

Fig. 5 A field photo showing protection of the hand-dug wells from sanding up by flash floods, by building up a high masonry wall around it (in W. Rahaba)



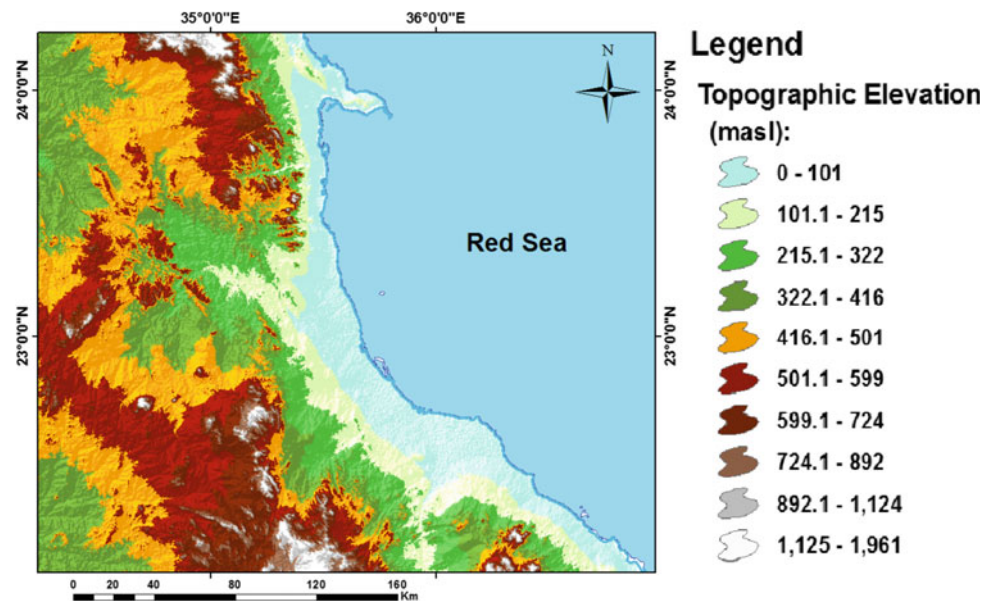
Table 1 Meteorological parameters, recorded at Shalatin Station (the period from October 1997 to October 1998), after Desert Research Institute (1998)

Month	Third of month	Average Temperature (°C)	Solar radiation K.W./M ²	AV. Wind velocity	Rainfall (mm)
October 1997	2nd	28.8	0.253	31.80	24.849
	3rd	26.4	0.22	26.56	–
November 1997	1st	25.3	0.219	32.88	–
	2nd	24.8	0.219	32.88	–
	3rd	23.6	0.195	29.19	–
December 1997	1st	22.4	0.192	29.65	–
	2nd	20.5	0.177	39.18	–
	3rd	20.4	0.173	29.81	–
January 1998	1st	20.3	0.169	39.8	–
	2nd	18.0	0.198	33.6	–
	3rd	18.9	0.208	28.3	–
February 1998	1st	20.7	0.220	27.4	–
	2nd	19.0	0.226	31.6	–
	3rd	20.4	0.236	41.3	–
March 1998	1st	20.3	0.246	34.2	–
	2nd	21.5	0.231	34.0	–
	3rd	21.0	0.226	28.2	1.27
April 1998	1st	22.7	0.305	40.3	–
	2nd	27.5	0.295	36.1	0.76
	3rd	25.2	0.279	37.2	–
May 1998	1st	28.5	0.308	33.7	–
	2nd	27.8	0.324	38.9	1.27
	3rd	29.7	0.317	40.0	–
June 1998	1st	28.5	0.315	36.6	–
	2nd	30.4	0.323	41.1	–
	3rd	29.8	0.320	39.1	–

(continued)

Table 1 (continued)

Month	Third of month	Average Temperature (°C)	Solar radiation K.W./M ²	AV. Wind velocity	Rainfall (mm)
July 1998	1st	31.7	0.319	36.3	–
	2nd	32.4	0.297	35.8	–
	3rd	32.9	0.302	35.5	–
August 1998	1st	33.2	0.314	36.4	–
	2nd	35.4	0.285	36.1	–
	3rd	35.8	0.310	35.0	–
September 1998	1st	28.2	0.317	31.50	–
	3rd	29.0	0.320	31.40	–
October 1998	1st	28.4	0.248	31.2	–
	3rd	28.0	0.211	25	–

Fig. 6 Topographic elevations of the study area (based on ASTER DEM of 30-m resolution)

El-Khamsin storm. Prior to the present arid nature of the climate, semi-arid or even wet climatic conditions were dominant in Egypt. Butzer (1959) and Said (1990), give some details of that period.

1.4 Topographic Features

The topography of the area ranges from gently sloping coastal plains to rugged mountainous and hilly lands, at the western and southwestern (SW) parts of the study area and heights up to 1961 masl (Fig. 6).

2 Materials and Methods

To accomplish the work objectives, the following tasks were performed which address the undertaken methods and techniques:

2.1 Satellite Image Collection, Preparation, and Processing

The ETM + 8 satellite image (acquired in 2014) was used, which has been designed to provide long-term continuity of data collection but with successive improvements in the technical capability and performance of the sensing systems involved.

The image is calibrated into geographic latitudes/ Longitudes, GRS 1980, and transformed from *.dat* format to *.img* format through the import module of Erdas Imagine 9.0[©] software and then converting them into Universal Transverse Mercator (UTM), WGS 1984, to be compatible with the different Geographic Information System (GIS) thematic layers (i.e., compatible with digital elevation model (DEM), enhanced thematic mapper images (ETM + 8), geological map for soil data, etc. (ERDAS Field Guide 2005).

2.2 Construction of Base Map

The map was constructed by using the published and validated maps of the Egyptian General Authority for Civil Survey (EGACS 1989) with multi-scales series and Google Earth maps and Satellite ETM + 8 images (Fig. 2). The constructed base map of geographic and drainage basins' data of the study area comprises the watershed boundaries of drainage basins shown in Fig. 7.

2.3 Construction of Geologic and Geomorphologic Maps

Lithostratigraphic and soil data were collected from Conoco geological maps of eastern Desert (CONOCO 1987) of 1:500,000 scale. Further enhancements' was performed by the interpretation of landsat ETM + 8 using ERDAS Imagine 10.1[©] software (Leica Geosystems GIS & Mapping 2008). The geomorphological map was constructed by visual interpretation of Landsat ETM + 8 false-color compiled image, (Fig. 2) of a scale 1:250000 (bands 4, 3, and 2).

2.4 Construction of Drainage Net Map

Construction of a drainage net is the basic GIS entity to perform any hydrological calculations or runoff watershed

modeling practices. In modern research methods, the reliance on DEMs and satellite imagery with high precision for the extraction of drainage networks and the boundaries of their basins are common (Jenson and Domingue 1988; Mark 1984; Moore et al. 1991; Martz and Garbrecht 1992; Tribe 1992).

Hydrologic process and water resource issues are commonly investigated by using distributed watershed models. These watershed models require physiographic information such as the configuration of the channel network, location of drainage divides, channel length and slope, and sub-catchment geometric properties. Traditionally, these parameters are obtained from maps or field surveys. The digital representation of the topography is called a DEM. The automated derivation of topographic watershed data from DEMs is faster, less subjective, and provides more reproducible measurements than traditional manual techniques applied to topographic maps (Tribe 1992). Digital data generated by this approach also have the advantage that they can be readily imported and analyzed by the GIS. The technological advances provided by the GIS and the increasing availability and quality of DEMs have greatly expanded the application potential of DEMs to many hydrologic, hydraulic, water resources, and environmental investigations (Moore et al. 1991). In the present work, the runoff calculations and assessing the potential for the RWH, was performed by dividing the study area into 52 watersheds (Fig. 8), which in turn, were subdivided into smaller sub-

Fig. 7 Base map of the study area constructed by GIS techniques

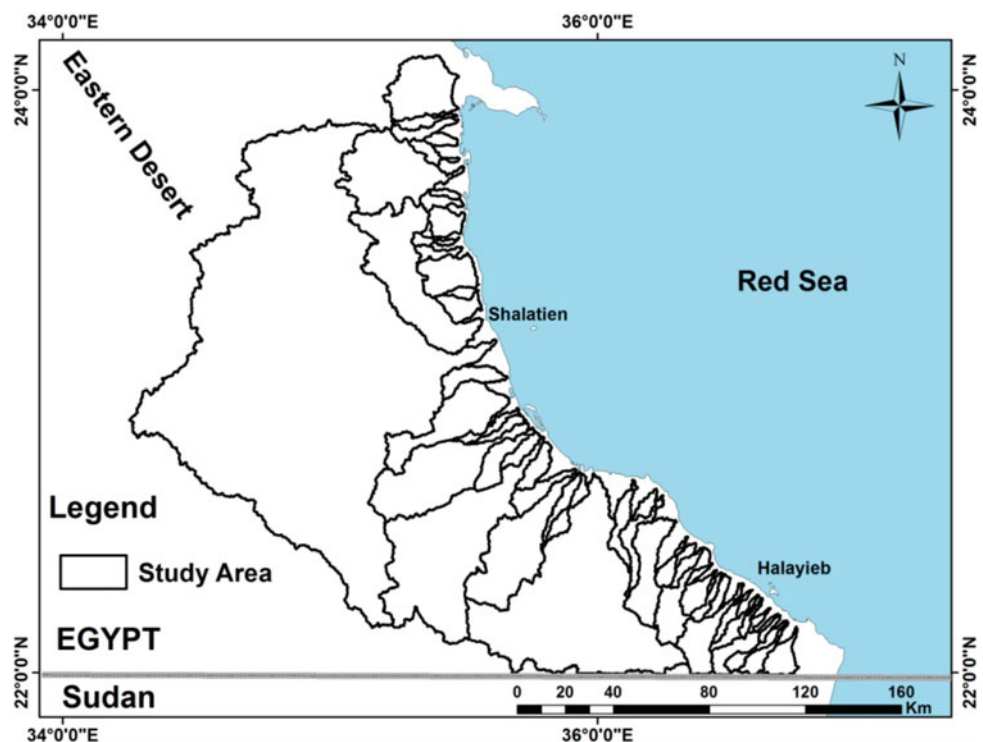
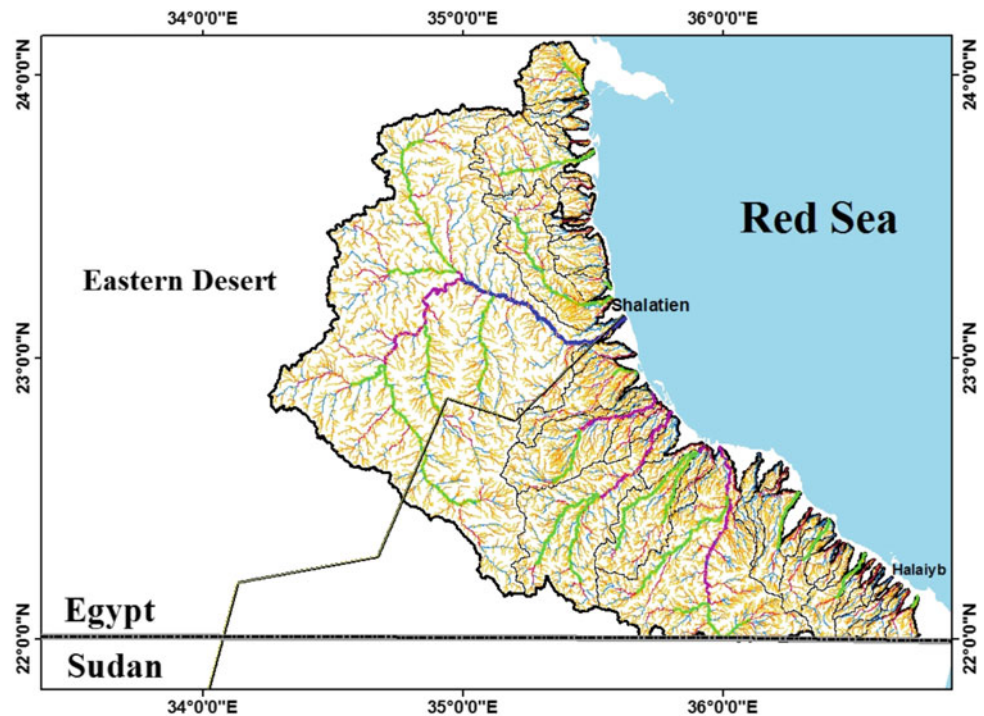


Fig. 8 Drainage net of study area comprising the: watersheds boundaries and drainage network



and sub-watersheds. The present work describes a process for determining site characteristics and developing an integrated approach including RS, GIS, and watershed modeling system software (WMS 8.0[©]) for performing such objectives.

DEM with a 30-m resolution of the study area has been obtained from the ASTER (Rabus et al. 2003), which was subsequently enhanced by the topographic contours and Landsat heights. One program that has been developed for the automatic delineation of watersheds and stream arcs on a DEM is the Topographic Parameterization (TOPAZ[©]) software (Garbrecht and Martz 1997). A special version of TOPAZ has been created for using within WMS software platform, which only requires an elevation grid as input and produces a flow direction grid and a flow accumulation grid as outputs. After defining basins with a DEM, the results are converted to drainage coverage for easier data storage and manipulation.

2.5 Runoff Calculations and Watershed Modeling

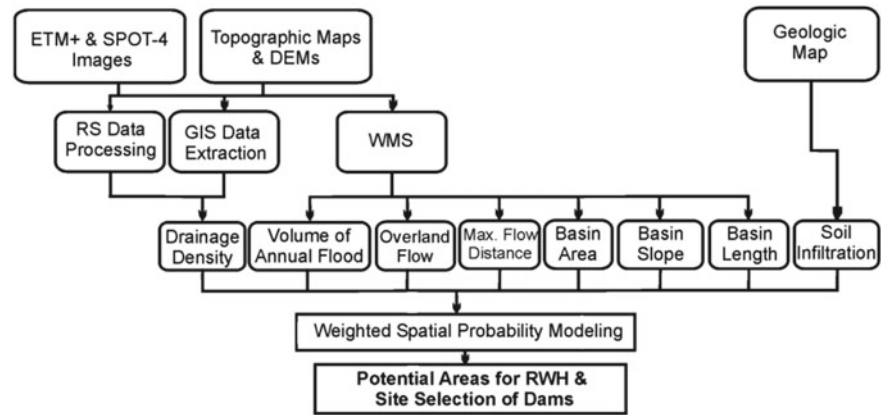
The hydromorphometric parameters of Halaib and Shalatin watersheds were determined using watershed modeling systems (WMS 8.0[©]) software (Aquaveo 2008), which

differentiated the basins and provided multiple watershed characteristics. Accordingly, several thematic maps, viz, volume of annual flood (VAF), average overland flow (OFD), maximum flow distance (MFD), infiltration number (IF), drainage density (Dd), basin area (BA), basin slope (BS), and basin length (BL) were integrated as input layers for the weighted spatial probability model (WSPM) to perform a determination for the efficient sites suitable for the RWH. The WMS 8.0[©] software calculated the hydromorphometric characteristics for each watershed value used in the WSPM. These values are provided for each of the delineated watersheds. These layers are generated in steps, i.e., digitization, editing, building a topological structure, and finally polygonization in ArcGIS 10.1[©] Spatial Analyst module (ESRI 2007).

Finkel (1979) method was used through the present work to calculate the volume of the annual flood which was run inside the WMS 8.0[©] software (Aquaveo 2008). Finkel (1979) used his method for the Araba Valley, which has similar climate conditions to Sinai Peninsula and arid regions in Egypt. It is a simple graphical method to determine the probability or frequency of occurrence of yearly or seasonal rainfall.

The Finkel empirical method (Finkel 1979) uses the following parameters (Eqs. 1 and 2):

Fig. 9 Flowchart of methodology



1. Peak flood flow (Q_{\max})

$$Q_{\max} = K_1 A^{0.67} \quad (1)$$

where Q_{\max} = Peak flood flows, in m^3/s .

2. Volume of the annual flood (v) in 1000 cubic meters

$$V = K_2 A^{0.67} \quad (2)$$

where A is the area of the basin in km^2 , and K_1 and K_2 are the constants depending on the probability of occurrence:

Probability of occurrence in a given year	K_1	K_2
10%	1.58	26.5

Here, we used 10% because it is very suitable for the developmental conditions.

The overall flowchart of the methodology is given in Fig. 9.

3 Geomorphological Setting, Geological Setting, and Soil Characteristics

3.1 Geomorphologic Features

Geomorphology is the face of the terrain, which reflects the geological setting of the area and has an important effect on accumulation, transportation, and percolation of rainfall. The investigated area comprises different types of landscapes including exogenic and endogenic landforms. The main geomorphologic units and features are:

3.1.1 Geomorphological Units

The study area can be classified into the following geomorphological units (Fig. 10):

Denudational landforms:

1. Low rocky land partially covered with sand and gravel
2. Low rocky highly fractured land
3. High relief mountainous area with sharp peaks
4. Moderately relief weathered and fractured mountainous area
5. Low rocky land with dense dyke swarms
6. Nearly flat sedimentary high land
7. Piedmont
8. Isolated hills
9. Hilly country.

Accumulated origin landforms:

1. Alluvial fan-like delta
2. Sand dunes
3. Wadi deposits.

Coastal plain:

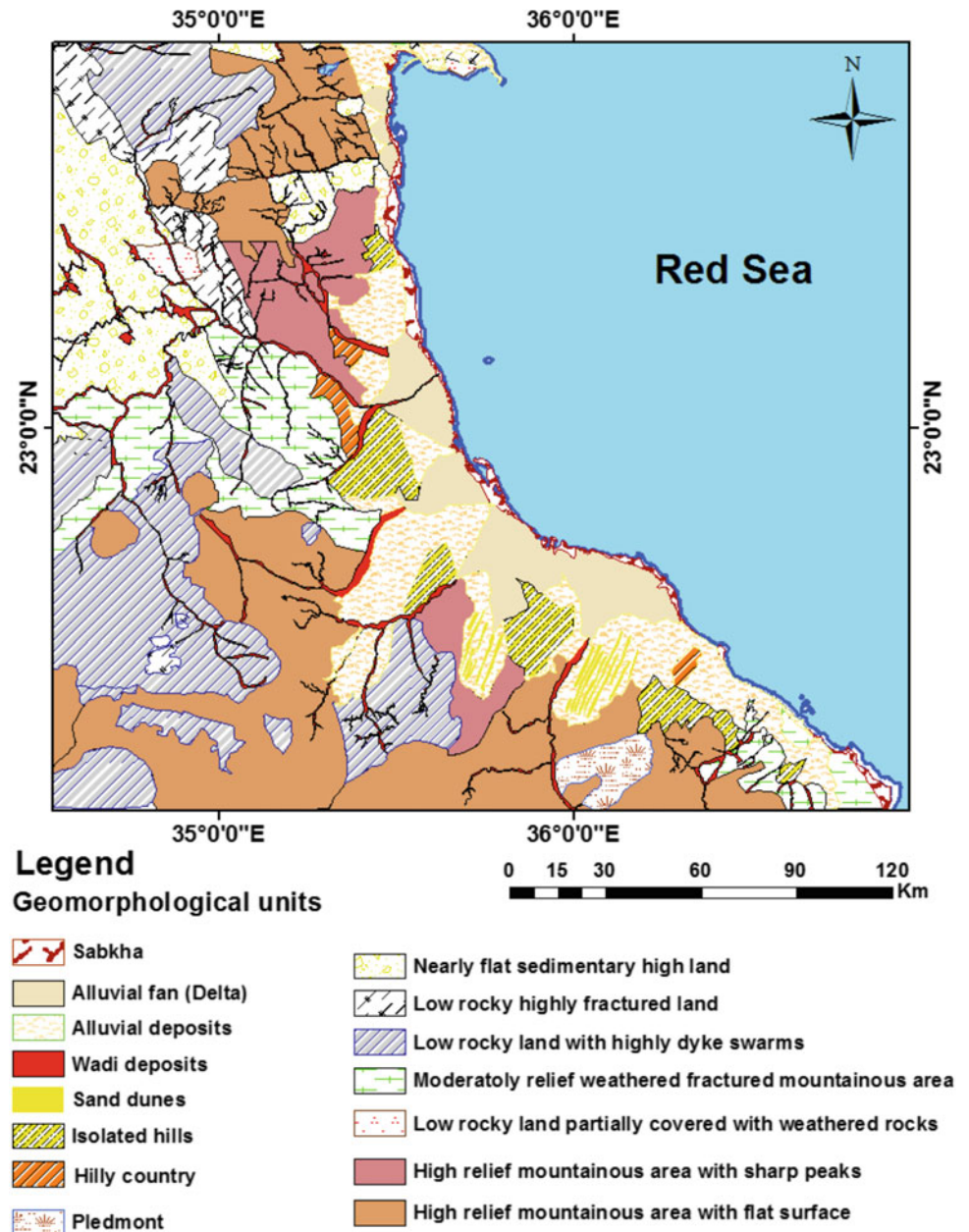
1. Beach
2. Sabkhas
3. Sand sheets.

In the following paragraph, a brief description of some of the major geomorphologic units recognized in the study area will be given.

Denudational Landforms

They are represented by nine geomorphic units (Fig. 10) formed chains of mountains that cover most parts of the study area. These mountains possess different slopes, but they are mostly ranging from steep to moderate slopes. Several pointed peaks are found in the study area such as those of Gebel Elba (1417 m), Gebel Shindeb (1334 m), and

Fig. 10 Geomorphologic map of the study area



Gebel Iss (1050 m). The eastern boundary of the mountainous chains is partially delineated by NNW to NNE faults, while the NE, NW, and ENE faults mainly shape the mountains. The hills range in topographic elevations from about 100 m to 400 m. They are formed of igneous, metamorphic, and sedimentary rocks, and range in size from tens to hundreds of meters. Major NE and NW faults as well as dykes of many trends and major wadis trace them. Most of these hills have gentle slopes and rounded peaks. Wadis have generally separated these hills and drain toward the Red Sea.

Some of these hills comprise some of the main economic minerals in the study area, such as magnesites, chromite, and iron oxides. These hills are mainly exposed at the area around Gebel Elba, W. Kraf, and the area between W. Hodein and W. Shaab deltas. The nearly flat sedimentary high land is well stratified and characterized by low to moderate topographic relief. They are represented by the Nubia Sandstone beds located at the northwestern (NW) part of the study area overlying the basement rocks. They are composed of sandstones with clay intercalation and are highly weathered and highly fractured with a consistent

mean elevation of about 500 m (masl). They are unconformably overlying the basement rocks and are faulted in different trends. From the field observation it was found that most of this unit developed in the investigated area is bounded by faults, especially those of NE–SW and NW–SE trends. Piedmonts are gently inclined slopes with slopes of about 1° extending from slopes cut in bedrocks down to an area of sediment deposition at a lower elevation. These morphologic features are represented by elongated areas in W. Shaab and W. Ibib.

Accumulated Landforms

Accumulated landforms include the following geomorphological forms:

Alluvial fan-like delta

The alluvial fans like delta occupy the foot slopes of the denuded mountains and large hills, and extend to large distances toward the sea to cover most of the coastal plain of the area studied, and have the fan-shaped form. These fans occupy different areas ranging from less than one square kilometer up to many square kilometers. They are usually formed of unconsolidated loose layers of boulders, gravels, sands and clays. These alluvial fans had been recognized from the Landsat (ETM + 8) images (Fig. 2) and they are connected with each other to form Bajada plain. Deltas are protuberances extending out from the shorelines formed where large alluvial channels enter the sea and supply sediments more rapidly than it can be redistributed by coastal

processes (Summerfield 1991). This features are somewhat represented in the area of study by the delta of W. Kraf which is probably represent an early stage developed delta, as depositional features are clear on the Landsat (ETM + 8) images (Fig. 2) where progradation of the coastal plain is only obvious in this sole characteristic wadi of the study area. This phenomenon could be attributed to the relative lower infiltration rate observed from the infiltration tests carried out in the vicinity of the wadi which gives a high possibility for channel sedimentation by the wadi into the Red Sea and building characteristic fan-like delta of W. Kraf.

Sand dunes

These sand dunes are of elongated type, of NE–SW direction. They covered an area of low land of granodiorite rocks along the coastal plain as well as located at the edges of some high mountains, as in Gebel Elba area, or along the eastern flank of W. Kraf (Fig. 11). The height of these dunes is about 13 m. The longitudinal dunes found in W. Kraf may comprise underneath buried paleo-drainage systems with probable groundwater bodies. On the coastal dunes, phreatophytes and other vegetation types are growing on, these dunes lie downwind of large sand supply and are characterized by localized vegetation sustained by near-surface groundwater that may be present. These dunes are sometimes called nebkhas and formed of dry sand grain size. About thirteen main dunes are interpreted from TM images with their bright yellow color.

Fig. 11 Field photo showing sand dunes in W. Kraf



Wadi and alluvial deposits

The wadis of the area of study are formed of bedrock and alluvial channels, the later flow into alluvial channels formed in unconsolidated sediments. These sediments may range in caliber from boulders (at the upstream channels) to clay-sized material at the downstream channels). Alluvial channels are “self-formed” and their morphology arises from the mobilization, transportation, and deposition of sediment and represents an adjustment to prevailing hydrological and sedimentological conditions. Alluvial channels differ significantly from bed rock channels which can usually change only slowly and whose morphology is dominated by structural and lithological controls.

Coastal Plain

The coastal plain of the study area is composed of different geomorphic features; beach, sabkhas, sand sheets, and alluvial terraces.

Sabkhas

Sabkhas occupy wide areas near the shoreline of the Red Sea from Abu Ramad in the north to Ras Halaib in the south. They are composed mainly of salts, clay, and silts with few grains of sand. They are wetlands and partially covered by seawater and salt. Some people extract NaCl salt from these sabkhas. They exhibited low topographic relief and were formed in the Quaternary age. The sabkhas are replaced by northward of the latitude of Abu Ramad by Beach sands which constitute quantitatively the most significant accumulations of subarially exposed sediment along the Red Sea coast.

Sand Sheets

Sand sheets are sand accumulations covered some small areas along the Red Sea coast. These sheets rarely give rise to significant topographic features but domes. The geomorphologic map (Fig. 10) may differentiate the infiltration capabilities of different areas as units characterized by high infiltration possibilities in terms of nearly flat surfaces, weathered surfaces, low rocky lands, low to moderately relief weathered fractured areas, nearly flat sedimentary high land, sand dunes and sand sheets, and areas characterized by low infiltration capabilities such as alluvial fans (deltas), wadi and alluvial deposits, sabkhas, high relief mountainous area with sharp peaks, piedmonts, isolated hills, and hilly country. The precipitation falling on a slope either run off on the surface, is held in surface depressions (surface detention), or infiltrates through the slope surface. Except on the slope of the impermeable rock where some proportion of the

precipitation reaching the slope almost invariably infiltrates the surface and either percolate down to the water table.

3.2 Geological Setting

The southern part of the Eastern Desert of Egypt represents a part of the Arabo-Nubian Shield. The area is almost occupied completely (exceptionally the area of Gebel Abra q and the upstream portion of W. Hodein are made of Nubia Formation) by basement rocks which form the mountainous ranges of high to medium topographic relief. The sedimentary rocks cover is a relatively small in area and forming moderately weathered bedded hills.

Quaternary deposits are present to cover the Red Sea Coastal plain and partly cover the sedimentary and Precambrian rock units. A geological map (Fig. 12) was prepared using Landsat ETM + 8 composite image (Fig. 2) followed by intensive field work where the geological contacts were sharpened and checked in the field and by matching it with the published Conoco geological map (scale:1:500,000), Sheet of Bemis).

3.2.1 Description of Rock Units

The following are different rock units from older to younger which could be identified in the study area:

- ***Precambrian basement rocks:***
 - Gneisses and Migmatites
 - Ultrabasic rocks
 - Metasediments rocks
 - Metavolcanic rocks
 - Gabbro–diorite Group
 - Older Granitoid rocks
 - Younger Granites
 - Alkaline Granite
 - Dykes
 - Ring Complexes.
- ***Cretaceous sedimentary rocks:***
 - Abu Aggag Formation
 - Timsah Formation
 - Umm Barmil Formation.
- ***Miocene carbonates rocks:***
 - Gebel El-Rusas Formation.
- ***Quaternary deposits:***
 - Wadi deposits
 - Sabkhas

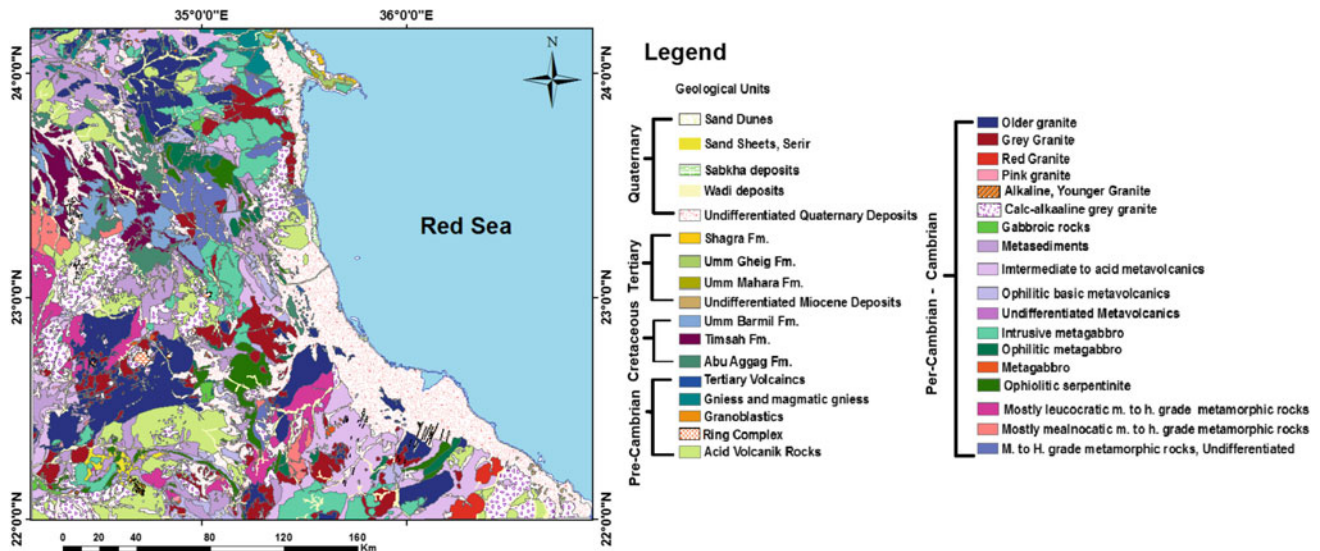


Fig. 12 Geological map of the study area (after Conoco 1987)

- Aeolian deposits
- Gravel plain.

These rock units formed the host environment for the groundwater occurrences as they provide favorable conditions for the groundwater aquifers and affect its hydro-chemical quality. The following is a brief description of these units.

Precambrian Basement Rocks

It is accepted now that Egyptian basement rocks in the Eastern Desert were developed during the Pan African progeny and were formed by the accretion of intraoceanic island arcs. These basement rocks essentially consist of ultrabasics, metamorphic complex, and granitic masses. The metamorphic sequence of interbedded metasediments and metavolcanics is presented in most localities. The granitic masses belong to late to post-orogenic. The following is a short description for the Precambrian basement rocks.

Gneisses and Migmatites

Gneisses and migmatites are the oldest outcrops of the basement rocks in the Eastern Desert of Egypt. Low topographic relief, highly weathered characterizes them, gneissose texture and highly fractured. They are present as isolated small hills partly covered by sands and exposed due to the NW part of W. Hodein. Gneiss and migmatite rocks are highly deformed with a high grade of metamorphism,

protruding melanosome bands of hornblende and leucosome. The latter is mainly quartz. Garnet crystals are abundant in these rocks.

Ultrabasic and Related Rocks

The ultramafic rocks occur at Sol Hamed area, as a belt of serpentinites striking in NE–SW trend. They show high topographic relief and exhibit green color. They are fractured in different directions and are also thrust. The marginal parts formed talc carbonate rocks with brown color, highly weathered, and weak in hardness. These rocks are composed mainly of olivine and pyroxene relics, antigorite, and comb-shape crysotile veinlets. They contain iron oxides and chromite bodies. There are some quartz veins of E–W trend cutting the rocks. Also the white and yellow color carbonates minerals filling the joints. Pale green talcoses surfaces are abundant in the eastern side of this serpentinites belt, with some aggregates of olivine and pyroxene.

Metasediments

These rocks are characterized by pale gray in color and schistose texture, flaky, and of bedding fabric, highly affected by tectonic structure processes and highly weathered. They show pencil-shape weathering products. The metasediments consist of green schist facies where they are composed mainly of actinolite and tremolite with rare chlorite, epidote, and iron oxides. These rocks are exposed at

different localities, such as the elongated areas around W. Hodein, W. Kraf, and great area at the SW part of the study area.

Metavolcanic Rocks

Nuweir and El-Sharkawi (1978) suggested that anywhere in the Eastern Desert of Egypt, the metavolcanic rocks are always associated and interbedded with the metasediment rocks. These rocks are of schistose greenschist facies composed mainly of actinolite, tremolite with few chlorites, and epidote with iron oxides and quartz veinlets. Many dykes in different directions cross them. These rocks are exposed to the south of Gebel Sul Hamid.

Gabbro–diorite Group

Akkad and Ramly (1960) gave the term of the gabbro–diorite group. These rocks are outcropped in Sol Hamed area and other greater parts of the study area. They are of medium to coarse grained in size, highly weathered, and highly fractured. These rocks are composed mainly of hornblende, calcic plagioclase, and iron oxides with few pyroxene and biotite crystals. There are chlorite and epidote in the joints.

Older Granitoid Rocks

These rocks are widely spread as isolated small hills with low topographic relief in the area of study. They show pale to deep gray colors and highly weathered with exfoliation fabric. These facies are named as gray granites by El-Ramly (1972) and previously named as syntectonic granites by Sabet (1972). The older granitoid rocks are medium to coarse grained and composed mainly of plagioclase, hornblende, biotite, and quartz and are cut by younger granites. They range in composition from granodiorite to adamellite.

Younger Granites

These granites were previously named as pink granites by Akkad and Ramly (1960). Sabet (1972) named them as late-tectonic granites. They are exposed as high topographic relief bodies with sharp contacts with the all other older basement rocks. They are composed mainly of orthoclase, microcline, quartz, and plagioclase, and they are of medium to coarse grained. Some quartz aggregates are present particularly at their contact with other rocks.

Alkaline Granites

These rocks are most probably belonging to Cretaceous age. They are of alkaline composition and composed mainly of alkaline feldspars (microcline and orthoclase) and quartz, of medium to coarse grain. These rocks are mainly represented in Gebel Elba with very high topographic relief. They are white in color and slightly weathered. They are jointed in vertical system, which filled with iron oxides; also there are some pockets of aggregated quartz.

Dykes

The Precambrian basement rocks were injected by a group of acidic and basic dykes. These dykes are penetrating the older basement rocks, which led to the creation of longitudinal ridges. The study area is affected intensively by these dykes which are responsible for the presence of several water points as, sometimes block the water in the wadis and form natural dams. Therefore, it was found that several water points were dug in the wadi beds. These wells are usually shallow, with depths range from 8 to 10 m. The intensive role of these dykes was observed in several localities and was responsible for the presence of their water points as in: W. Rahaba, W. Hodein (W. Fiqo and W. Gimal, W. Ibib, W. Kraf, and W. Meisah). Most of these dykes are striking in NE–SW direction with vertical walls.

Ring Complex

Gebel Meshbeh and Naqroub El-Fokani is a typical ring complex of syenite rocks in the southern Eastern Desert of Egypt. They have a ring shape of very high topographic relief. They are composed mainly of syenite, trachyte, and younger granite rocks. They are not cut by any dykes but are cutting by NE–SW faults and belong to Cretaceous age. They show pale and deep red color of fine to medium grain size.

Cretaceous Sedimentary Rocks (Nubia Sandstone)

The Cretaceous rocks in the area of study are composed of alternating sequences of fine- to coarse-grained sandstone intercalated with silt or clayey beds. These rocks are exposed in the NW part of the study area, the region of W. Hodein, in Gebel Abraq and Abu Saafa area (Fig. 13).

The Nubia Sandstone succession is composed of the following formations, from older to younger.

Fig. 13 Field Photo showing the Nubia sandstone outcrops at W. Abu Saafa area



Abu Aggag Formation

El-Naggar (1970), noted that Abu Aggag Formation is composed of conglomeratic to coarse-grained kaolinitic sandstone. The predominant structures are large to small-scale trough cross-bedding and ripple laminations. Superimposed channel sandstones can be assigned to a low-sinuosity or braided river environment. The upper part of the formation shows fining upward sequences of lens-shaped channel sands and thick paleosoles. In the type area, it has a thickness of 30–40 m. The bottom of this formation is not exposed or reached by drilling in the area of study.

Timsah Formation

The Timsah Formation is composed of nearshore marine to deltaic sequences of silt and fine-grained sandstone with thick shale intercalations. Two or three oolitic iron ore beds occur in this formation (El-Naggar 1970). The thickness of this formation ranges from 5 to 130 m. Timsah Formation conformably overlies the Abu Aggag Formation and disconformably overlain the fluvial section of Umm Barmil Formation. The age of Timsah Formation ranges from Coniacian to Santonian (El-Naggar 1970).

Umm Barmil Formation

The Umm Barmil Formation is composed of coarse to medium-grained sandstones of large-scale tabular and trough cross-bedded originated from a low sinuosity fluvial

environment (El-Naggar 1970). Paleo-current direction of forests points to N–NW. In the upper part, the sequence contains fining-upward cycles with intercalation of gray siltstone and ripple-laminated sandstone.

The thickness of this sequence at the type area is about 40 m, but may exceed 260 m in Wadi Dif area (Abdel Razik 1972; Endriszewitz 1988). Accordingly all the drilled groundwater wells in the area of study especially, in Abu Saafa and Dif areas did not encounter the base of this formation. In the subsurface, this formation consists of fine to coarse-grained sandstones, white to gray in color, mostly silty and clayey and slightly ferruginated. Umm Barmil Formation overlies Timsah Formation with an erosional contact and its age ranges from Santonian to Lower Campanian (Klitzsch et al. 1986; Hendricks and Luger 1987).

Miocene Carbonates Rocks

The Miocene sediments are found as isolated hills located to the west of Abu Ramad and Halaib areas in W. Serimtai, W. Aideib, W. Daaet, W. Kraf, W. Darera, and the region of W. Hubal. They mainly consist of alternating limestone and marl beds, and they are equivalent to the beds of Gebel El-Rusas Formation. The rocks of Gebel El-Rusas Formation are composed of alternating beds of marls and limestones interbedded with clay layers, which are covered by gravel, and boulders detached from the surrounding rocks. The Gebel El-Rusas Formation is characterized by the presence of a great number of manganese and calcite ore-bearing veins. These veins are affected by a group of faults generally striking NW–SE direction, i.e., parallel to the Red Sea. Also another group of faults having the general

direction of NE–SW with a lateral displacement affects them. This displacement led to the appearance and disappearance of the Miocene rocks with its ore veins in some places in the study area.

The Quaternary Sediments

The Quaternary sediments comprise gravel plain, wadi deposits, sabkhas, aeolian sediments, etc. The following is some details about these units:

Gravel Plain

The coastal plain of the investigated area is mostly covered by gravel sheet (s) depending on the topography of the plain. The western side of the plain faces the high range of the basement rocks from which the separated blocks and boulders are rested nearby this side. As far as, at the shoreline of the Red Sea, the size of these blocks and boulders decreases gradually to flint and pebble size.

Wadi Deposits

These deposits formed terraces like islands, especially near the downstream of the wadis, and they are composed of gravels and pebbles graded in different sizes and interbedded with thin bands of coarse-grained sands.

Sabkhas

These deposits are extending along the Red Sea coast and occupy different pans according to the topography of the area. These deposits are formed of mud horizons intermingled with sands and salt. Some pans are partially covered by seawater depending on the extent of the tide, while others are permanently covered by water. The salt formed in these pans may reach in thickness to 5 cm.

Aeolian Deposits

These sediments are composed of windblown sands and generally form the serir feature. Also, these blown sediments form the longitudinal or crescent-shaped dunes in the area. The heights of these sand dunes range from 5 to 10 m above the ground surface. The length, height, and width of these dunes are increasing toward the Red Sea coast, where some of these dunes may reach 10 km in length. These movable sand dunes formed parallel groups of ridges beginning from the basement rocks to the near of the Red Sea coast. Some of the sand dunes are not movable and form stabilized sand dunes. This type of dunes is found along the eastern flank of W. Kraf. These dunes may be trapped in a local structural control and wetness of the ground. The importance of these

dunes area is that they may comprise a buried paleo-drainage system along with W. Kraf. On the other hand, this aeolian sand may contain black sand derived from the Precambrian basement rocks.

3.2.2 Tectonics

The study area, as the other parts of the Eastern Desert, was subjected to different deformation processes, which affected the Precambrian basement and the overlying sediments. The faulting systems are one of the main factors, which control the occurrences of groundwater and its flow. The main structural elements affecting the study area are:

Faults

Many wadis and tributaries in the study area were channeled their preferred pass routes on the faults or fractures zones. The promising faulting system which affecting the study area can be summarized in the following sets:

Red Sea faulting system: These are the main faults, and having the trend N 25°–35° W, which is parallel to the Red Sea rifting system. In this system, the faults may extend more than 50 km. They possess strike–slip movements but some of them are of the normal type with their downthrown side toward the east.

Gulf of Aqaba (Dead Sea) system: This is the main secondary trend, which affected the study area. It has a direction of N 20° E.

The third set of faults have the N 50°–60° E trend which is considered as the oldest trend (Cretaceous) which affected the basement rocks. This trend is encountered in Gebel Elba at the southern part of the study area.

Fractures

Most of these structural features were formed as an echo of the major faulting systems, and others are primary structures; hence, they are numerous and intensified along the whole areas, with relatively shorter lengths than the main fault trends. These fractures are very important in groundwater studies as they are responsible for the presence of many hand-dug wells and springs in the study area, as will be discussed later.

Dykes

The different basement rock units outcropped in the investigated area is injected by swarms of dykes of acidic, intermediate, and basic composition. Generally, these dykes are arranged in parallel groups forming swarms of different trends and of longitudinal ridges. Also, these dykes are intersecting each other. As mentioned before, the rock types encountered in the area of study are highly fractured and

jointed. They are together with the dyke swarms play an important role in preserving water. Where the former (fractures and joints) acts as passage ways and when they are intersecting with each other's tubular water bodies are formed among them (Davis 1965), while the later (sealed dykes) preserve and block water, especially when they are intersected with each other's or intersected with fractures and faults. The dyke swarms are easily detected on the Landsat images. The trends and orientations of these dykes are very important in groundwater movement, occurrences, and exploration, as when they are crossing the wadis they capture the groundwater at the upstream side of the wadis. Such case was observed in the field, where these dyke swarms (masked and not seen on the Landsat ETM + 8 images) are responsible for the occurrence of the famous water point of Bir Gahelia, in W. Rahaba.

3.3 Soil Characteristics

The present pedological setting of the study area is based on the interpretation of satellite images, field work survey, and analytical data. HS area is characterized by many types of soil as described in the following terms:

3.3.1 Soil Types in Halaib–Shalatin Area

Soil of the Wadies

These soils are sedimentary movable, sandy textures in some areas with a crumbs of rock and gravel in the elevated areas

changed to loamy sand in moderate elevation areas and there are Celtic crust layers with thickness of 1 cm approximately cover the surface of the soil shows in Fig. 14, while at the end of the wadi, there is compacted soil which shows signs of water erosion (Figs. 15 and 16).

The morphological features of soil profiles representing this unit show that the dry soil color is very pale brown (10YR7/4) to brownish yellow (10YR 6/6) and it is pale brown (10YR 6/3) to yellowish brown (10YR 5/6) in moist condition was determined with the aid of Munsell Color Charts, (Anon 1975), the texture class is sandy loam for the surface layers. Soil profiles are characterized by deep soils, soil structure is sub-angular blocky and massive in the surface layer. The consistency is soft to slightly hard, non-sticky to slightly sticky, non-plastic to slightly plastic. Based on the morphological feature of the representative's profile of this unit and chemical analysis, the soils are classified as typic Torrifuvents.

Soil of the Delta and Alluvial Fans

These soils are sedimentary movable with water or wind, soil profiles are characterized by deep soils and moderately deep, soil texture is sand, loamy sand, and sandy loam.

The morphological features of soil profiles representing this unit show that the dry soil color is very pale brown (10YR7/4) to yellowish brown (10YR5/4) and it is pale brown (10YR 6/3) to dark yellowish brown (10YR 4/4) in moist condition, and the texture class is sandy loam to loamy sand for the surface layers. Soil structure is sub-angular blocky and massive in the surface layer. The consistency is

Fig. 14 Loamy crust on surface soil of the wadi



Fig. 15 Compacted soil in the upstream parts of the wadi

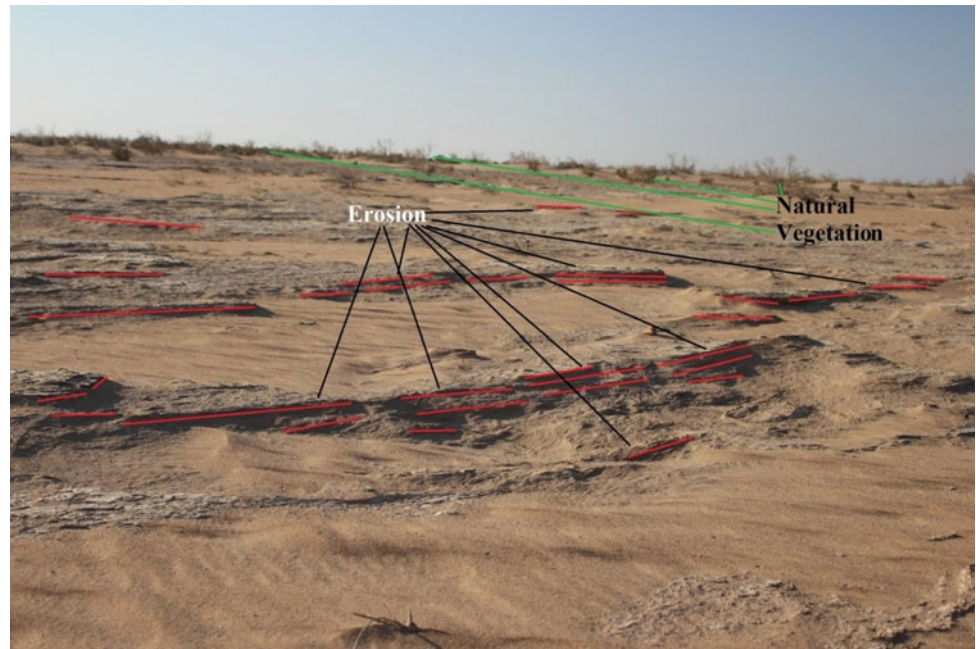


Fig. 16 Water erosion in the upstream parts of the wadi



soft to slightly hard, non-sticky to slightly sticky, non-plastic to slightly plastic. The horizon boundary is clear smooth. The morphological features of soil profiles representing this unit show that, most of the studied soil profiles contain a small percentage of salts, gypsum, and calcium carbonate. The depth of drilled soil profile is moderate to deep (Fig. 17). Based on the morphological feature of the

representative's profile of this unit and chemical analysis the soils are classified as Typic Torrifuvents.

– Soil of Sabkhas

These soils are sandy and too salty which is flat to undulating and found in the low lying areas and extended with the

Fig. 17 The drilled soil profile in the alluvial fan of wadi Hodein



coastline, exist mainly in depressions and originated as a result of sea intrusion which rises water table. The soil profile is shallow and water table depth of 30–80 cm. Soil profile contains mostly on salic horizon or gypsic horizon.

The morphological features of soil profiles representing this unit show that the dry soil color is very pale brown (10YR 7/4) to brownish yellow (10YR 6/6). It is yellowish brown (10YR 5/6) in moist condition, the texture class is coarse sand. Soil profiles are characterized by shallow to moderately deep soils (30–80 cm), soil structure is single grained structure and very friable in the surface layer. The consistency is slightly hard, no sticky and no plastic. The horizon boundary is a clear smooth and diffuse smooth boundary. This unit is shallow deep water table. Salt is increased with depth. It is mainly present in fine salt crystals forms for the surface layer and the accumulation of salts for soil. Gypsum content present in the studied layers is in the form of small shiny crystals. The soils of this unit are classified as Typic Aquisalids.

Soil of Sand Sheet

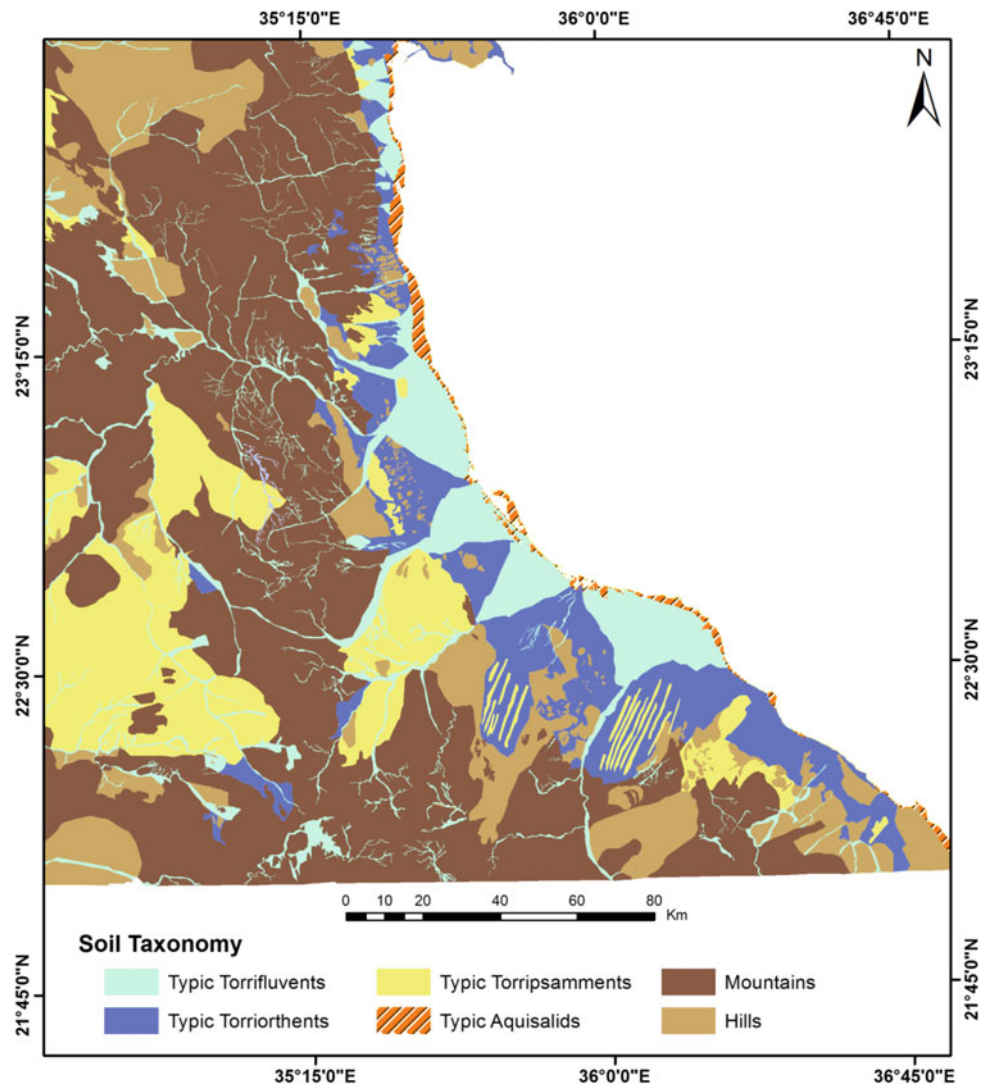
Soil profiles are characterized by deep soils, soil texture is sandy. The morphological features of soil profiles representing this unit show that the dry soil color is very pale brown (10YR7/4) to brownish yellow (10YR 6/6) and it is pale brown (10YR 6/3) to yellowish brown (10YR 5/6) in moist condition, the texture class is sandy for the surface layers. Soil structure is single grained and massive in the surface layer. The consistency is soft to slightly hard non-sticky, non-plastic. The horizon boundary is clear smooth. Most of the studied soil profiles are a small percentage of salts, gypsum, and calcium carbonate. The soils of this unit are classified as Typic Torripsamments.

3.3.2 Soil Classification of Halaib–Shalatin Area

The American Soil Survey Staff system (USDA 2010) was applied down to the sub-great group level for the studied soil mapping unit. Table 2 shows the calculated area for each

Table 2 Soil classification according to USDA (2010) for HS area

Soil order	Soil sub-order	Soil great group	Soil sub-great group	Units
Aridisols	Salids	Aquisalids	Typic Aquisalids	Wet and dry Sabkhas
Entisols	Psamments	Torripsamments	Typic Torripsamments	Sand sheet and sand dunes
	Fluvents	Torrifluvents	Typic Torrifluvents	Wadi, Alluvial fans and Delta
	Orthents	Torriorthents	Typic Torriorthents	Alluvial deposits

Fig. 18 The soil map of HS area

soil classification unit. The spatial distribution of these soil great groups is illustrated in Fig. 18.

The defined diagnostic horizons of Aridisols are salic and gypsic horizons. Salic horizon usually exists in soils close to salt marches and poorly drained area such as salt marshes are also common in these areas. The process of soil salinization is more often connected with rising of water level and high evaporation rate. These areas mostly located in the northern parts near the coast.

Diagnostic horizons (salic and gypsic) are different in presence with each other in accordance to the conditions associated with the configuration in the arid and semi-arid regions due to poor rainfall and relatively high evaporation which, in turn results in the accumulation process. Precipitations of salts arise from processes of evaporation and thus, at least soluble salt (carbonate) precipitates first followed by the most soluble salt (gypsum), where calcic horizon exists are down the profile and gypsum above calcic horizon.

Either in the presence of groundwater level (such as salt marshes), the movement of the water to down, and, thus, it consists of salic horizon followed by gypsic horizon.

The soil of the study area contains two orders of soil classification; the Entisols, which includes Psamments, Orthents, and Fluvents suborders and the Aridisols, which include Salids suborders.

3.3.3 Land Evaluation

Land Capability Classification

Land capability classification was carried out using the Applied System of Land Evaluation (ASLE software) which has been developed by (Ismail et al. 2005). ASLE software is inserting for soil database and calculates possible indices combinations between the major factors. The soil properties factor was used to calculate land capability. This property is

Table 3 Land capability index classes and ratings used by ALES of HS area

Class	Description	Rating (%)
C1	Excellent	>80
C2	Good	60–80
C3	Fair	40–60
C4	Poor	20–40
C5	Very poor	10–20
C6	Non-agricultural	<10

irrigation system, number of layers and layers depth, physical properties (e.g., clay content, available water, profile depth, landform, slope, and level of surface), and chemical properties (e.g., pH, soil salinity, CEC, gypsum content, and carbonate content). Ranges of land capability classes are represented in Table 3. According to ASLE software, the studied area was classified into four capability classes as follows (Fig. 19).

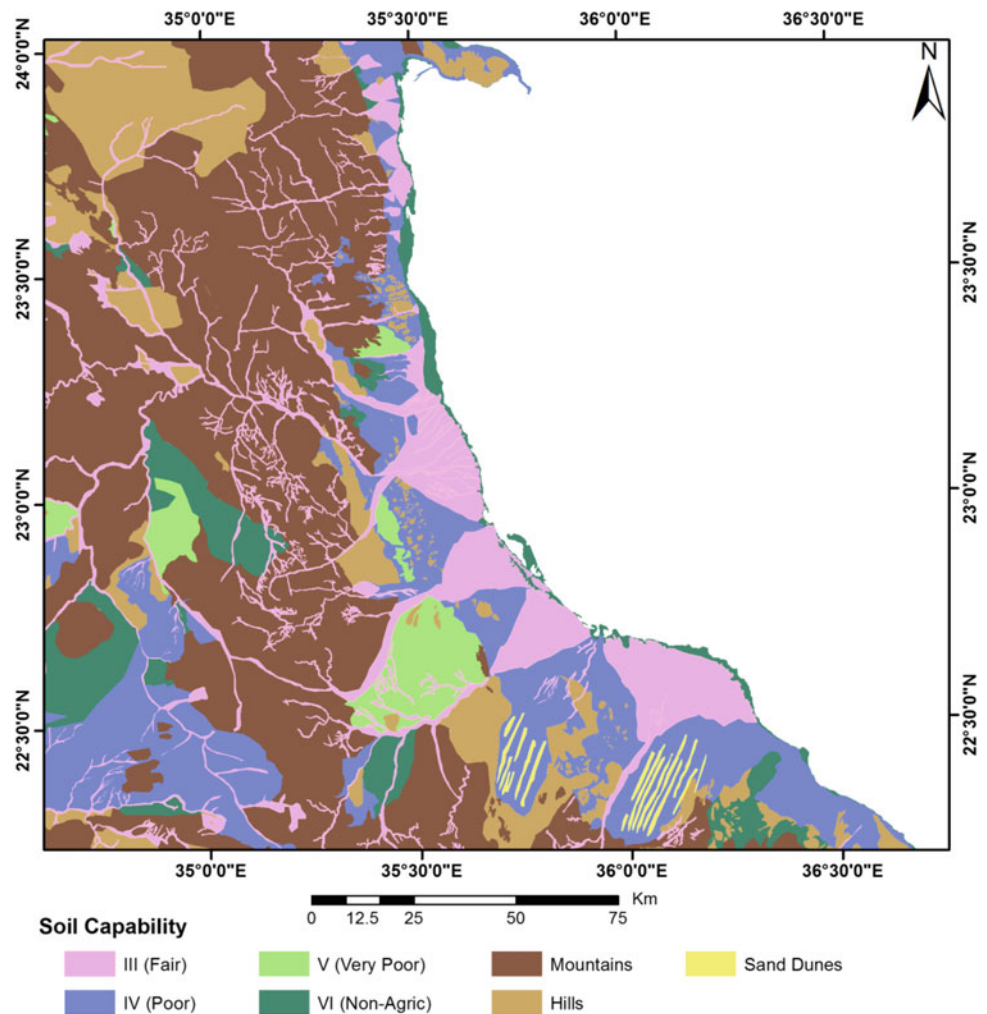
Soils With Fair Land Capability (C3)

Soils in this class have more than slight limitations and more than moderate limitations that require moderately intensive management practices or moderately restrict the range of crops, or both. Soils in this class have fair soil index between 42.64 and 57.47%. These soils are deep to moderately well drained, moderately affected by alkaline and electric conductivity (EC). Accordingly, these soils need slightly good management practices to improve their current situation. So, the current capability of this soil map unit can be changed to be good with moderately intensive management practices. This class represented wadi and alluvial fans.

Soils With Poor Land Capability (C4)

Soils in this class have more than slight limitations and more than moderate limitations that require moderately intensive management practices or moderately restrict the range of crops, or both. Soils in this class have poor soil index

Fig. 19 Capability soil index of HS area



between 20.3 and 38.3%. Accordingly, these soils need good management practices to improve their current situation. So the current capability of this soil map unit can be changed to be fair with moderately intensive management practices. This class represented some soils of alluvial deposits.

Soils With Very Poor Land Capability (C5)

Soils in this class have one or more severe limitations that exclude the use of land, or with one or more severe limitations that require special management practices or severely restrict the range of crops, or both. These soil units have some limitations such as salinity, soil depth, and content of CaCO_3 because it has low soil index (10.37–18.32%). These lands require good and proper management. These soil units will be improved to be fair or good. They are moderately high in productivity for a fair range of crops. This class is represented on the plain with rock out crop.

Soils With Non-Agriculture Land Capability (C6)

Soils in this class have severe or very severe limitations that cannot be corrected such as texture, high salinity, high contents of gypsum, and very shallow soil profile. It has low soil index ranging 1.39%. This class is represented by sabkhas.

4 Results of Watershed Modeling and Discussions

4.1 Generalities

HS area is classified into 52 watersheds, each has its geographical location and own hydromorphological parameters (Fig. 20 and Table 4).

4.2 Criteria of Runoff Water Harvesting (RWH) Potentiality Determination in Halaib-Shalatin Area

RWH could play a vital role in reducing flood proneness and providing household consumption (Sepehri et al. 2018). The RWH potentiality of the study area was determined by spatially integrating eight thematic layers, which represent the most important hydrographic and hydromorphometric parameters or criteria for determining the RWH potentiality. After defining the watershed attributes with the DEMs inside the platform of WMS 8.5[©] software, the multi-criteria decision support (MCDSS) layers are to be converted into data coverage for easier data storage and manipulation. The input criteria (layers) and their ranges used in the construction of the weighted spatial propability model (WSPM) are

Fig. 20 Landsat satellite ETM + 8 image showing HS Watersheds

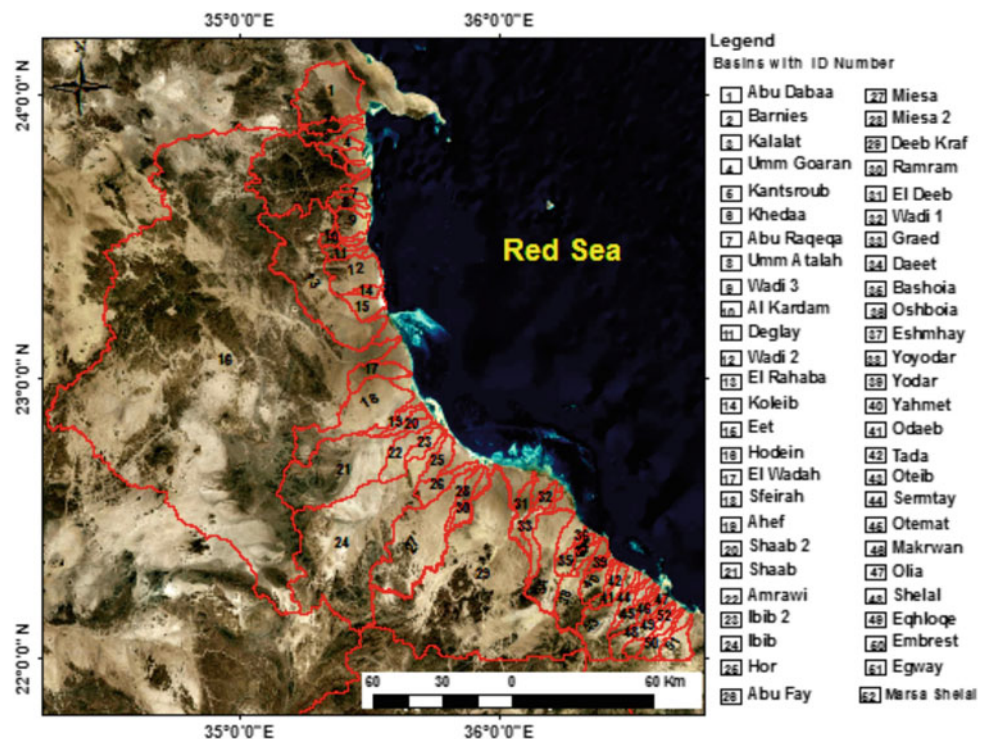


Table 4 WMS 8.0[®] software hydrographical output criteria used for demarcating the watersheds' characteristics of HS area

Basin ID	Watershed	Volume of annual flood (VAF) (10^3 m^3) Finkel method	Peak flood flow (Q_{\max}) (m^3/s) Finkel method	Overland flow distance (OFD) (km)	Max. flow distance (MFD) (km)	Basin infiltration No. (IF)	Drainage density (Dd) (km^{-1})	Basin Area (BA) (km^2)	Basin slope (BS) (m/m)	Basin length (BL) (km)
<i>Halaib-Shalatin watersheds</i>										
1	Olia	218.10	36.72	0.63	14.11	0.97	1.25	23.24	0.04	12.61
2	Mersa Shalal	225.11	38.50	0.72	15.91	0.88	1.43	24.37	0.02	12.65
3	Yodar	225.77	38.67	0.72	14.58	0.77	1.45	24.47	0.01	13.16
4	Abu Raqeqa	249.07	44.77	0.59	14.21	0.67	1.18	28.34	0.15	12.21
5	oshboiya	254.37	46.20	0.70	17.54	1.00	1.39	29.24	0.02	13.95
6	Makrawan	282.15	53.93	0.57	20.14	0.84	1.14	34.13	0.05	16.74
7	Shaab 2	418.66	97.19	0.72	30.39	0.77	1.43	61.51	0.06	23.84
8	Kolieb	302.00	59.69	0.66	30.48	0.91	1.32	37.78	0.01	14.53
9	Al kardam	335.48	69.83	0.53	17.33	0.72	1.05	44.20	0.01	18.25
10	El Laqd	364.60	79.07	0.58	17.08	0.67	1.15	50.05	0.08	14.77
11	Odaeb	395.16	89.16	0.59	20.60	0.92	1.18	56.43	0.01	21.37
12	Eshmhay	396.39	89.58	0.69	24.95	0.92	1.38	56.69	0.20	20.10
13	Tada	401.15	91.19	0.68	25.12	0.80	1.36	57.71	0.02	18.68
14	Deglay	411.04	94.56	0.52	24.74	0.72	1.05	59.85	0.08	17.99
15	Sermatay	413.38	95.37	0.57	21.12	0.79	1.14	60.36	0.21	25.64
16	Umm Atalah	424.41	99.19	0.50	22.00	0.72	1.00	62.78	0.16	16.45
17	Kanstroub	434.67	102.79	0.56	24.22	0.83	1.13	65.06	0.18	16.45
18	Ahef	442.72	105.65	0.71	36.81	0.75	1.43	66.87	0.01	28.06
19	Barnies	449.91	108.22	0.57	29.74	0.63	1.13	68.49	0.12	24.19
20	Bashoia	472.76	116.52	0.60	27.18	0.80	1.20	73.75	0.03	22.03
21	Otemat	497.33	125.68	0.59	35.63	0.80	1.18	79.54	0.08	28.55
22	Ibib 2	507.81	129.65	0.58	27.54	0.75	1.16	82.06	0.02	20.26
23	Ehqloqe	511.50	131.06	0.63	38.89	0.75	1.27	82.95	0.11	29.64
24	Embrest	528.26	137.52	0.55	33.95	0.62	1.10	87.04	0.10	27.05
25	Misa 2	543.27	143.39	0.64	42.76	0.66	1.28	90.75	0.01	33.35
26	Kalalat	563.65	151.49	0.55	37.78	0.66	1.09	95.88	0.17	25.93
27	Ramram	579.00	157.69	0.63	41.45	0.75	1.27	99.81	0.01	41.50
28	Yahemt	622.99	175.90	0.60	28.95	0.72	1.20	111.33	0.01	21.36
29	Hor	625.16	176.82	0.65	27.90	0.70	1.29	111.91	0.10	21.45
30	Eet	642.03	183.99	0.61	27.45	0.74	1.22	116.45	0.01	18.99
31	Abu Mad	656.27	190.11	0.57	21.12	0.74	1.15	120.32	0.14	15.05
32	Graed	701.58	210.03	0.60	63.24	0.67	1.20	132.93	0.02	41.50
33	El Deeb	703.34	210.82	0.62	51.54	0.64	1.24	133.43	0.02	35.58
34	Egway	712.90	215.11	0.61	31.52	0.79	1.22	136.15	0.05	23.98
35	Abu Fay	713.09	215.20	0.46	38.38	0.24	0.92	136.20	0.02	28.35
36	Shelal	740.71	227.75	0.56	40.15	0.72	1.13	144.15	0.15	33.61
37	El Wadah	752.35	233.12	0.60	35.81	0.73	1.20	147.54	0.01	25.97
38	Amrawi	845.35	277.41	0.62	45.80	0.90	1.23	175.57	0.02	32.22
39	Kelibtab	1109.47	416.25	0.60	39.35	0.81	1.19	263.45	0.09	25.13

(continued)

Table 4 (continued)

Basin ID	Watershed	Volume of annual flood (VAF) (10^3 m^3) Finkel method	Peak flood flow (Q_{\max}) (m^3/s) Finkel method	Overland flow distance (OFD) (km)	Max. flow distance (MFD) (km)	Basin infiltration No. (IF)	Drainage density (Dd) (km^{-1})	Basin Area (BA) (km^2)	Basin slope (BS) (m/m)	Basin length (BL) (km)
40	Yoyodar	1118.38	421.25	0.56	52.23	0.73	1.11	266.61	0.11	40.72
41	Otieb	1147.92	437.97	0.58	60.46	0.79	1.16	277.19	0.18	40.14
42	Daect	1427.07	606.09	0.61	53.74	0.74	1.22	383.60	0.04	42.13
43	Abu Dabaa	1678.51	772.20	0.79	40.10	1.68	1.58	488.73	0.06	28.52
44	Sfeirah	1900.70	929.63	0.64	72.93	0.81	1.27	588.37	0.05	53.70
45	Meisa	2357.61	1282.18	0.54	90.19	0.69	1.09	811.51	0.07	64.02
46	Khedaa	2439.80	1349.47	0.47	68.63	0.59	0.95	854.09	0.20	49.57
47	Shaab	2547.82	1439.61	0.60	100.17	0.77	1.19	911.15	0.09	68.16
48	Rahaba	2834.56	1688.00	0.57	101.65	0.76	1.13	1068.3	0.09	64.56
49	Ibib	4115.46	2944.85	0.52	129.72	0.70	1.04	1863.8	0.13	92.44
50	Kraf (from Egypt)	5563.66	4618.49	0.56	146.27	0.75	1.12	2923	0.09	82.23
51	Hodien	13989.60	18288.53	0.34	303.83	0.19	0.69	11575	0.07	143.64
52	Um Goran	342.22	71.94	0.68	24.88	0.9	1.36	45.5	0.20	12.6

Table 5 Ranges of input criteria used in the WSPM for HS area

Watershed RWH Criteria	Very high	High	Moderate	Low	Very Low
Volume of annual flood (1000 m^3)	>11590	11580–8603	8602–5512	5511–2476	<2475
Overland Flow Distance (km)	>0.6218	0.6217–0.5733	0.5732–0.5125	0.5124–0.4392	<0.4391
Maximum Flow Distance (km)	>247.2	247.1–175.1	175–112.3	112.2–61.03	<61.02
Basin infiltration number	>1.169	1.168–0.7715	0.7714–0.6022	0.6021–0.3804	<0.3803
Drainage density (km^{-1})	>1.244	1.243–1.147	1.146–1.026	1.025–0.8782	<0.8781
Basin Area (km^2)	>9279	9278–6455	6454–3586	3585–1309	<1308
Basin Slope (m/m)	>0.1368	0.1367–0.1038	0.1037–0.07783	0.07782–0.04807	<0.04806
Basin Length (km)	>117.6	117.5–91.8	91.79–64.56	64.55–38.82	<38.81

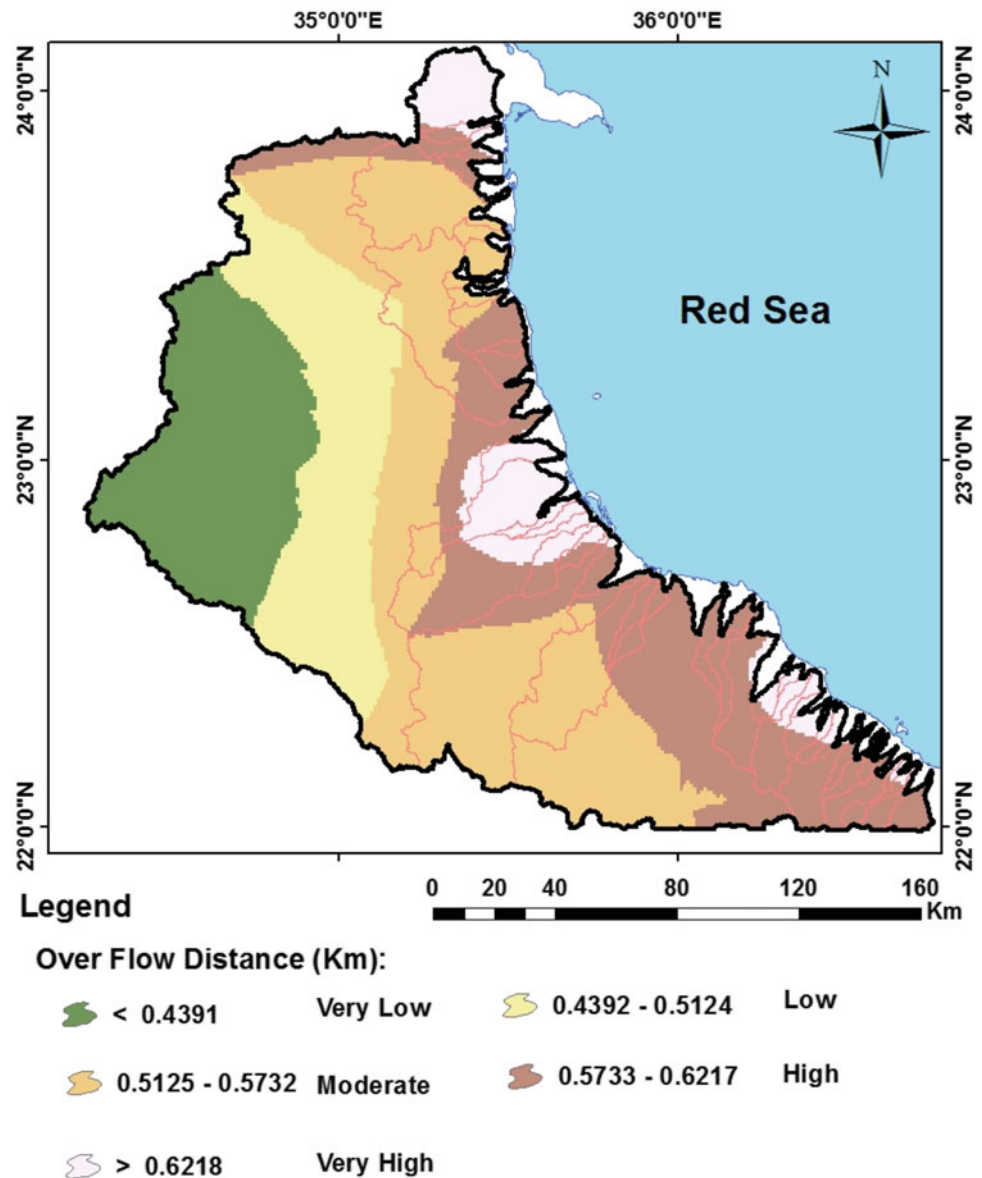
given in (Tables 4 and 5). Integration of these criteria in the GIS-based WSPM will result in the production of comprehensive maps determining the efficient sites suitable for RWH, with a number of classes. These thematic layers, which represent the WSPM model inputs, include: average overland flow distance (OFD), VAF, BS, Dd, BL, BA, basin infiltration number (IF), and MFD (Table 4). The following is a short description of these themes:

– Average Overland Flow Distance (OFD)

The average OFD within the basin is computed by averaging the overland distance traveled from the centroid of each

triangle to the nearest stream. The overland flow is the water that flows over the slopes of the drainage basin and is then concentrated into stream channels. Also, it is known as surface flow. It is affected by the type of soil and surface topography that govern the erosion rates caused by the overland flow (Montgomery and Dietrich 1989). High–very high OFDs (>247.2 km) are represented by the eastern side of the study area constitute a strip parallel to the Red Sea coast. It covers most of the small watersheds that are close to the coast such as (Embrest, Egway, Mrasa Shelal, El-Deep, El-Laqd, El-Wadah, Sfeirah, Abu Dabaa, Baranies, and Kalalat Watersheds) (Fig. 21). Additionally, it covers the downstream parts of larger watersheds such as (Hodein, Ibib,

Fig. 21 The OFD thematic layer used in the WSPM



and Deep Kraf. The thematic layer of the OFD indicates a pronounced decrease in value toward the western side of the study area reaching to very low (<0.4391 km) at the upstream parts of Hodein Watershed (Fig. 21 and Table 5). The moderate class of OFD (0.5732–0.5125 km) was occupied by the most parts of Miesa, Khedaa, Wadi 3, and Ibib Watersheds in addition to some parts of Hodein, Deep Kraf, and Sfeirah Watersheds. This layer was assigned a weight of 12.5 in the WSPM (Table 6).

– Volume of Annual Flood (VAF)

The availability of a pronounced VAF in a drainage basin is one of the most important parameters for the success of the

RWH (Elewa and Qaddah 2011). The VAF reflects the quantity of water available for harvesting. The values of VAF were calculated and listed in Tables 4 and 5 in units of 1000 m³.

The VAF was calculated by Finkel's method (Finkel 1979). Figure 22 shows the classes of VAF, where the high–very high classes (>11590) occur mostly in the western corner of study area mainly in W. Hodein Watershed at its upstream parts (Fig. 22). The moderate class (8602–5512) of the VAF occurs as a small strip in the central part of W. Hodein Watershed in addition to a very small part in Shaab Watershed at its upstream. The low and very low VAF classes (<2475) comprises large parts of the study area represented mainly by the eastern side parallel and close to

Table 6 The first WSPM scenario (equal weights to criteria), ranks, and degree of effectiveness of themes used in the RWH potentiality mapping of HS area

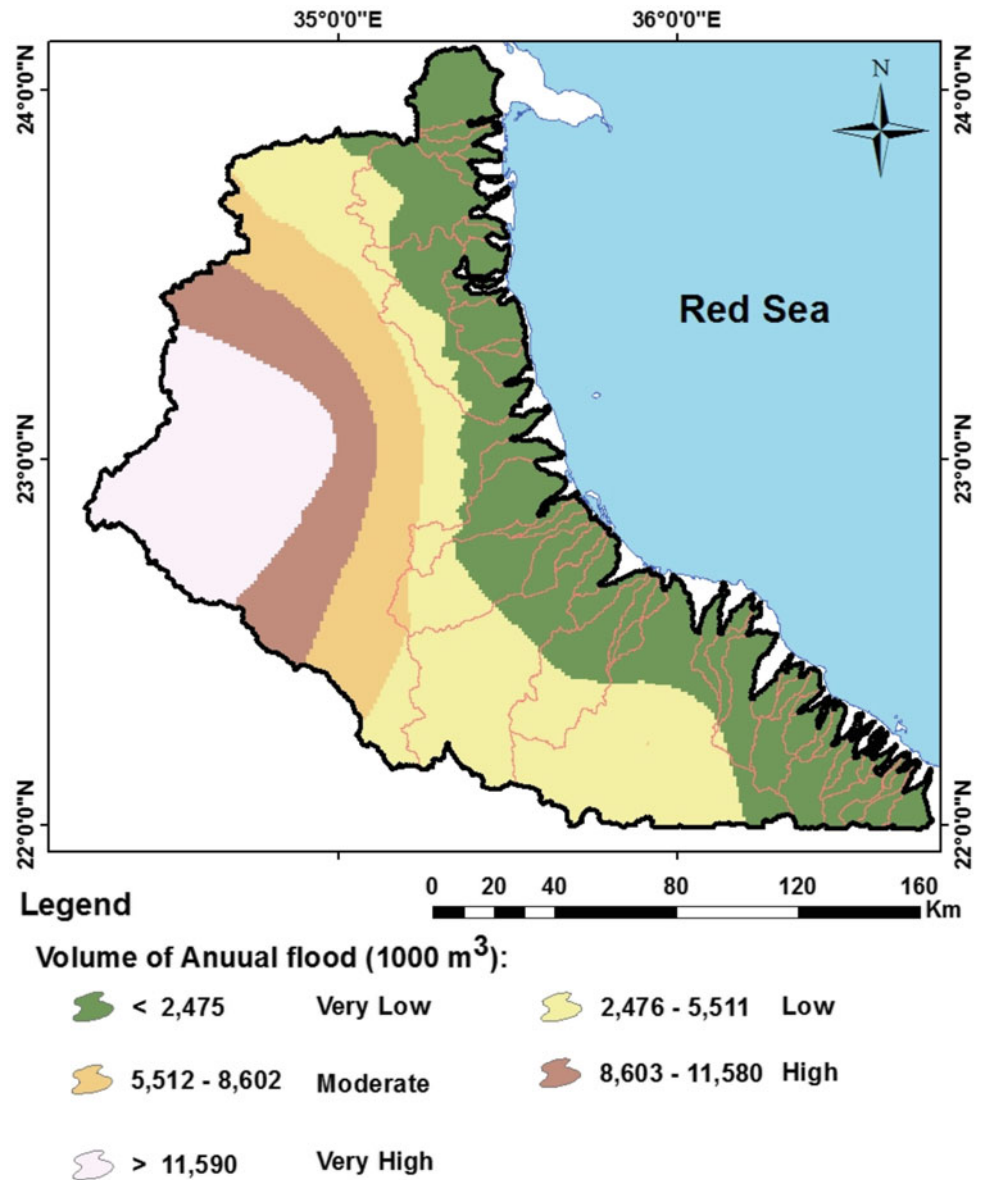
Thematic layer (Criterion)	RWH potentiality class	Average rate (Rank) (R_c)	Weight (W_c)	Degree of effectiveness (E)
Volume of annual flood (VAF)	I (Very high)	0.9	12.5	11.25
	II (High)	0.7		8.75
	III (Moderate)	0.5		6.25
	IV (Low)	0.3		3.75
	V (Very low)	0.1		1.25
Average overland flow distance (OFD)	I (Very high)	0.9	12.5	11.25
	II (High)	0.7		8.75
	III (Moderate)	0.5		6.25
	IV (Low)	0.3		3.75
	V (Very low)	0.1		1.25
Maximum flow distance (MFD)	I (Very high)	0.9	12.5	11.25
	II (High)	0.7		8.75
	III (Moderate)	0.5		6.25
	IV (Low)	0.3		3.75
	V (Very low)	0.1		1.25
Basin infiltration number (IF)	I (Very high)	0.9	12.5	11.25
	II (High)	0.7		8.75
	III (Moderate)	0.5		6.25
	IV (Low)	0.3		3.75
	V (Very low)	0.1		1.25
Drainage density (Dd)	I (Very high)	0.9	12.5	11.25
	II (High)	0.7		8.75
	III (Moderate)	0.5		6.25
	IV (Low)	0.3		3.75
	V (Very low)	0.1		1.25
Basin area (BA)	I (Very high)	0.9	12.5	11.25
	II (High)	0.7		8.75
	III (Moderate)	0.5		6.25
	IV (Low)	0.3		3.75
	V (Very low)	0.1		1.25
Basin slope (BS)	I (Very high)	0.9	12.5	11.25
	II (High)	0.7		8.75
	III (Moderate)	0.5		6.25
	IV (Low)	0.3		3.75
	V (Very low)	0.1		1.25
Basin length (BL)	I (Very high)	0.9	12.5	11.25
	II (High)	0.7		8.75
	III (Moderate)	0.5		6.25
	IV (Low)	0.3		3.75
	V (Very low)	0.1		1.25

the Red Sea coast extending from northeast to southeast (Fig. 22). These classes are represented by all watersheds with different areas ranging from small parts as in Hodein Watershed to hole watershed area as in the other watersheds (Fig. 22). In general, the spatial distribution of the VAF classes was degraded from the very high to very low classes passing by high, moderate, and low classes from the western to the eastern parts of the study area (Fig. 22). This layer was assigned a weight of 12.5 in the WSPM for the RWH (Table 6).

– Basin Slope (BS)

The BS of the drainage basin is a key factor for the selection of water-harvesting locations in order to get the maximum storage capacity in the channel. It is the average slope of the triangles comprising this basin (Horton 1945; Leopold and Maddock 1953). Reasonable care should be taken into account when determining this parameter, as the peak discharge and hydrograph shape is sensitive to the slope value used for the basin (Jones 1999). In the present work, the

Fig. 22 The VAF (calculated by Finkel's method) thematic layer used in the WSPM



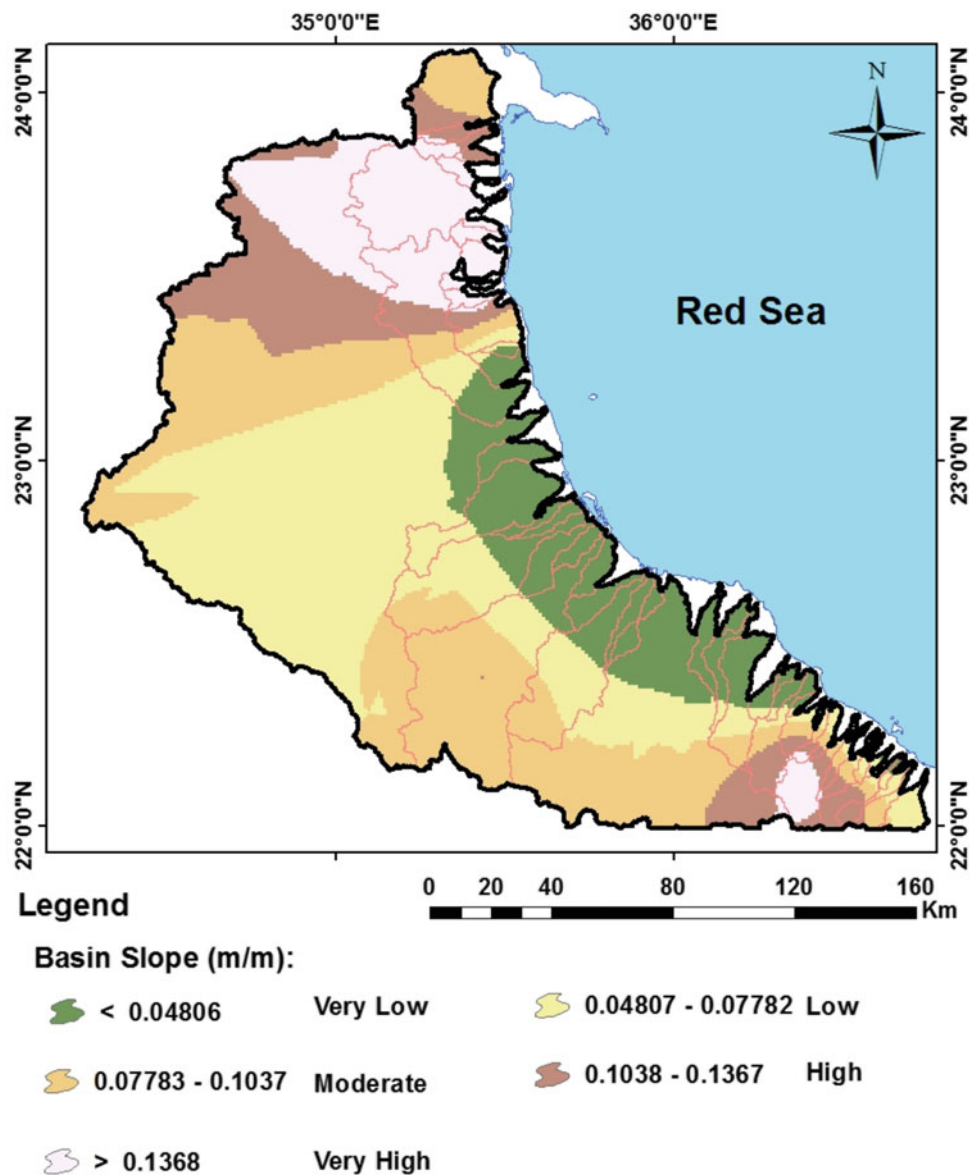
slope map is generated from the ASTER DEM. Five slope classes were generated (Fig. 23). The slope map was merged with the basin map to create the slope attributes of each drainage basin. The thematic layer of the BS indicates that high–very high slope (>0.1368) are represented by the SE corner of the study area occupying the upstream parts of many watersheds such as (Marsa Shelal, Egway, Embrest, Eghloqe, Shelal, Deep Kraf, and Otieb Watersheds). These classes also represented by Umm Goaran, Kantsroub, Khedaa, Abu Ragea, and Umm Atalah Watersheds in the northeastern (NE) side of the study area in addition to some parts of Hodein, Rahaba, Kelibtab, and Deglay Watersheds (Fig. 23). Moderate class of BS (0.1037 – 0.07783 m/m) are represented by a considerable strip in southern parts of the study area covering the upstream parts of Shaab, Ibib, Miesa,

and Deep Kraf Watersheds in addition to some parts of Hodein, Rahaba, Kelibtab Watersheds in the northern parts of the study area (Fig. 23). Moderate class is decreased to low–very low BS classes (<0.04806 m/m) to the eastern side mainly in the central parts of the study area extending from central parts to the outlet of many Watersheds (Fig. 23) which doubles the possibilities of the RWH. The possibility of RWH is higher in gentle or medium-sloped basins parts. This layer was assigned a weight of 12.5 in the WSPM (Table 6).

– Drainage Density (Dd)

The Dd was classified into five classes and were ordered as: >1.244 , 1.243 – 1.147 , 1.146 – 1.026 , 1.025 – 0.8782 ,

Fig. 23 The BS thematic layer used in the WSPM

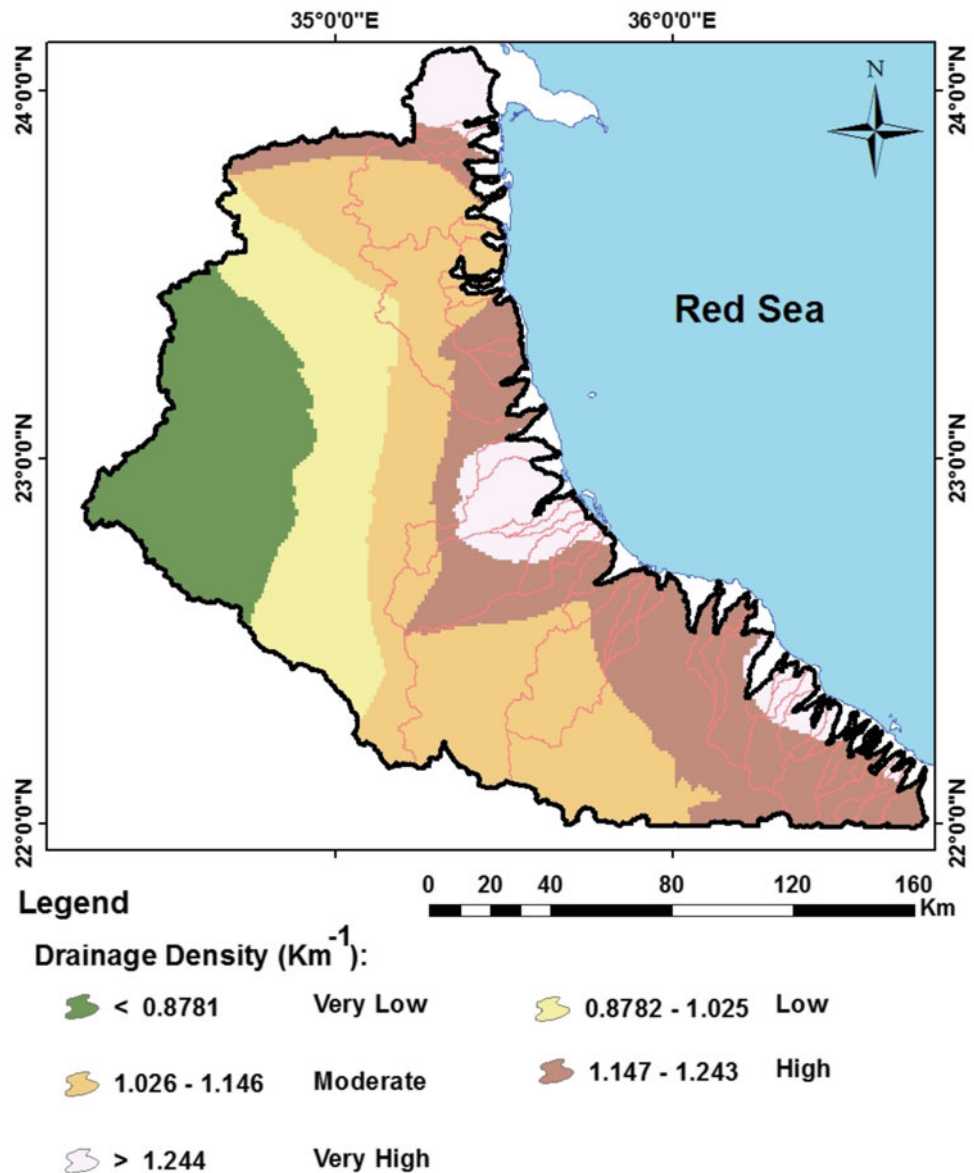


and $<0.8781 \text{ km}^{-1}$ for the very high, high, moderate, low, and very low potential for the RWH, respectively (Table 5; Fig. 24). The general decrease in the Dd values due to the western parts (watershed upstream areas). The thematic map of Dd arranged the Dd classes from very low, low, moderate, high, and very high, respectively, from west to east parts of the study area (Fig. 24). It is also observed that there are many watersheds in the eastern side of the study area are totally covered by high–very high Dd classes as in Abu Dabaa, Baranis, Kalalat, Amrawi, Ibib 2, Shelal, Ehqloqe, Embrest, Egway, Marsa Shelal, Oteib, and Otemat Watersheds (Fig. 24). This layer had been assigned a weight of 12.5 in the WSPM (Table 6).

– Basin Length (BL)

The BL is defined as the distance which cut the basin into two similar parts (Horton 1945). The longer the BL the lower the chances that such a basin will be flooded; this is because, the longer the basin, the lower its slope, and hence the higher the possibilities for the RWH. The longer basins in the study area (High–very high BL classes; $>117.6 \text{ km}$) are represented only by Hodein Watershed mainly in its central and upstream parts (Fig. 25). High–very high flowed by moderate BL class and represented by considerable parts of Shaab, Ibib, Miesa, and Deep Kraf watersheds. The general decrease in BL is due to the east parts of the study

Fig. 24 The Dd thematic layer used in the WSPM

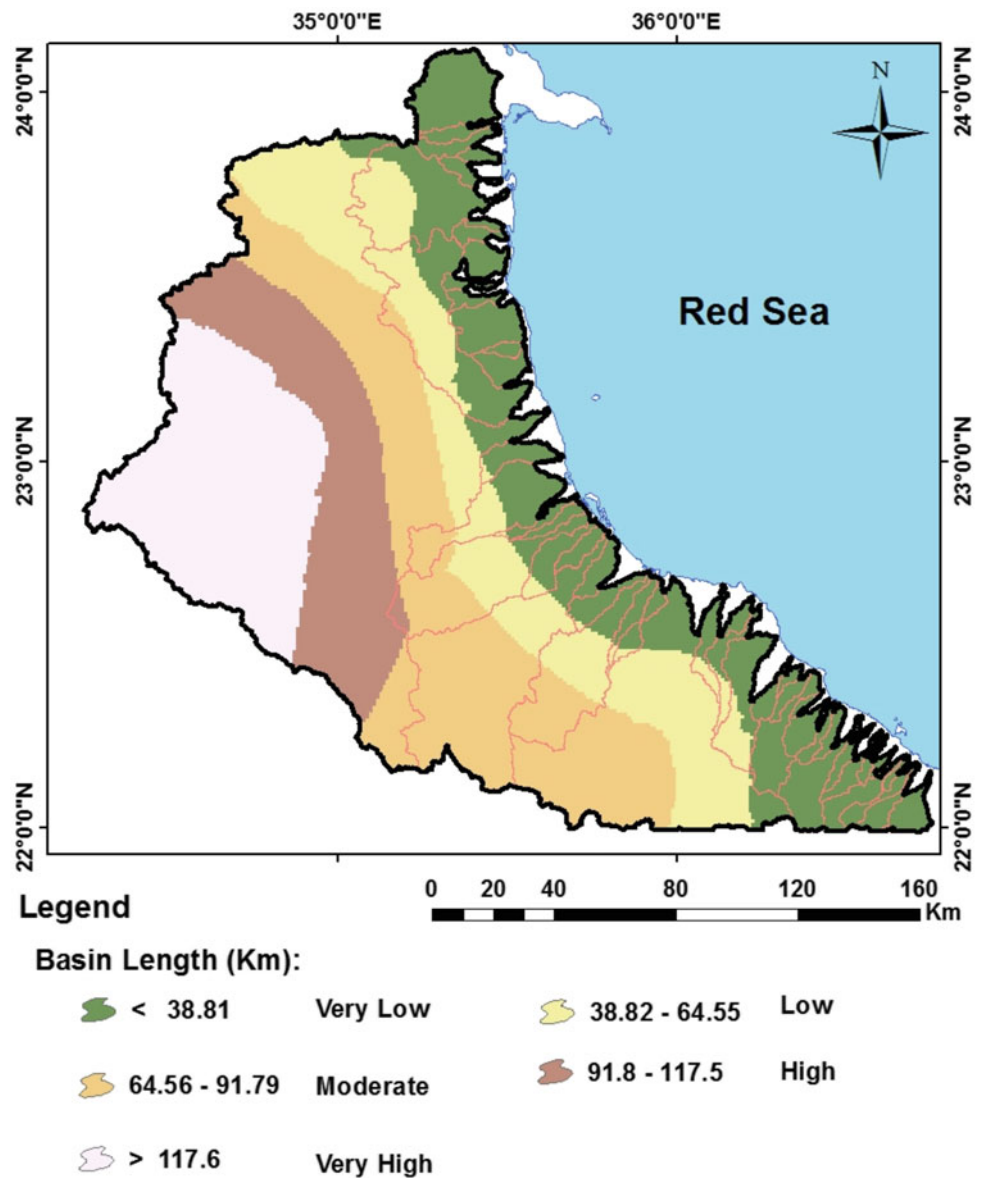


area, whereas the low–very low classes totally covered the micro-watersheds extending along the eastern side in addition to some parts of larger watersheds (Fig. 25). Micro-catchment RWH practices are more successful in shorter BLs (i.e., Abu Dabaa, Baranis, Kalalat, Amrawi, Ibib 2, Shelal, Eghloqe, Embrest, Egway, Marsa Shelal, Oteib, and Otemat Watersheds), whereas the macro-catchment procedures are more applicable in the longer BLs (i.e., Hodein, Ebib, and Miesa Watersheds). This is because, the longer the basin the lower its slope and, hence, the higher the possibilities for the RWH. This layer was assigned a weight of 12.5 in the WSPM (Table 6).

– Basin Area (BA)

The BA is the total area in square kilometers enclosed by the basin boundary (Horton 1945). BA is the most important of all the morphometric parameters controlling the catchment runoff volume and pattern. This is because, the larger the size of the basin the greater the amount of rain it intercepts and the higher the peak discharge that result (Morisawa 1959; Verstappen 1983). Another reason for the high positive correlation between BA and the discharge is the fact that the BA is also highly correlated with some of the other catchment hydromorphometric characteristics, which

Fig. 25 The BL thematic layer used in the WSPM

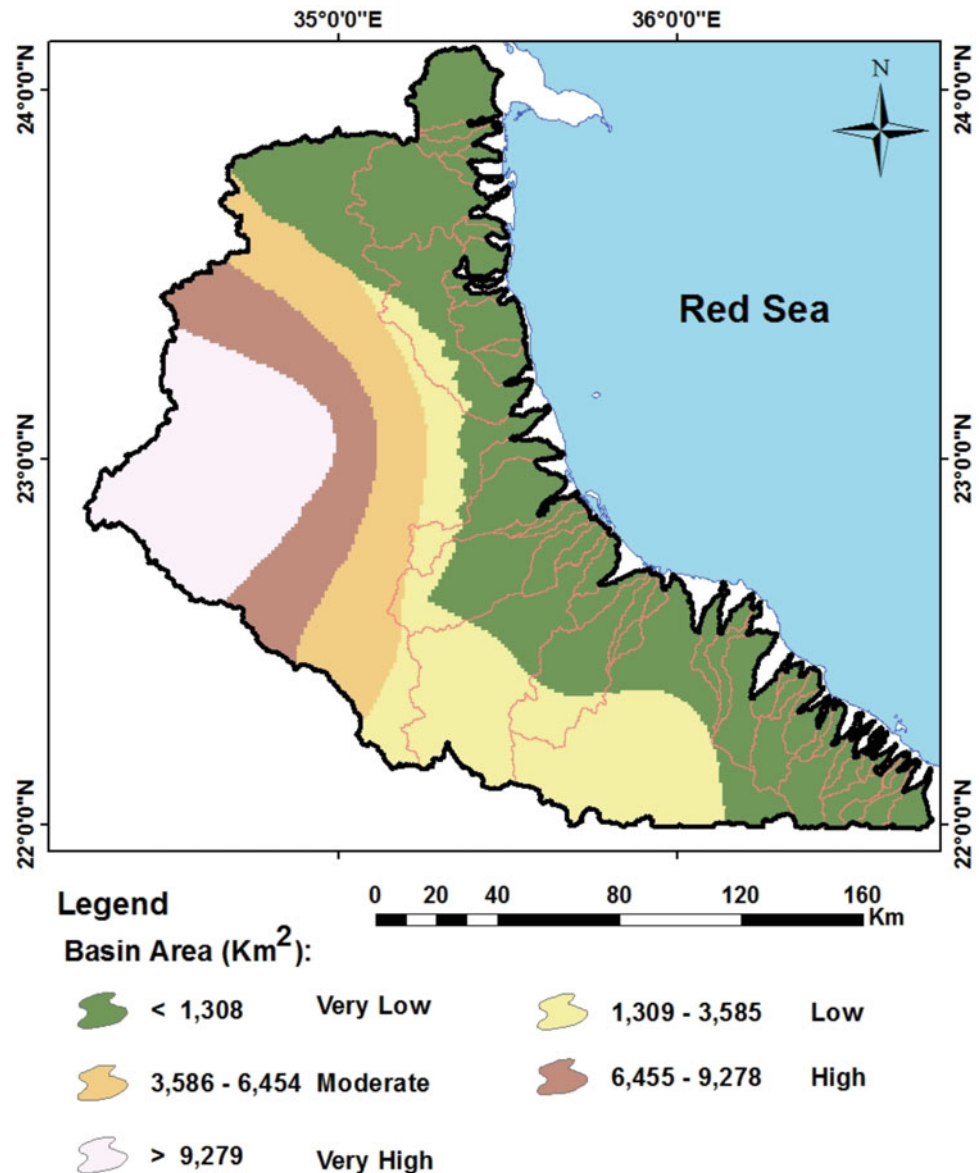


influence runoff, such as BL (i.e., the larger the BA the longer its length), average OFD, and the MFD (Gregory and Walling 1973; Jain and Sinha 2003). A thematic layer of the BA with five classes was generated (Fig. 26). The very high–high BA classes ($>9279 \text{ km}^2$) occur in W. Hodein upstream Watershed. The moderate BA class ($6454\text{--}3586 \text{ km}^2$) is represented by a curved zone in the central part of Hodein Watershed in addition to a very small part of W. Shaab Watershed (Fig. 26). The low–very low classes ($<1308 \text{ km}^2$) are represented by the other parts of the study area, which occur in the eastern and the central parts. This layer was assigned the weight of 12.5 in the WSPM (Table 6).

– Basin Infiltration Number (IF)

The IF is defined as the product of Dd and drainage frequency (Df) (Faniran 1968). The higher the infiltration number the lower will be the infiltration and consequently, higher will be the runoff. This leads to the development of higher Dd. IF gives an idea about the infiltration of a drainage basin. The IF thematic map reflects that most of the study area is represented by moderate IF class (0.7714–0.6022) which are characterized by moderate RWH potentialities and infiltration capabilities. The low–very low IF classes (<0.3803) are represented by the upstream and central parts of W. Hodein Watershed in addition to very small

Fig. 26 The BA thematic layer used in the WSPM



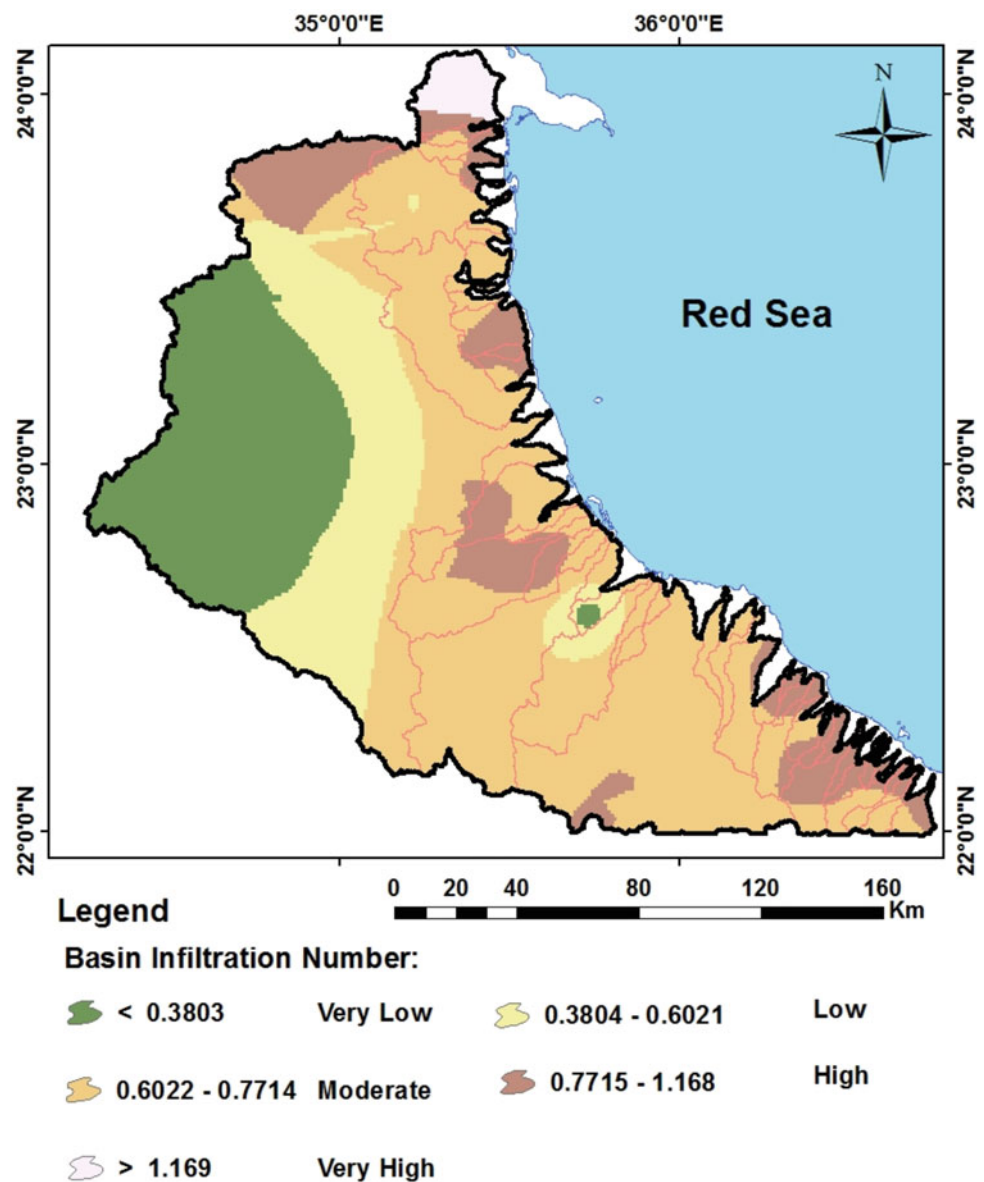
parts of Ibib, Hor, Miesa, and Khedaa Watersheds (Fig. 27). The very high IF class only occurs in Abu Dbaa watershed at the NE part. High IF class is distributed as scattered areas in northern, central, and southern parts (Fig. 27). This layer was assigned a weight of 12.5 in the WSPM (Table 6).

– Maximum Flow Distance (MFD)

The MFD of a basin includes both overland and channel flow (Horton 1945). It is the maximum length of the water's path in the drainage basin in kilometers. This factor is important in determining the RWH capability of a drainage

basin, as the higher the MFD the higher the RWH possibilities, and vice versa. The high–very high MFD classes (>247.2 km) occur mainly in central and upstream parts of W. Hodein Watershed. The moderate MFD class (175–112.3 km) occurs as longitudinal zone extending from north to south through the central and SW parts of the study area occupying central and upstream parts of Hodein, Rahaba, Sfeirah, Shaab, Ibib, Miesa, and Deep Kraf Watersheds. The moderate MFD class if decreased further to the eastern strip of the study area reaching to very low class (<61.02 km) covering mostly micro-watersheds close to Red Sea coast and downstream parts of larger watersheds (Fig. 28).

Fig. 27 The IF thematic layer used in the WSPM



4.3 Weighted Spatial Probability Models (WSPMs) for RWH in Halaib–Shalatin Area

The MCDSS (Malczewski 1996, 2006) represented by the previously discussed eight thematic layers, were ranked according to their magnitude of contribution to the RWH, thus they were categorized from the very high to very low contribution, and the same classes were used in the RWH potentiality mapping.

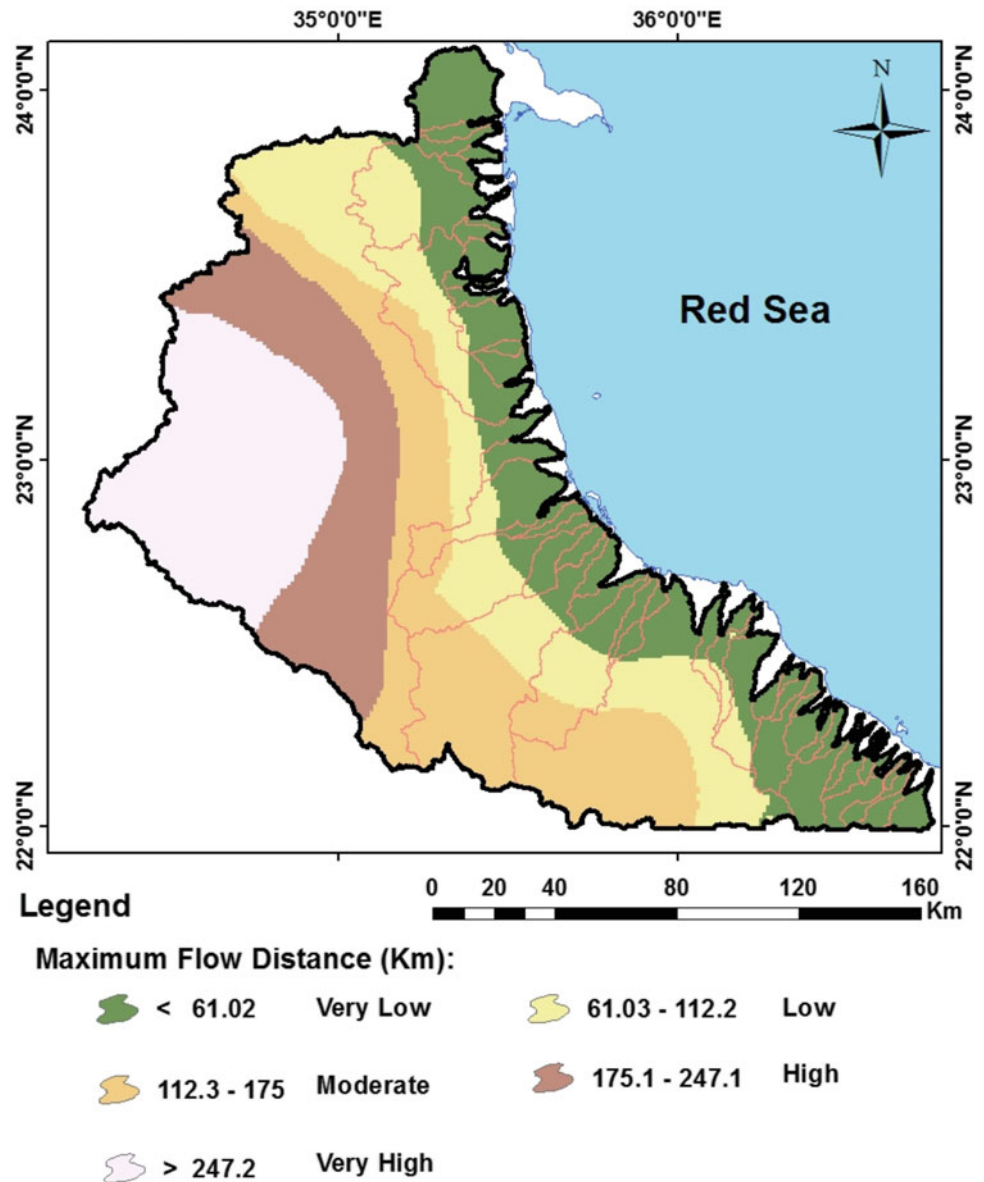
Three weighted spatial probability models' scenarios (WSPM) were generated, where the model was running three times by using criteria of: (1) Equal weights, (2) Weights proposed by the authors' judgments, and (3) Weights justified by the sensitivity analysis. The model's running implied the integration of all criteria as thematic

layers in the WSPM. Accordingly, an output map for each scenario with several classes indicating the categories of RWH potentiality (i.e., very high, high, moderate, low, and very low) was obtained.

4.3.1 WSPM's Scenario I (Equal Weighting of Criteria) for Halaib–Shalatin Area

In this model's scenario, the previously discussed criteria had been proposed to have the same magnitude of contribution in the RWH potentiality mapping (Table 6; Fig. 29). However, some criteria work positively, while others work negatively in the RWH potentiality mapping. For example, the BS criterion works negatively in the RWH potentiality mapping, whereas the VAF, OFD, BA, BL, Dd, and MFD, work positively. The weights and rates of the previously

Fig. 28 The MFD thematic layer used in the WSPM



discussed MCDSS were assumed and optimized here to have equal weights of contribution in the RWH potentiality mapping (Table 6), where the integrated criteria were given an equal weight of 12.5% with a summation of 100% for all data themes. After proposing criteria weights, categorization was applied to each of the five classes among each criterion. For example, the classes were graded from I (very high potentiality) up to V (very low potentiality) in the RWH potentiality mapping (Table 6; Fig. 29). Taking 100% as the maximum value for the rank, thus for the five classes, ranks will be classified as: 100–80, 80–60, 60–40, 40–20, and 20–0%, respectively. Consequently, the average ranking for each class will be 0.90, 0.70, 0.50, 0.30, and 0.10% for classes from I to V, respectively (Table 6).

The degree of effectiveness (E) for each thematic layer was calculated by multiplying the criterion weight (W_c) with the criterion rank (R_c). For example, if the weight of VAF equals to 12.5% and this is multiplied by the average rank of 90 (for class I), the E will be 11.25 (Eq. 3).

$$E = W_c \times R_f = 0.125 \times 90 = 11.25 \quad (3)$$

According to this method of data manipulation, the assessment of the effectiveness of each decision criterion provides a comparative analysis among the different thematic layers. Therefore, it is clear from Table 6 that the class I in all data themes (i.e., $E = 11.25$) represent the most effective criteria in performing the RWH potentiality mapping, compared to the least effective class V (i.e., $E = 1.25$)

Fig. 29 WSPM's Scenario I map showing the potential areas for the RWH in HS area

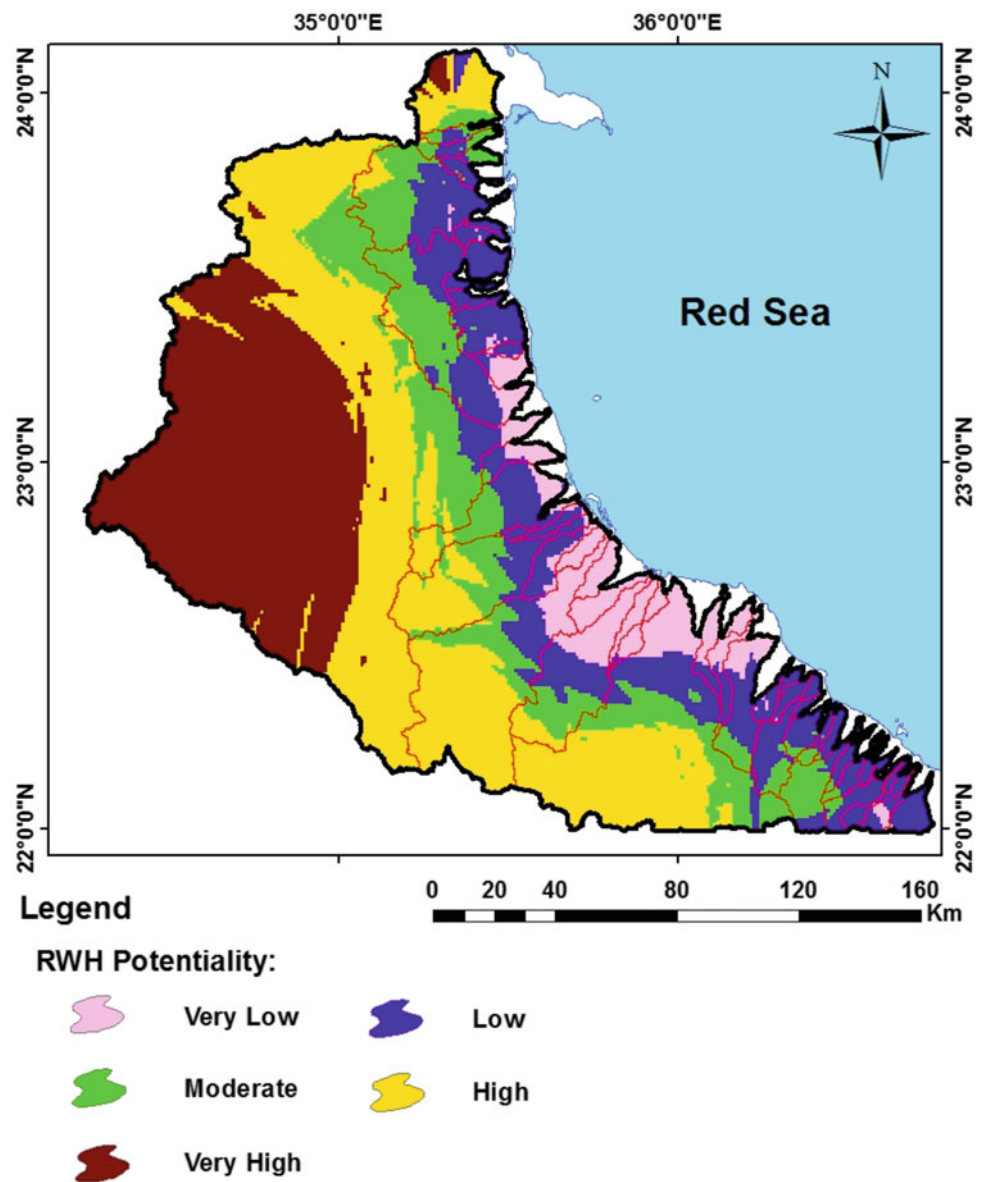


Table 7 Areas of RWH potentiality classes (WSPM Scenario I) in HS area

RWH potentiality map					
RWH potentiality class	Very low	Low	Moderate	High	Very high
Area (km ²)	2091.55	4841.74	4207.38	7989.81	6261.96
Area (in % relative to the total studied area) (Total study area: 25392.4 km ²)	8.24	19.07	16.57	31.47	24.66

in all criteria. Therefore, an arithmetic overlay approach was built within the ArcGIS 10.1[©] Spatial Analyst Model Builder to conduct the WSPM. The overlay processing manipulates both continuous and discrete grid layers and the derived data are continuous grid data layer. Thus, the WSPM output map for the RWH potentiality with five classes

ranging from the very low to very high potentiality was produced (Fig. 29).

The percentage of the spatial distribution of the resulting RWH potentiality classes to the total study area of the study area: 8.24 (very low), 19.07 (low), 16.57 (moderate), 31.47 (high), and 24.66% (very high) (Fig. 29; Table 7).

From the WSPM's map, it can be concluded that most of studied area is of high to very high potential for the RWH (i.e., 31.47 and 24.66% of total study area, respectively), especially, in its up streams areas of larger watersheds in the central and western parts (i.e., Hodein, Sfeirah, Ibib, Shaab, Miesa, Deep Kraf, Khedaa, and Abu Dabaa Watersheds. RWH potentiality is moderate (16.57%), which is noticeably decreasing to low and very low RWH (19.07 and 8.24%, respectively) in the downstream eastern parts of the study area (Fig. 29; Table 7).

4.3.2 WSPM's Scenario II (Weights Assigned by the Authors' Experience and/or Judgment) in Halaib–Shalatin Area

Based on the authors' experience, the eight thematic layers of the WSPM had been overlain by the ArcGIS 10.1[©] within the Spatial Analyst Model Builder for performing the WSPM taking the new assigned weights as: average OFD (17%), VAF (16%), BS (12%), Dd (12%), BL (12%), BA (11%), MFD (10%), and IF (10%) (Table 8). According to this scenario, the E for each thematic layer was calculated by

Eq. 1, for the eight criteria. For example, if the weight of VAF equals 16% and this is multiplied by the average rank of 90 (for class I), the E will be 14.4, whereas the least effective class V has a E of 1.6 (Table 8).

The resulted WSPM's map has five classes ranging from the very low to the very high potentiality for the RWH. The spatial distribution of these classes relative to the total studied area was: 8.09% for the very low, 16.09% for the low, 18.27% for the moderate, 33.10% high, and 24.44% for the very high potentiality for the RWH (Fig. 30; Table 9). It is observed from the resulted map that the promising watersheds for the RWH were represented by watersheds of Hodein, Sfeirah, Ibib, Shaab, Miesa, Deep Kraf, Khedaa, and Abu Dabaa, which characterized by high–very high RWH potentiality classes (about 59% of total studied area), especially in its upstream and central parts (Fig. 30). High–very high RWH classes generally decreased to the eastern side in the direction of Red Sea coast, where it followed by moderate RWH class reaching to low–very low classes which covered mainly most of the micro-watersheds.

Table 8 The WSPM scenario II using an unequal weighting of criteria based on authors' judgment; ranks and degree of effectiveness of themes used in the RWH potentiality mapping

Thematic layer (Criterion)	RWH potentiality class	Average rate (Rank) (R_c)	Weight (W_c)	Degree of effectiveness (E)
Average volume of annual flood (VAF)	I (Very high)	0.9	16	14.4
	II (High)	0.7		11.2
	III (Moderate)	0.5		8
	IV (Low)	0.3		4.8
	V (Very low)	0.1		1.6
Average overland flow distance (OFD)	I (Very high)	0.9	17	15.3
	II (High)	0.7		11.9
	III (Moderate)	0.5		8.5
	IV (Low)	0.3		5.1
	V (Very low)	0.1		1.7
Maximum Flow Distance (MFD)	I (Very high)	0.9	10	9
	II (High)	0.7		7
	III (Moderate)	0.5		5
	IV (Low)	0.3		3
	V (Very low)	0.1		1
Basin infiltration number (IF)	I (Very high)	0.9	10	9
	II (High)	0.7		7
	III (Moderate)	0.5		5
	IV (Low)	0.3		3
	V (Very low)	0.1		1
Drainage density (Dd)	I (Very high)	0.9	12	10.8
	II (High)	0.7		8.4
	III (Moderate)	0.5		6
	IV (Low)	0.3		3.6
	V (Very low)	0.1		1.2
Basin area (BA)	I (Very high)	0.9	11	9.9
	II (High)	0.7		7.7
	III (Moderate)	0.5		5.5

(continued)

Table 8 (continued)

Thematic layer (Criterion)	RWH potentiality class	Average rate (Rank) (R_c)	Weight (W_c)	Degree of effectiveness (E)
Basin slope (BS)	IV (Low)	0.3	12	3.3
	V (Very low)	0.1		1.1
	I (Very high)	0.9		10.8
	II (High)	0.7		8.4
	III (Moderate)	0.5		6
Basin length (BL)	IV (Low)	0.3	12	3.6
	V (Very low)	0.1		1.2
	I (Very high)	0.9		10.8
	II (High)	0.7		8.4
	III (Moderate)	0.5		6
	IV (Low)	0.3		3.6
	V (Very low)	0.1		1.2
	I (Very high)	0.9		10.8
	II (High)	0.7		8.4
	III (Moderate)	0.5		6

Fig. 30 WSPM's Scenario II map showing the potential areas for the RWH in HS area

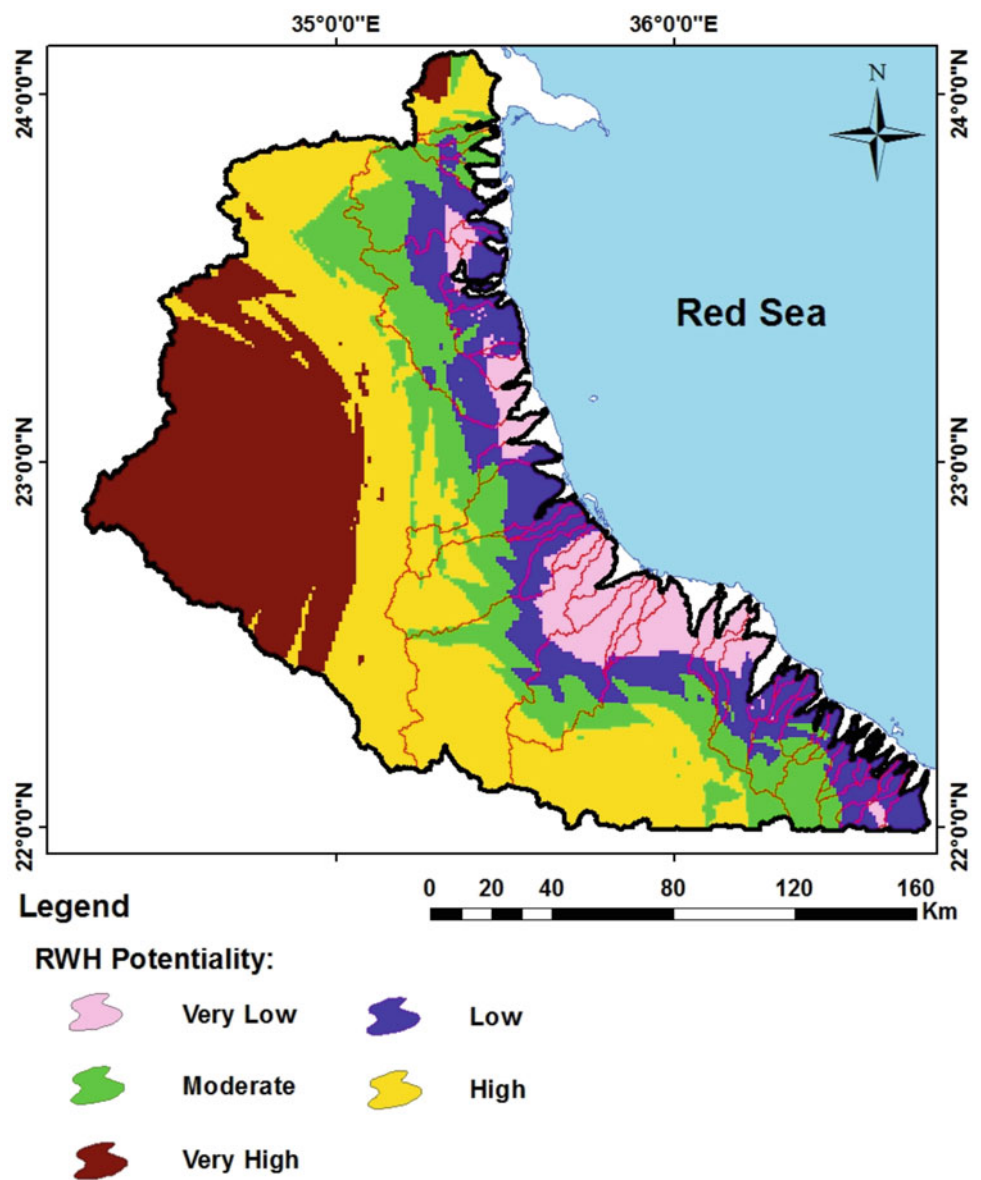


Table 9 Areas of RWH potentiality classes (WSPM Scenario II) in HS area

RWH potentiality map					
RWH potentiality class	Very low	Low	Moderate	High	Very high
Area (km ²)	2055.03	4085.24	4639.91	8405.47	6206.81
Area (in % relative to the total studied area) (Total study area: 25392.4 km ²)	8.09	16.09	18.27	33.10	24.44

4.3.3 WSPM's Scenario III (Justified Weights by the Sensitivity Analysis) in Halaib-Shalatin area

In the third scenario, a sensitivity analysis (Van Griensven et al. 2006) was performed to justify the weights of the WSPM's criteria in order to attain a more justified or optimum RWH potential areas in the study area.

However, to justify the WSPM's weights and results, we have to take all the scenarios as alternatives with different proposals for assigning weights of the criteria. The WSPM's sensitivity analysis for the determination of RWH potentiality was performed through three steps as follows:

- The first step (Scenario I) involves assuming that all the WSPM's eight thematic layers or criteria have the same magnitude of contribution or weights in the RWH potentiality mapping. In this scenario, all criteria were assigned an equal weight of 12.5% (equal effect).
- The second step involves the authors' experience or judgment to assess the weight of each criterion and/or also taking into consideration the experience gained from the similar literatures (i.e., Adiga and Krishna Murthy 2000; Javed et al. 2009; Montgomery and Dietrich 1989; Ponce and Hawkins 1996; Elewa and Qaddah 2011; Elewa et al. 2012, 2013, 2014).
- The third step was to determine the RWH potentiality by applying the sensitivity analysis to justify the weights of decisive criteria. The RWH potentiality assessment of a site involves the necessity to assess the reliability of the parameters used in the prioritization. A small perturbation in the decision weights may have a significant impact on the rank ordering of the criteria, which subsequently may ultimately alter the best choice and the model results. However, the uncertainties associated with MCDSS techniques are inevitable and the model outcomes are open to multiple types of uncertainty. In each WSPM's running operation, seven parameters had been kept with equal weights of 10%, while assigning only one parameter with the remaining 30% (Figs. 31, 32, 33, 34, 35, 36, 37 and 38).

The previously discussed WSPM's running practice is necessary to apply the variance-based global sensitivity analysis (GSA) or what is called the ANOVA (ANalysis Of VAriance), which subdivides the variability and apportions it to the uncertain inputs (Ha et al. 2012; Feizizadeh et al. 2004). GSA is based on perturbations of the entire parameter space, where input factors are examined both individually and in combination (Ligmann-Zielinska 2013). Variance-based GSA has been used in the present work, where this approach is identified as one of the most appropriate techniques for justifying the factors' weights of the WSPM (Saltelli et al. 2000; Saisana et al. 2005). The goal of variance-based GSA is to quantitatively determine the weights that have the most influence on model output, in this instance, on the RWH categorization computed for each cell of the watershed area by the decisive factors. With this method we aim to generate two sensitivity measures: first-order (S) and total effect (ST) sensitivity index. The importance of a given input factor (X_i) can be measured via the so-called sensitivity index, which is defined as the fractional contribution to the model output variance due to the uncertainty in (X_i). For (k) independent input factors, the sensitivity indices can be computed by using the following decomposition formula for the total output variance ($V(Y)$) of the output (Y) (Saisana et al. 2005) (Eqs. 4–6):

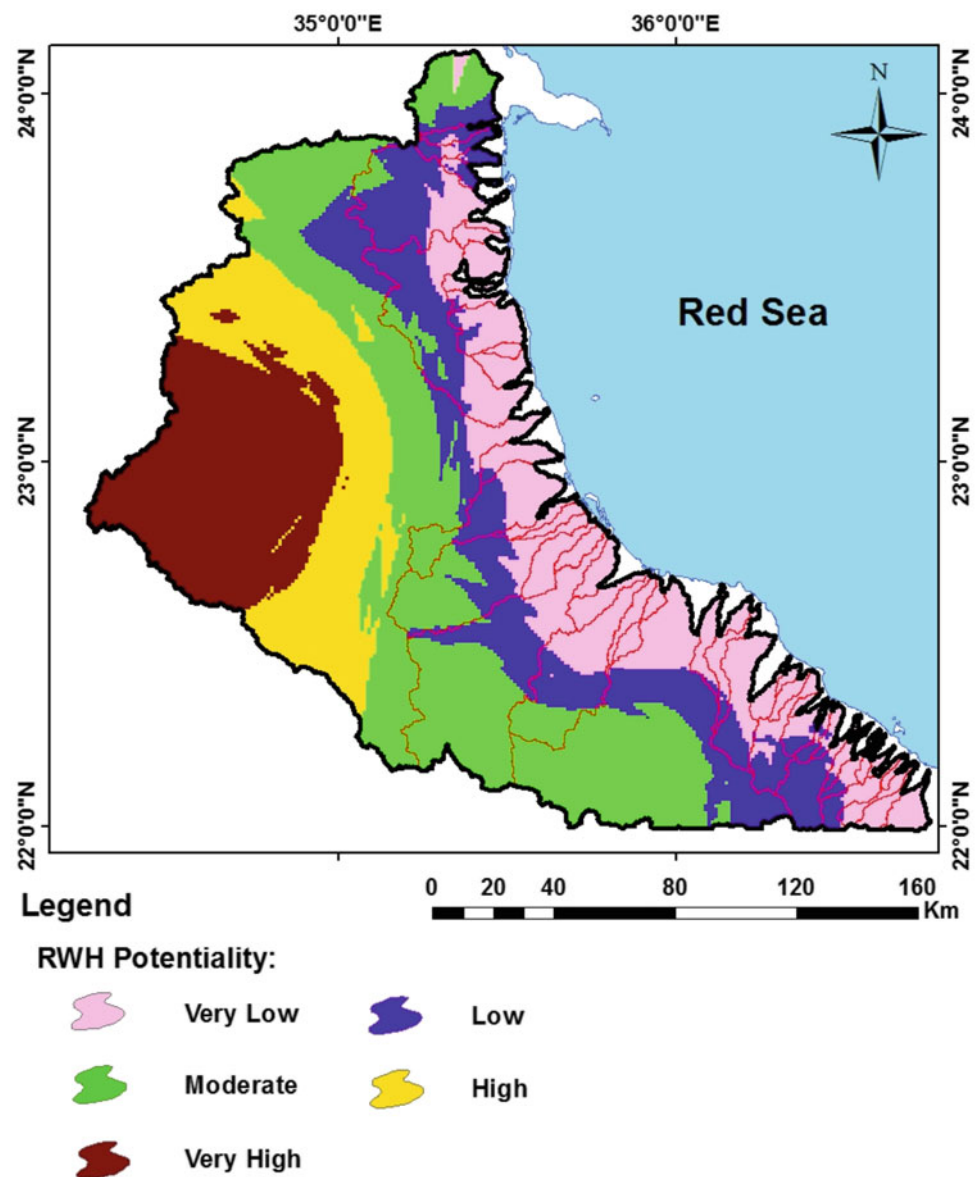
$$V(Y) = \sum_i V_i + \sum_i \sum_{j>i} V_{ij} + \dots + V_{12,\dots,k} \quad (4)$$

$$V_i = V_{xi}\{E_{x-i}(Y|X_i)\} \quad (5)$$

$$V_{ij} = V_{xij}\{E_{x-ij}(Y|X_i, X_j)\} - V_{xi}\{E_{x-i}(Y|X_i)\} - V_{xj}\{E_{x-j}(Y|X_j)\} \quad (6)$$

A partial variance (V_i) represents the repeated variation of a single criterion (i) (i.e., one of the eight model criteria) that affects the other model criteria, which constitutes the inputs of the WSPM. In other words, one of the WSPM eight parameters is changed, while the rest remain constant. However, in Eq. 4, higher order effects ($V_{1, 2, p}$) are combined effect for two or more inputs. The partial effects

Fig. 31 WSPM map showing the potential areas for the RWH (unequal weights: 10% for each thematic layer except the BA with 30%)



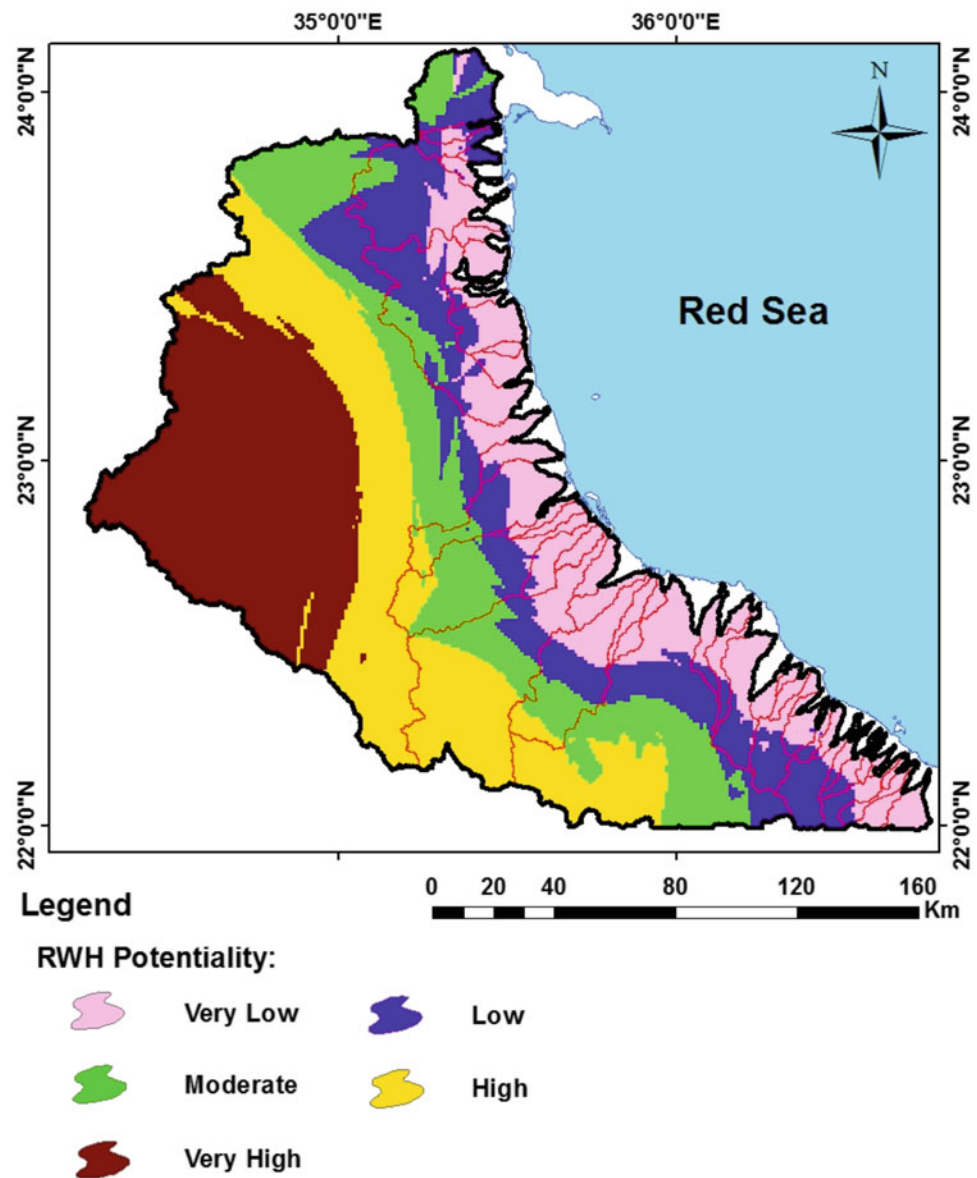
can be calculated with special sampling schemes that are often computationally demanding (Saltelli et al. 2000). Accordingly, the effect of each model criterion was calculated by comparing its effect on the summation of classes that have high and very high RWH potentiality, in case that the criterion was assigned a unique weight value of 30% compared to the first scenario of equal model weights.

Figure 39 shows the classes of the high–very high RWH potentiality and their summation area (green columns),

which resulted from scenario I (equal weighting) and the Scenario III, in which all criteria have equal weights of 10% unless only one criterion with a weight of 30%.

Figure 40 represents the percentage of variance in the total area of high and very high potentiality classes for the RWH, which had been resulted from scenario III comparable to the scenario I. So, it could be noticed that the length of overland flow has a higher effect value, followed by volume of annual runoff and the smallest effect resulted from MFD and IF.

Fig. 32 WSPM map showing the potential areas for the RWH (unequal weights: 10% for each thematic layer except the BL with 30%)



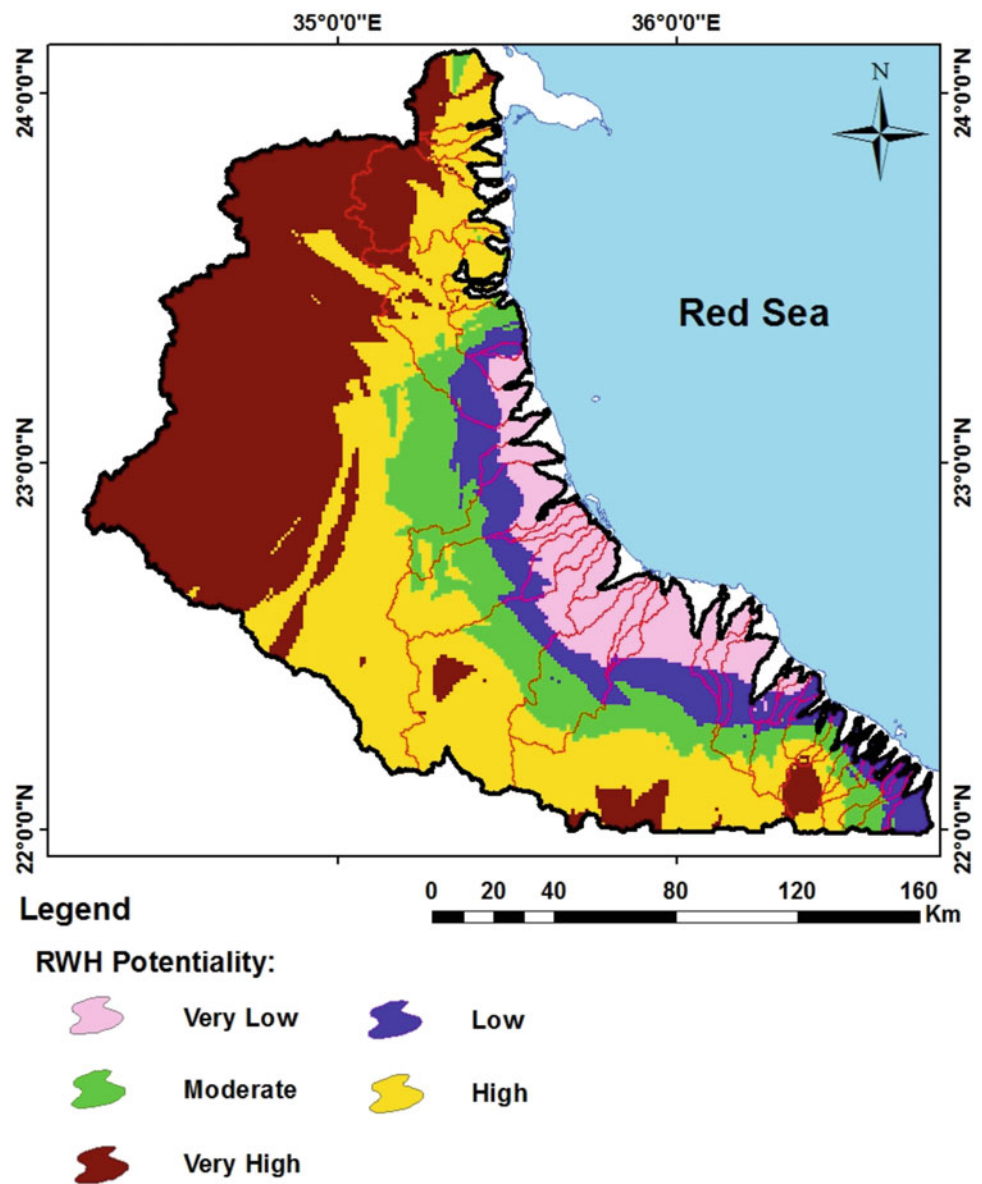
From Fig. 40 and Table 10, the summation of all variance ratios in the high–very high RWH potentiality classes in scenario III for each criterion with respect to their areas in scenario I is 272.96%.

Accordingly, the justified weight of each criterion was calculated by dividing the variance ratio shown in Fig. 40 and Table 10 by the sum of all variance ratios. For example, the justified or optimum weight of the length of over land

flow distance (OFD) could be obtained by dividing the variance ratio (60%) by the summation of all variance ratios (272.96), which is equal to 21.99% (Table 10).

Depending on the justified or optimum weights of the thematic layers, another run for the WSPM was carried out taking into consideration these new weights as: OFD (21.99%), VAF (12.54%), BS (7.65%), Dd (21.99%), BL (7%), BA (17%), IF (1.95%), and MFD (9.88%).

Fig. 33 WSPM map showing the potential areas for the RWH (unequal weights: 10% for each thematic layer except the BS with 30%)



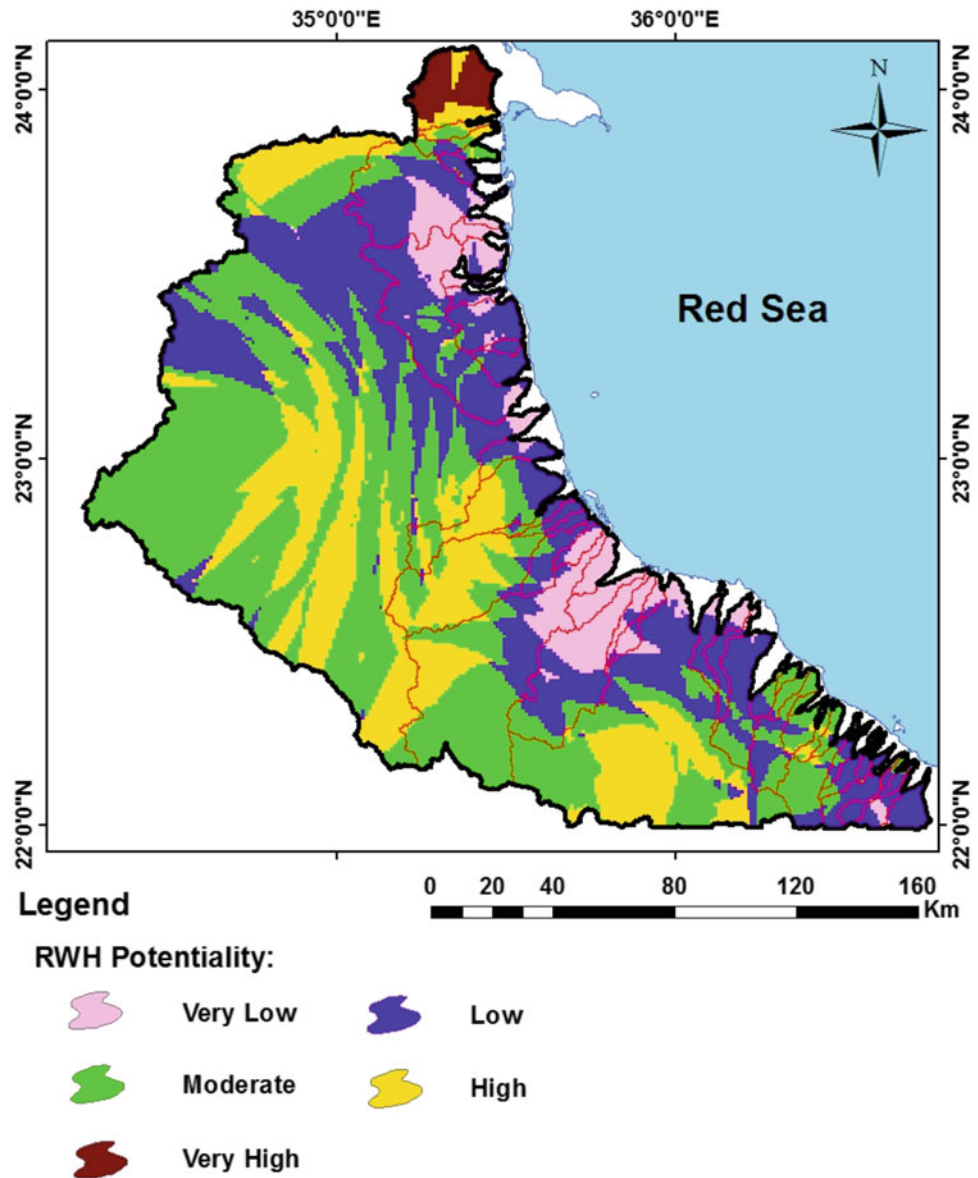
The WSPM output map with five classes ranging from very low to very high potentiality was obtained (Fig. 41). The spatial distribution of these classes relative to the total studied area was: 5.62% for the very low, 18.26% for the low, 28.9% for the moderate, 29.51% for the high, and 17.7% for the very high potentiality for the RWH (Fig. 41; Table 11).

From the justified WSPM's map, it could be concluded that about 47.2% of the study area was represented by high-very high RWH potentiality distributed mainly in larger watersheds at its upstream and central areas (i.e., Hodein,

Sfeirah, Ibib, Shaab, Deep Kraf, and Abu Dabaa watersheds). Moderate RWH potentiality class was represented by 28.91% decreasing to low-very low RWH potentiality classes due to downstream eastern parts.

In conclusion, the WSPM's map of scenario III, which had been constructed by the justified weights, was compared with scenarios I and II, and with the field verification carried out by the research team. Hence, a good correlation among the three scenarios was noticeable, where the moderate, high, and very high classes are dominating the study area. Accordingly, the justified scenario III could be considered as

Fig. 34 WSPM map showing the potential areas for the (unequal weights: 10% for each thematic layer except the Dd with 30%)



a product of high reliability for determining the RWHPotentiality, where it also coincides with the local inhabitants' experience and needs.

4.4 Proposals of Surface Storage Projects

4.4.1 Proposed R.W.H Construction in Halaib–Shalatin Watersheds

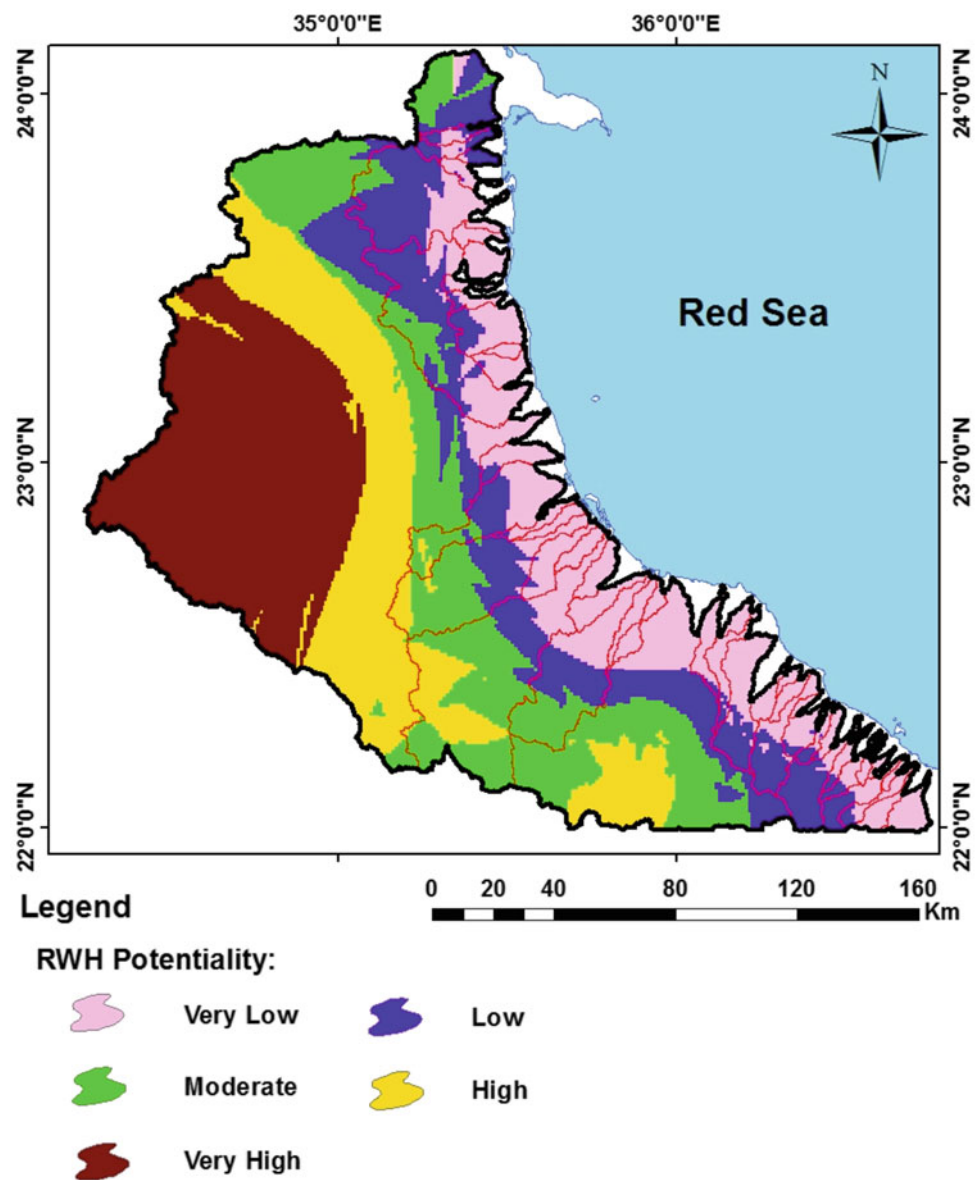
RWH technique in the basins of the studied area of HS on the coast of Red Sea in the SE of Arab rubabic of Egypt was made by the construction of 11 small dams in the main

basins of that area. The water-harvesting system in the study area also comprises a six ground cisterns cross the basins main stream in addition to the infiltrated water into the soil surface. This volume of water would be sufficient for some human activities and drinking water for local habitants of the study area. The locations of these dams and cisterns were shown in Fig. 42 and Tables 12 and 13.

In present work, the criteria used for the site selection of proposed dams include:

Collection of runoff water at the outlets of HS basins, which are characterized by adequate VAF.

Fig. 35 WSPM map showing the potential areas for the RWH (unequal weights: 10% for each thematic layer except the MFD with 30%)



The results of the WSPM for determining RWH potentialities (moderate to very High).

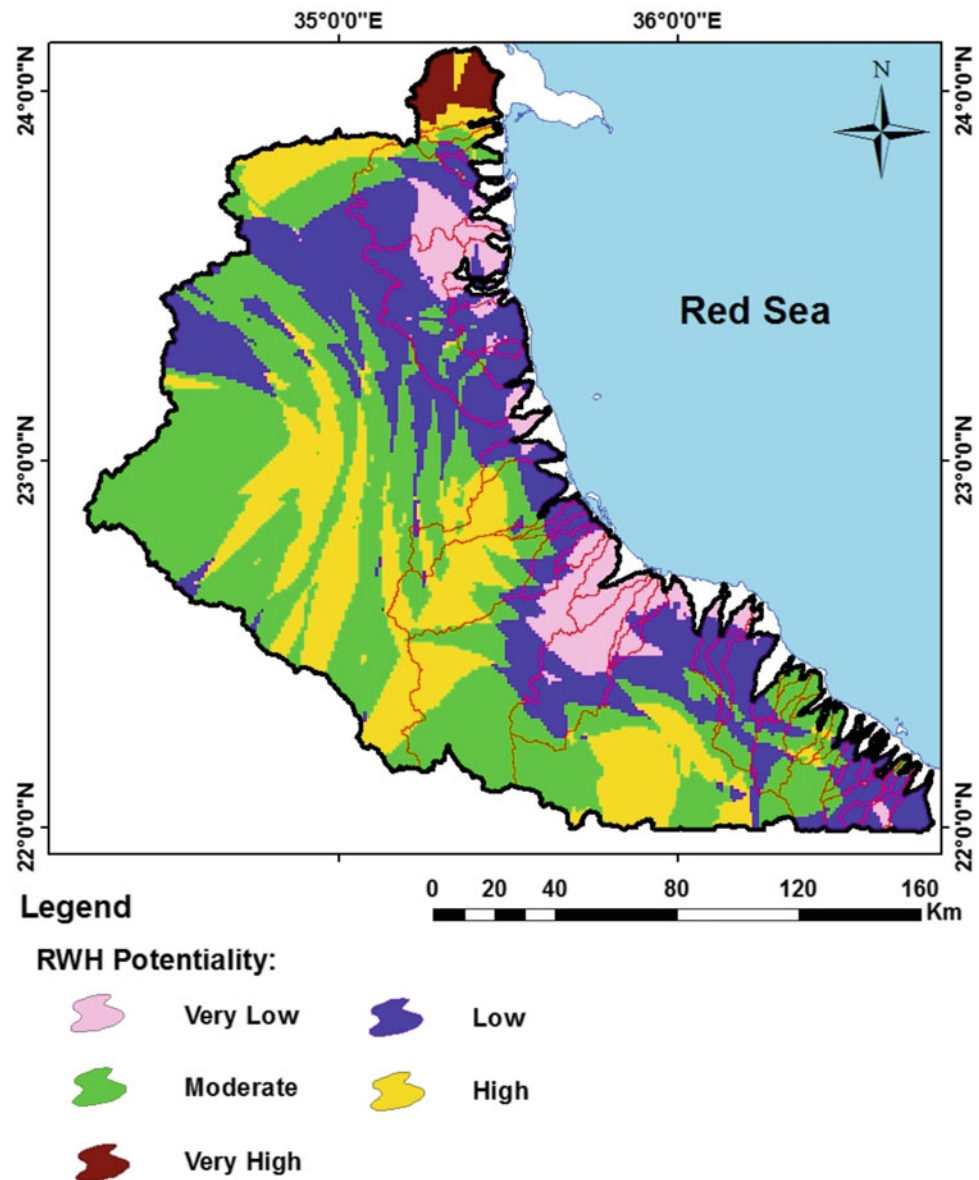
The soil characteristics, which will provide a good environment for agriculture (alluvial or wadi deposits).

Existing land use pattern, which should be outside the present inhabited areas. The harvested runoff water will provide new areas suitable for the settlement of new communities. Surface topography in terms of side slopes, which provide shoulders for the proposed dams to maintain reasonable stability for the installed proposed dams.

The successful design, construction, and operation of a reservoir of a dam project over a full range of loading require a comprehensive site characterization, a detailed design of each feature, and continuous evaluation of the project features during operation (McMahon 2004).

The proposed dams were aligned with respect to their heights to be straight or of the most economical alignment fitting to the topography and founding conditions. Additionally, the dams were designed to satisfy the basic design criteria of crest levels, minimum top widths, in addition to

Fig. 36 WSPM map showing the potential areas for the RWH (unequal weights: 10% for each thematic layer except the OFD with 30%)



the basic technical and administrative requirements of an embankment dam (Greimann 1987), to meet the dam safety requirements (i.e., the dam foundation and abutments stability under all static or dynamic loading conditions, seepage control, freeboard, spillway, and outlet capacity, etc.).

The proposed dams in HS basins are embankment dams of the rock-fill type. The rock-fill dam can be classified into few groups by the configuration of dam sections (Kunitomo 2000). The selected rock-fill type consists of various layers

of rock materials with an inclined core of impervious materials. The main body of the rock-fill dams, which should have a structural resistance against failure, consists of rock-fill shell and transitional zones, core and facing zones, which have a role in minimizing the leakage through the embankment. Filter zone should be provided in any type of rock-fill dams to prevent loss of soil particles by the expected erosion resulting from the seepage flow through the embankment.

Fig. 37 WSPM map showing the potential areas for the RWH (unequal weights: 10% for each thematic layer except the IF with 30%)

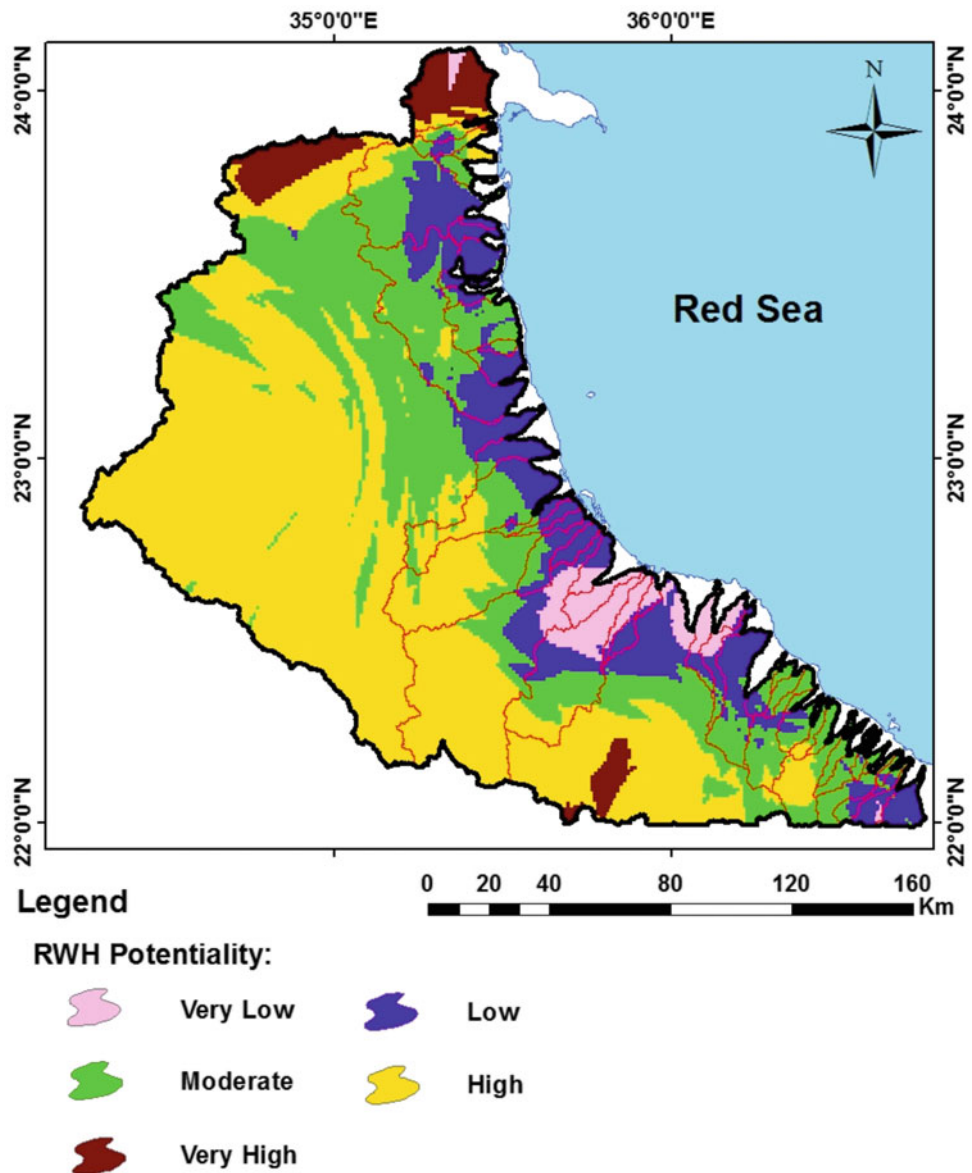


Figure 43 shows a vertical cross section through the proposed dams in HS basin. The proposed dam allows its reserved water flow through a pipe which has an adequate inclination.

The economic feasibility is the major constraints that control the dam construction. Therefore, the types of proposed dams were selected to satisfy the economic feasibility by using, to a large extent, the available local building materials.

With reference to the proposed dams' cross sections illustrated in Fig. 43, it is shown that they consist of different

building materials in layers (i.e., well-faced rock surface using cement mortar, previous layer of rolled fill material, and core layer from impervious rolled fill material). The cross sections of dams were designed according to the dam layout and topographical conditions with respect to the dam heights throughout each cross section.

Construction Stages of Proposed Dams

Upon beginning the construction stages of dams, additional detailed work is necessary, which includes:

Fig. 38 WSPM map showing the potential areas for the RWH (unequal weights: 10% for each thematic layer except the VAF with 30%)

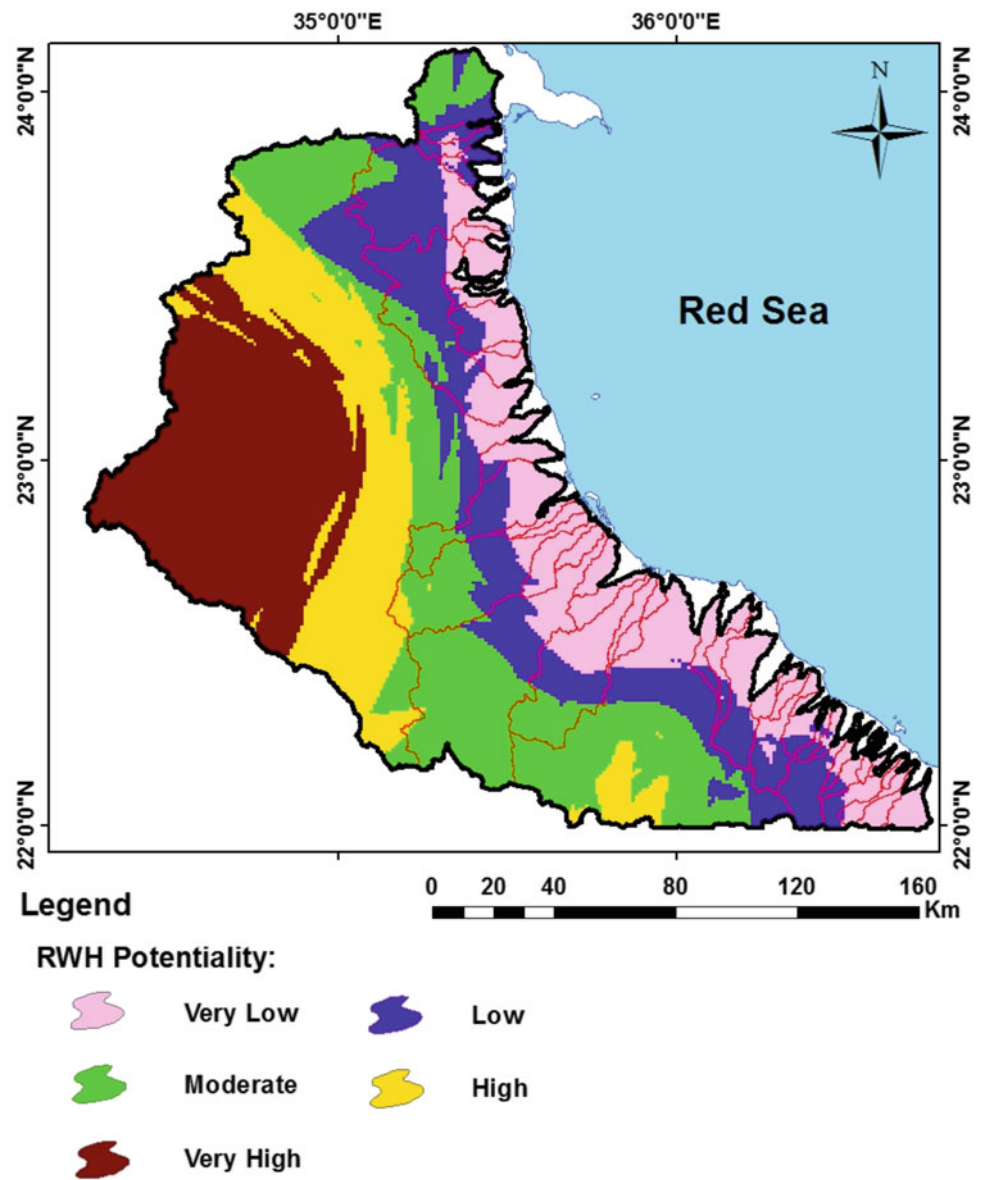
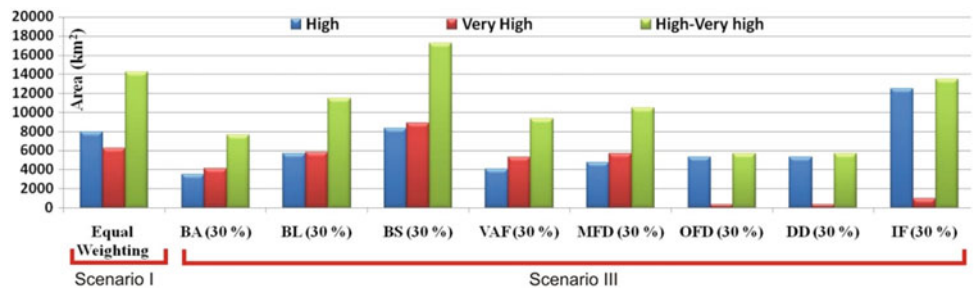


Fig. 39 Areas (in km²) of the high–very high RWH potentiality classes and their summation in the two WSPM scenarios in HS area



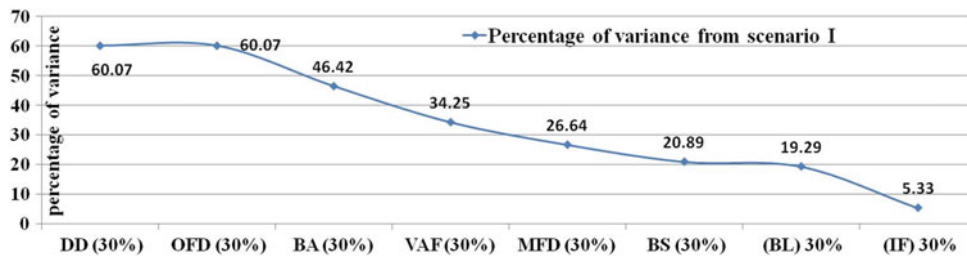


Fig. 40 A graph indicating the variance ratios of the high–very high classes in scenario III with respect to their areas in scenario I in HS area

Table 10 The variance ratios and justified weights of the WSPM's criteria used in the RWH potentiality mapping in HS area

WSPM Criterion	Overland flow distance	Volume of annual flood	Basin slope	Drainage density	Basin length	Basin area	Basin infiltration number	Max. flow distance
Variance ratio (%)	60.07	34.25	20.89	60.07	19.29	46.42	5.33	26.64
Justified weight (%)	21.99	12.54	7.65	21.99	7	17	1.95	9.88

Complete Design and Site Investigations:

Data collection (i.e., geotechnical works).

Selection of construction method.

Complete structural design of dams' cross sections and outlets.

Preparation of dam layouts taking into consideration the required facilities (i.e., roads, bridges, etc.).

Site Preparation:

Validation of dams' layouts and design details with the actual in situ conditions and locations.

Preparation of dams' foundations.

Fulfilling the compaction requirements of the base soil.

Follow-up Stages:

Construction of different structural elements of water outlets, pipe instalment, inlets and outlets of pipes.

Construction of different dam layers according to the details of cross sections.

Smoothen and finishing the surface of the dam with a layer of cement mortar and construction of different dam layers according to the details of cross sections.

Smoothen and finishing the surface of the dam with a layer of cement mortar and allocating the road pathways in the vicinity of the reservoirs.

The proposed six ground cisterns cross the basins will store yearly storage of 3,000 m³. The location of these cisterns was shown in Table 13 and Fig. 42. Also the proposed cisterns will increase the protection from the dangerous effects of flooding on the Red Sea coastal road.

Figures 44 and 45 show a typical cross section in the elevation view and complete plan view for the proposed ground cisterns, respectively. These cisterns have a storage capacity of 500 m³ for each, where it consists of 8-m-long rectangular side and storage height of 4 m.

5 Land Use Master Plan

5.1 Generalities

All the previously discussed issues about the developmental parameters of HS triangle area constitute a fruitful foundation for constructing an overall Land Use Master Plan (LMP). The objective of this plan is ensuring a sustainable vision for the development of the HS area according to the development capabilities of this area.

Fig. 41 WSPM map based on sensitivity results (scenario 3) showing the potential areas for RWH in HS area

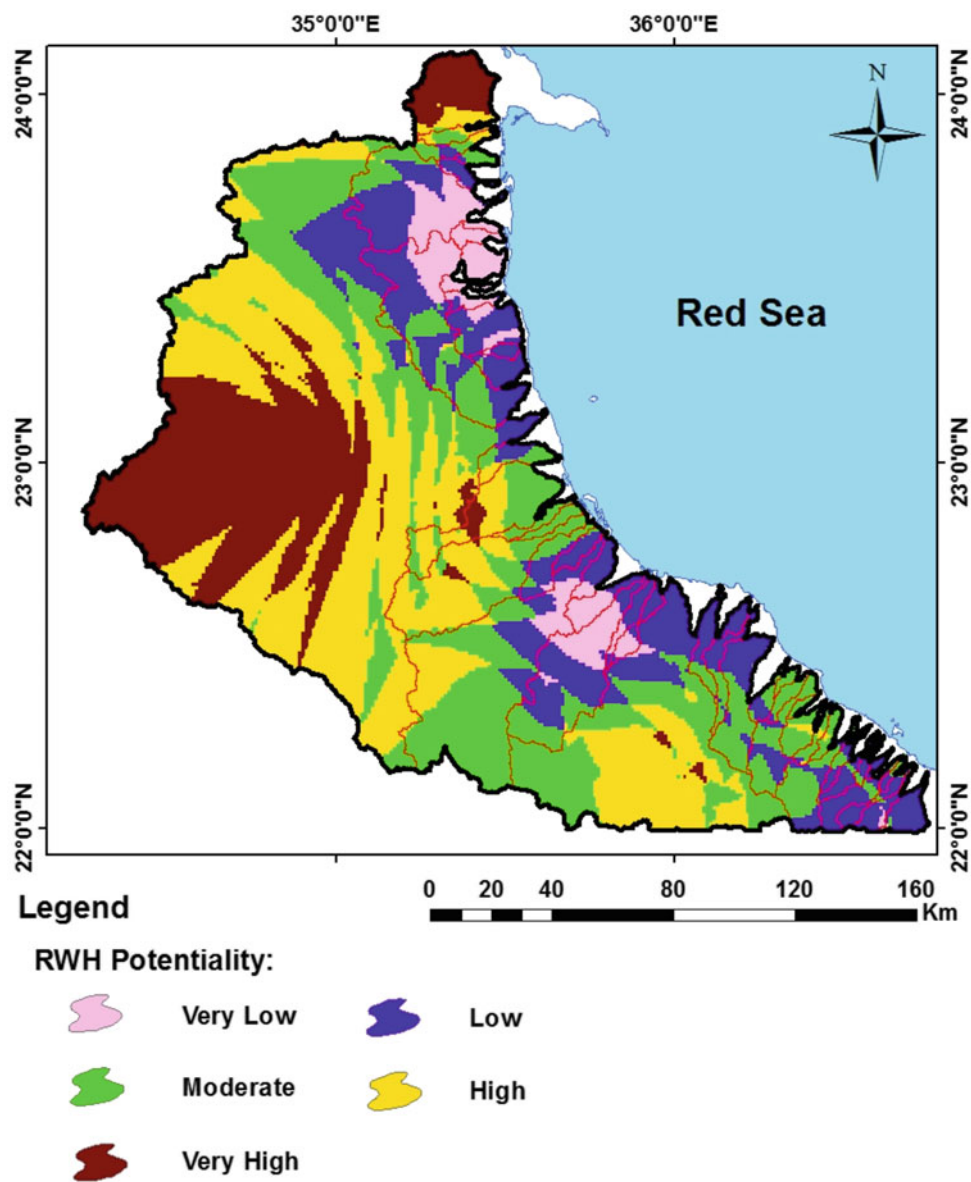


Table 11 Areas of RWH potentiality classes (WSPM Scenario III; based on the results of sensitivity analysis) in HS area

WSPM's map for the RWH potentiality classification					
RWH potentiality class	Very low	Low	Moderate	High	Very high
Area (km ²)	1425.99	4637.7	7340.02	7493.48	4495.276
Area (in % relative to the total studied area) (Total study area: 25392.4 km ²)	5.62	18.26	28.91	29.51	17.70

Fig. 42 Location of proposed dams and cisterns in HS watersheds

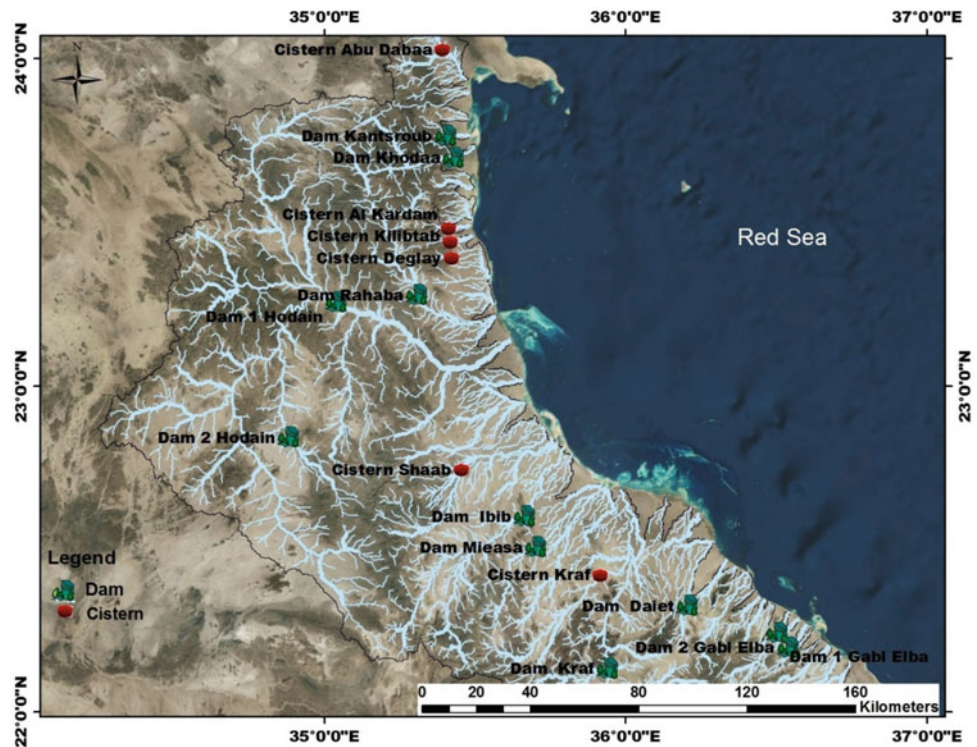


Table 12 Location of proposed dams in HS basins

Dam no.	Location	Lat.	Long.
1	Gabl Elba (1)	22°14'38.56" N	36°30'07.10" E
2	Gabl Elba (2)	22°11' 56.70" N	36°32' 22.87" E
3	Hodain	23°15' 23.87" N	35°02' 24.96" E
4	Hodain (2)	22°50' 43.44" N	34°52' 53.10" E
5	Dalet	22°19' 36.08" N	36°12' 20.79" E
6	Ibib	22°36' 10.71" N	35°39' 55.95" E
7	Kantsroub	23°45' 54.95" N	35°24' 12.90" E
8	Khodaa	23°41' 55.56" N	35°25' 45.26" E
9	Kraf	22°08' 03.34" N	35°56' 25.46" E
10	Mieasa	22°30' 25.69" N	35°42' 09.09" E
11	Rahaba	23°16' 48.72" N	35°18' 23.31" E

Table 13 Location of proposed cisterns in HS basins

Cistern No.	Location	Lat.	Long.
1	Abu Dabaa	24°01'44.55" N	35°23'30.79" E
2	Al kardam	23°29'04.33" N	35°04'43.55" E
3	Deglay	23°26'33.75" N	35°25'09.02" E
4	Kilibtab	23°23'36.11" N	35°25'20.19" E
5	Kraf	22°25'23.33" N	35°54'58.64" E
6	Shaab	22°44'49.40" N	35°27'20.51" E

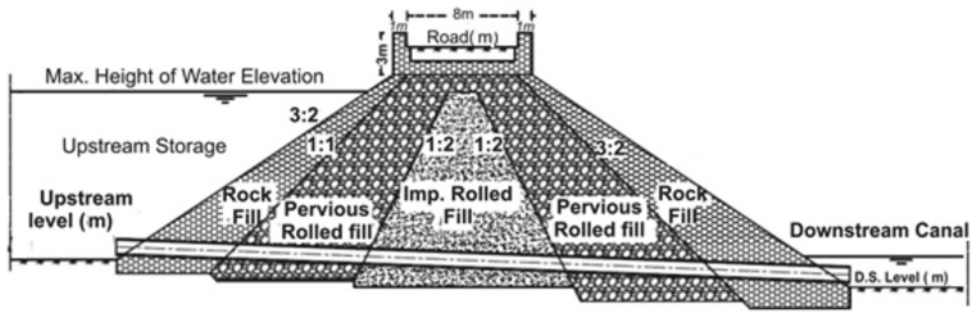


Fig. 43 Typical cross section of the proposed dams in HS basins (Elewa et al. 2013)

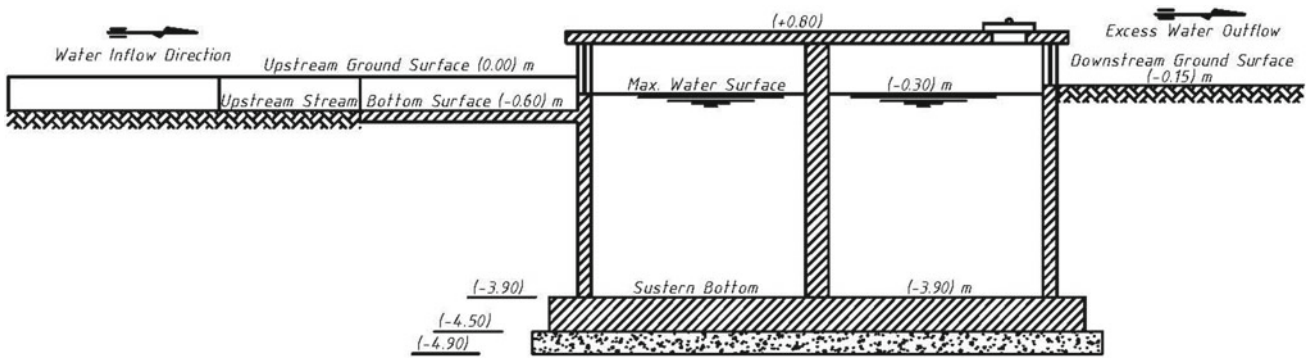


Fig. 44 Typical cross-sectional elevation in proposed cisterns in HS basins

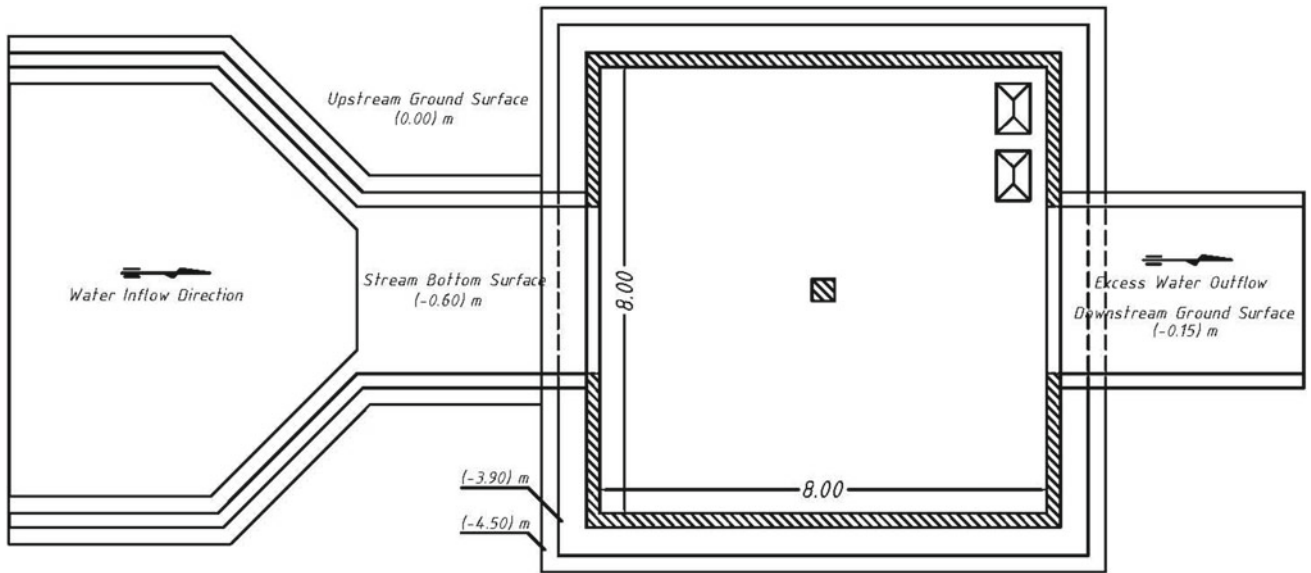


Fig. 45 Typical plan view in proposed cisterns in HS basins

The data used for the constructing the LMP were collected from:

- Different thematic maps and results of the present work.
- Ministry of Agriculture and Land Reclamation.
- Groundwater resources field inventory from 1992 uphill 2016.
- Previous works (Dissertations, Reports, articles, Web, etc.
- Geological data from EGS and Conoco Coral, 1987.
- General Authority for Rehabilitation Projects and Agricultural Development (GARPAD).
- National Water Research Center (NWRC), Egypt.
- National Authority for Remote Sensing & Space Sciences (NARSS).

5.2 Master Plan Objectives

The overall LMP has been elaborated to achieve, among the others, the following main objectives:

- To design the LMP for the whole HS region;
- To support a growth pattern for the area based on sustainable Green Economy;
- To promote the integration among different sectors and economic activities, as they are interfingering each other;
- To promote the integration among the economic activities to be developed, the infrastructure system, and the urban settlements;
- To promote the creation of clusters and urban settlements composed by a mix of economic and urban functions, guarantying the integration with the physical environment;
- To preserve the natural beauties and the heritage assets as a unique and inalienable patrimony of HS;
- To promote variety in use, therefore flexibility in planning according to the possible changes in socioeconomic conditions;
- To integrate within the LMP design the outcomes of all thematic maps previously discussed and the recommendations received from the research team involved in the present work;
- To build and design the LMP on the outcomes of the land suitability carried out for the HS region;
- To establish development criteria for sustainable use of the region:

HS area has great potential due to its geographic position on the Red Sea coast, which allows internal connectivity across the in-desert roads to the Nile Valley territory and sophisticated airports, toward Cairo and the delta area, to the

North, and international connectivity toward the rich countries of the Arab Peninsula, to the west. This connectivity is facilitated by the presence of:

- Two international airports: Hurghada and Mersa Allam to the south and Luxor to the West;
- The HS region has a surface of almost 23,000 km²; it includes a wide range of potential resources, well known since Pharaohs and Romans' times;
- Mineral resources, located in the mountains in an area between 10 and 80 km from the Red Sea coast; mineral resources include gold, granite, manganese, zinc, tantalum, and construction materials;
- Agriculture, due to the water scarcity in this area, most of its crops are exported from other areas located along the Nile River valley. However, small areas in the desert in Abu Saafa area (NW reaches of W. Hodein) were used as a pilot agricultural project in the form of greenhouses on limited groundwater resources. These significant water systems need to be matched by more efficient irrigation systems targeting water at the roots of each plant;
- Tourism, located mainly along the Red Sea coastline from north Shalatin to Halaib. This portion of the Red Sea coast presents a great potential for the tourism development to the uncontaminated coastline and reefs;
- Ecotourism–heritage tourism; the area presents a bulk of potentially exploitable sights in the old part of the Abraha and Abu Saafa, Abu Ramad, and along the historic connection routes, where roman ancient graffiti engravings in G. Abraha survives.

5.3 The Infrastructure System is Simple and Not Yet Efficient

One main road is connecting Shalatin to Halaib with minor paved and unpaved roads connecting its villages. Red Sea main highway is the principal road for accessibility. The local roads include about 45-km crosscut road between Shalatin and Bir El-Gahelia and then about 30-km road toward Bir Abraha. These roads are local rather than primary or secondary.

The main urban centers are the main cities of Shalatin, Abu Ramad, and Halaib.

These cities are located on the Red Sea corridor. Their location is favorable for the international market for export/import trading and for tourism; thanks to the international airports of Hurghada and Mersa Allam.

Within this system there are isolated nomadic nodes, separated from each other by a gap of 40 km of empty coastline and separated from the Nile Valley by a nearly about 220 km of mountains and desert zone.

5.4 Land Suitability Analysis

5.4.1 The Physical Environment

The present work carried out an assessment of the HS physical environment in the frame of the objectives and available baseline data. During the LMP construction, the work utilized the information previously collected in order to identify the main features of the area in view of the identified development opportunities. Following such an approach, the study areas/features have been identified and mapped:

1. **Map 1** (see Fig. 46): “Proposed Protected Areas” within HS area. The map includes:
 - Proposed protected Areas by the present work, which include G. Elba, W. Gimal, G. Abraç, Abu Saafa, rock engravings in G. Abraç and Abu Saafa, coral reefs, and mangroves sites along the Red Sea shoreline.
2. **Map 2** (see Fig. 47) “Slope,” which indicates the areas with slope in range under 5% and between 5% and 30% and those over 30% (using “DEMs”). The map shows the level of constraining in the mountain area to the west of the coastal zone.
3. **Map 3** (see Fig. 48): “Wadis and flood areas,” which shows the wadi network, and the areas subjected to flash floods. The map shows the wadi systems:

- Nine main wadis bed from the western mountain area toward the Red Sea, the average length of 40–80 km; the longest ones exist in the vicinity of Shalatin area, while the shortest ones are characterizing those of G. Elba and Halaib areas.
- The wadi width varies and there is no fixed width; the length of the wadies does not give an indication on the hazard, which depends on many factors. In the LMP, the indication for any development will be included (i.e., RWH capabilities, flood hazards, groundwater, etc.).

5.4.2 Analysis of Exploitable Natural–Heritage Resources for Economic Activities

The natural and heritage resources identified in the area are listed and analyzed in the following maps:

1. **Map 4** (see Fig. 49): shows proposed “Agriculture areas,” Agriculture areas are located mainly in the lower parts of the major wadi beds directly connected to Red Sea. Salt tolerant crops with low water requirements (i.e., medical herbs) are highly encouraged for small areas close to the Red Sea coastline. RO water desalination plant in Shalatin area (3600 m³ daily capacity) could be used as a minor source for pilot cultivated areas of low water consumption. In-desert pilot agricultural areas are proposed depending on the seasonal harvested flood water, which was determined feasibly in the present work.

Fig. 46 Protected and tourism areas within HS region

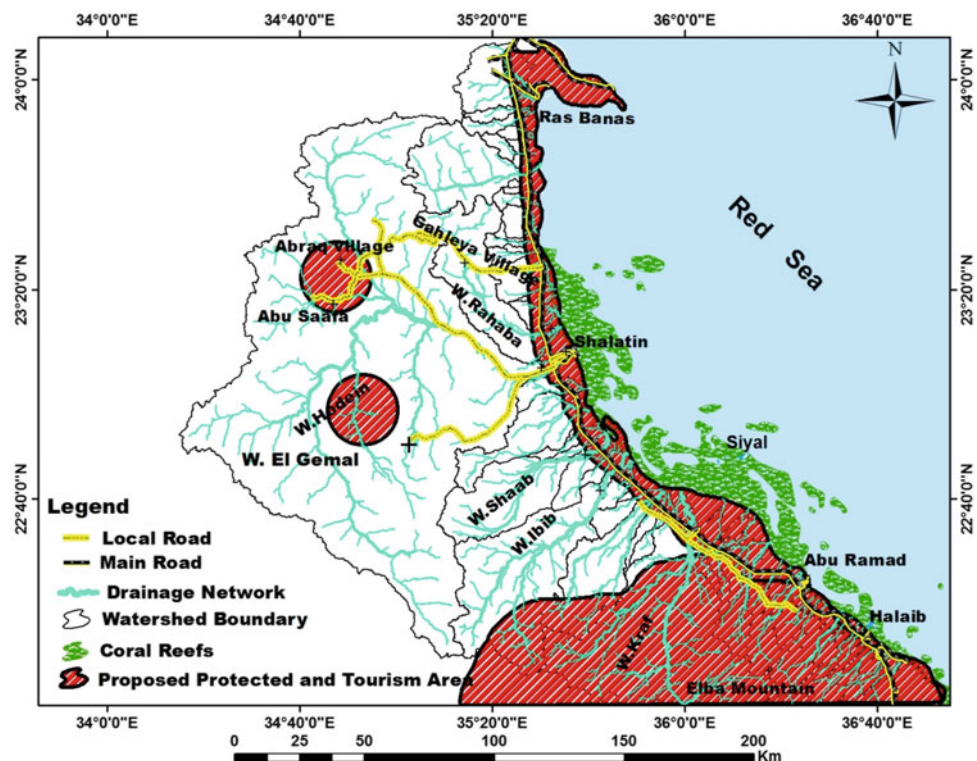


Fig. 47 Slope map of HS area (based on a 30-m resolution ASTER DEM)

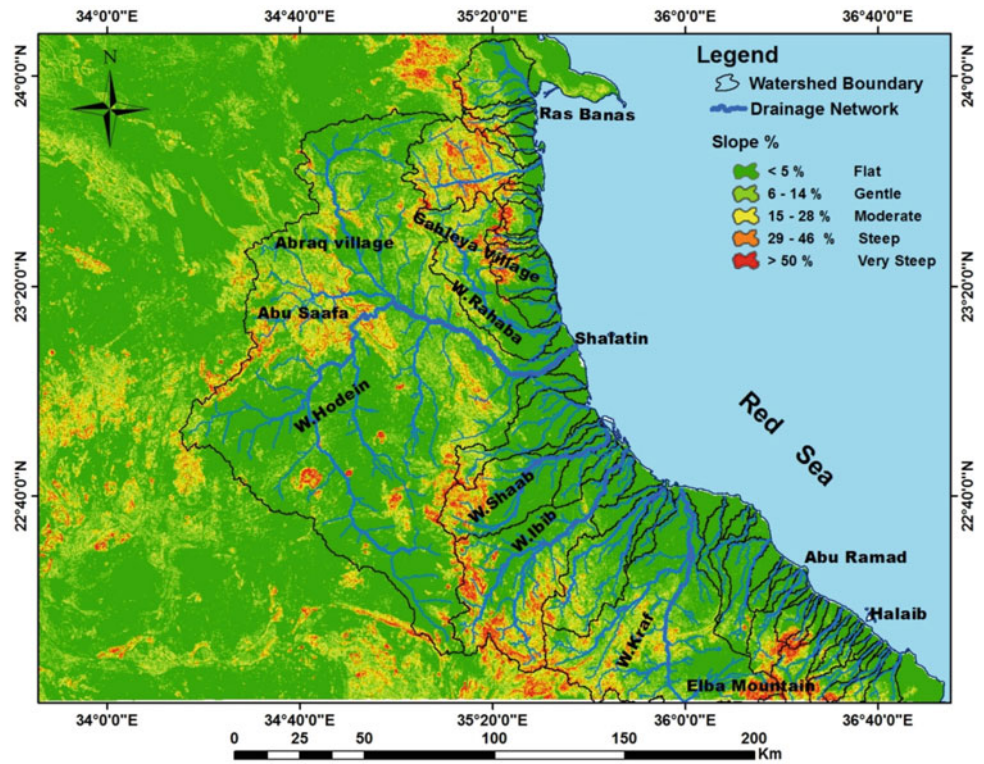
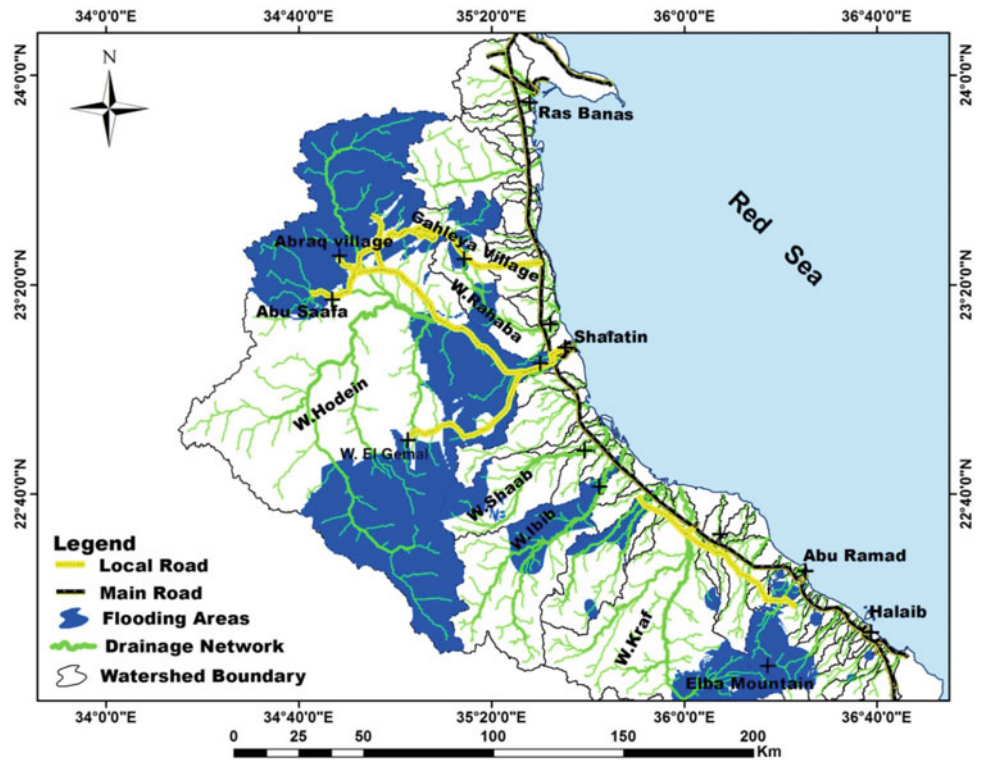


Fig. 48 Drainage network and flooding areas of HS region



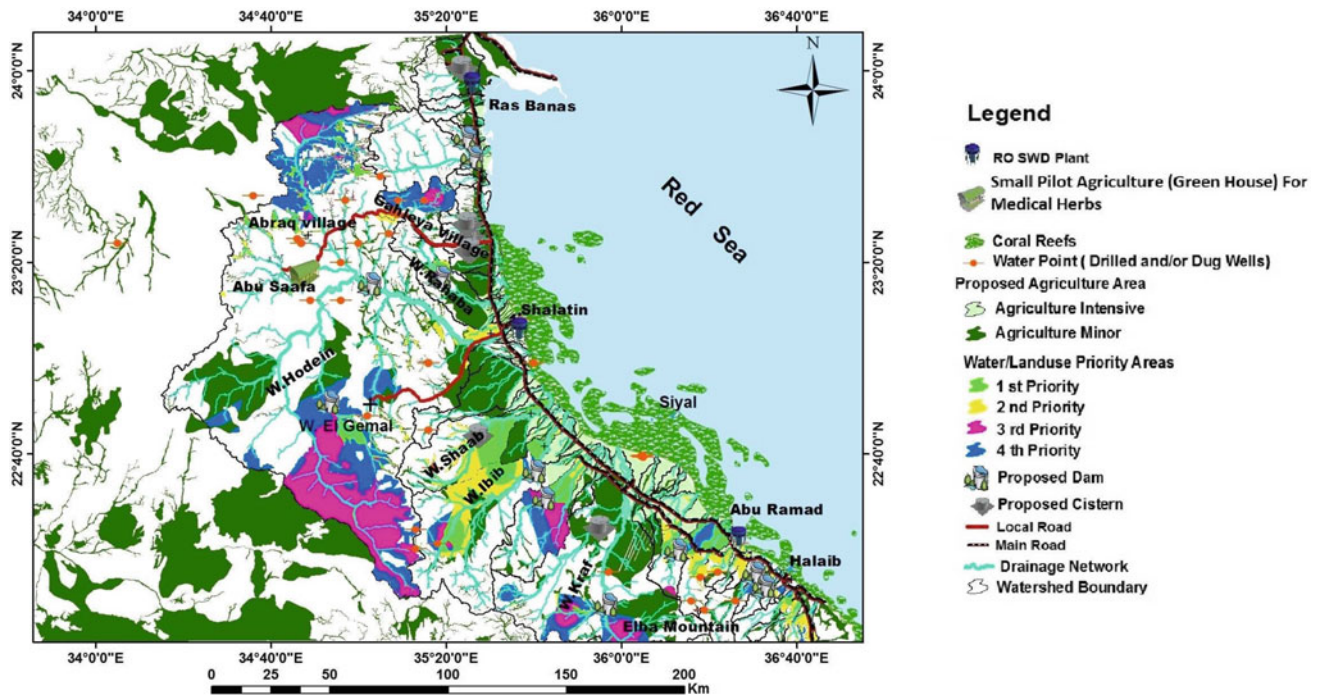


Fig. 49 Map of agriculture areas of HS region

2. **Map 5** (see Fig. 50): “Heritage and natural attraction”. The map has been designed according to the baseline data and tourism strategy showing natural attraction and heritage sites, which are mainly located along the Red Sea Coast and in some remote desert areas with ancient rock inscriptions from roman times in G. Abraq and Abu Saafa. The in-desert cultural attractions (i.e., old hand-dug wells) could be a destination of safari ecotourism. In addition, the coral reefs, mangroves along the Red Sea coast are also suitable for ecotourism safari destination.
3. **Map 6** (see Fig. 51): “Mining Sites”. The map shows locations of mineral resources in accordance with the information provided by the published geological maps and satellite images. The basement rocks territory was detached as the main source for minerals, building, or ornamenting stones. These minerals or rocks include, in particular, zinc, muscovites, granites, granodiorites, manganese, or gold. It has to be noted that the map reflects the regional baseline data suitable for industrial mining sector strategy for which such area is suitable for predominant mining activity. In the LMP, the “predominant activities” has been indicated characterizing each zone.
4. **Map 7** (Fig. 52): “Energy Production”. The map shows the location of areas for energy production suitable for solar energy plants: all the other areas outside mountains

and in the proximity of main power trunks and urban centers are suitable for solar energy plants. The planned solar plants are also plotted on the map (ongoing by the Egyptian Government) (PI self-communications). On the contrary, according to the baseline data and energy sector strategy, there are no areas extremely suitable for wind energy.

5.4.3 Analysis of Infrastructures and Network

The infrastructures and utilities networks existing in the area are listed and analyzed in the following maps:

1. **Map 8** (see Fig. 53): shows the current infrastructure network. Four main roads bound HS territory connecting its main cities:
 - Red Sea coastal main road connecting Shalatin to Halaib area.
 - Local roads crosscutting the main coastal Red Sea road toward local villages (Gahelia, Abu Ramad, Hodein).

These roads represent a potential for the integrated development of HS.

2. **Map 9** (see Fig. 54): shows the current utilities networks.

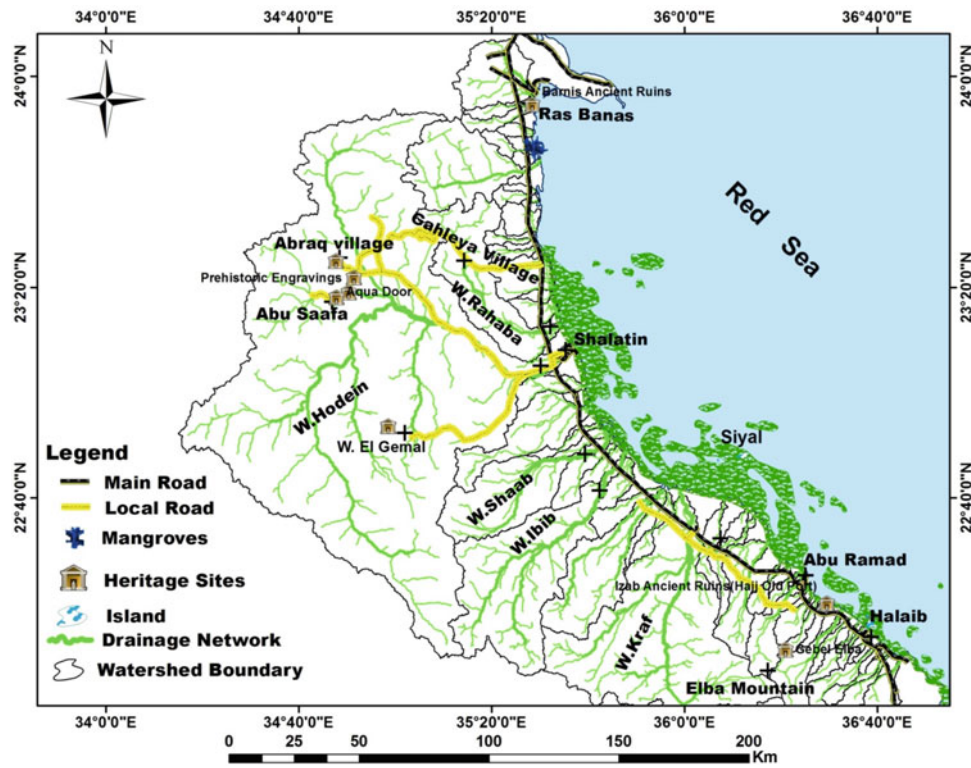


Fig. 50 Map of Heritage and natural attraction sites in HS area

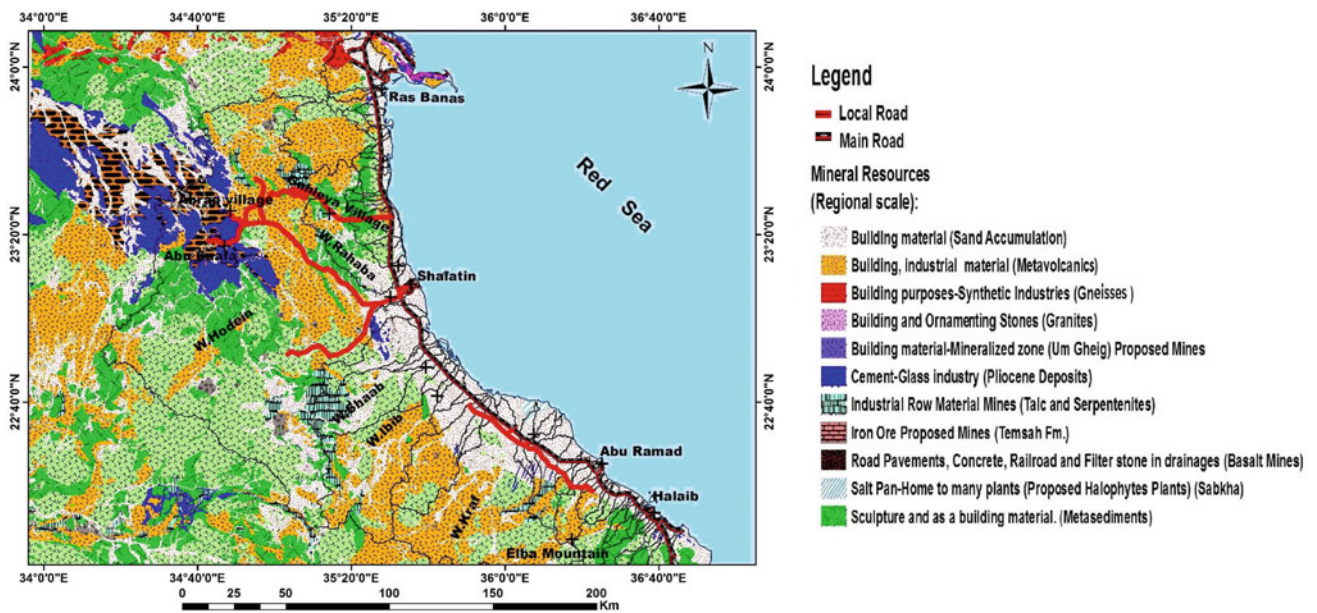


Fig. 51 Map of mining sites in HS area

Fig. 52 Map of energy production sites in HS area

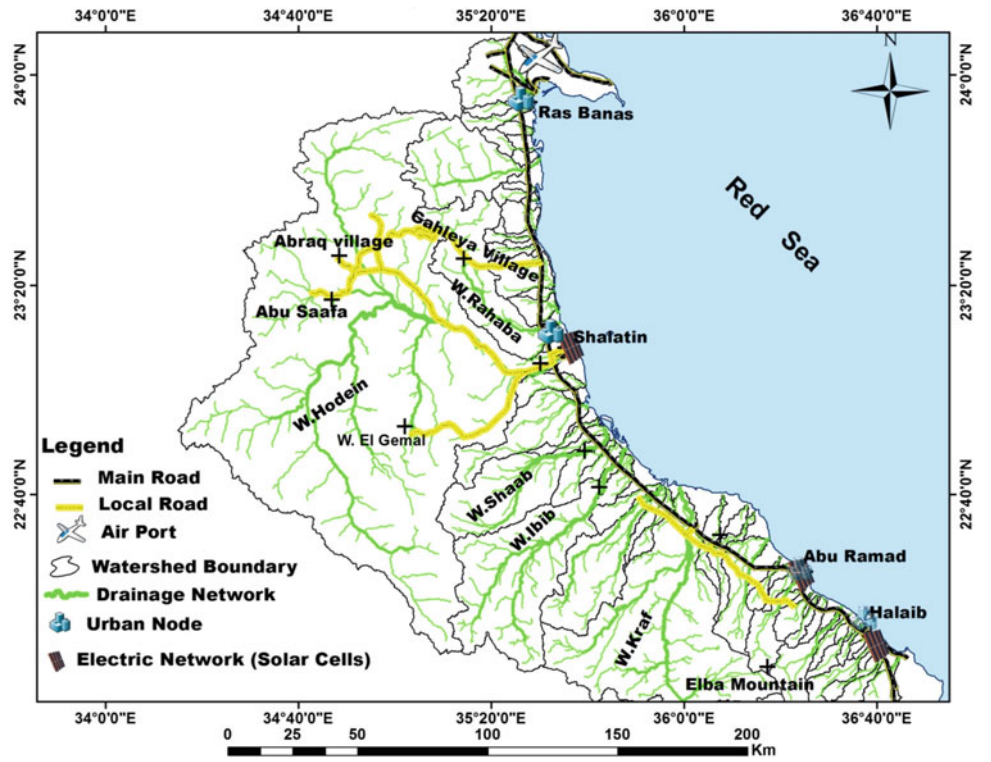


Fig. 53 Infrastructure network map of HS area

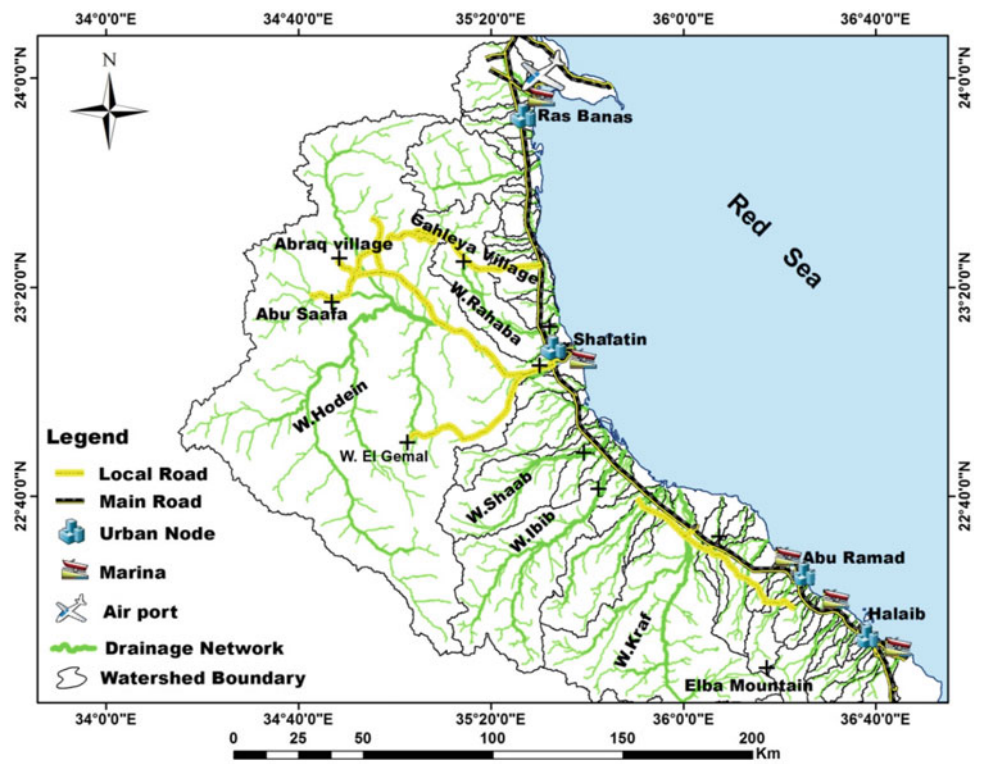


Fig. 54 Utilities networks map of HS area

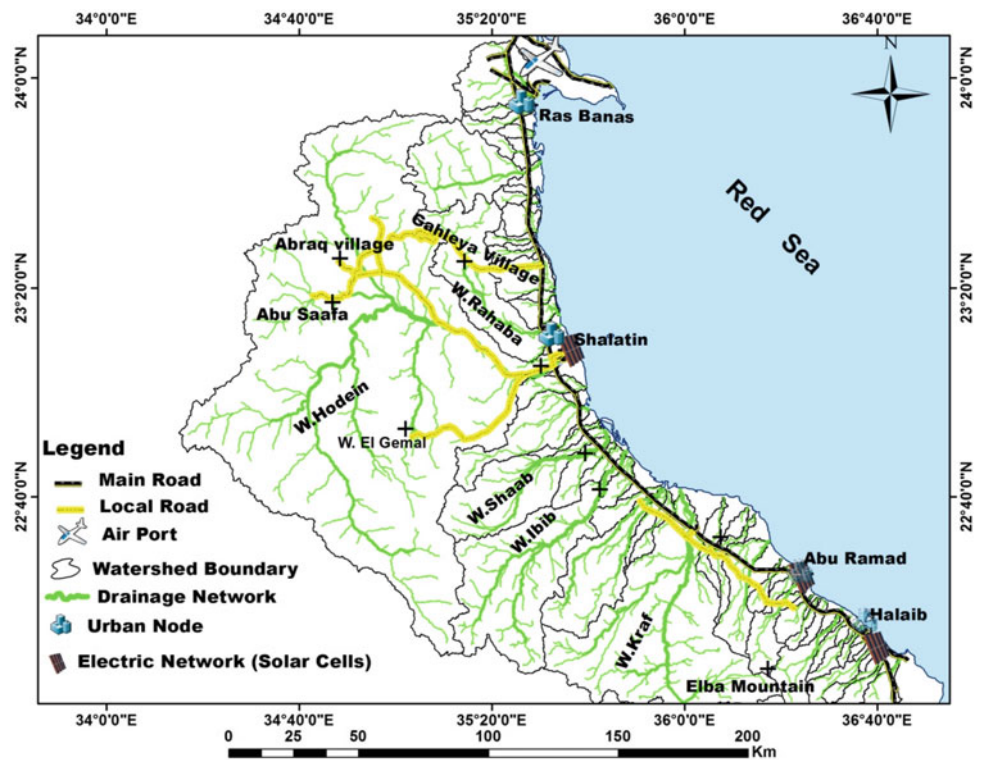
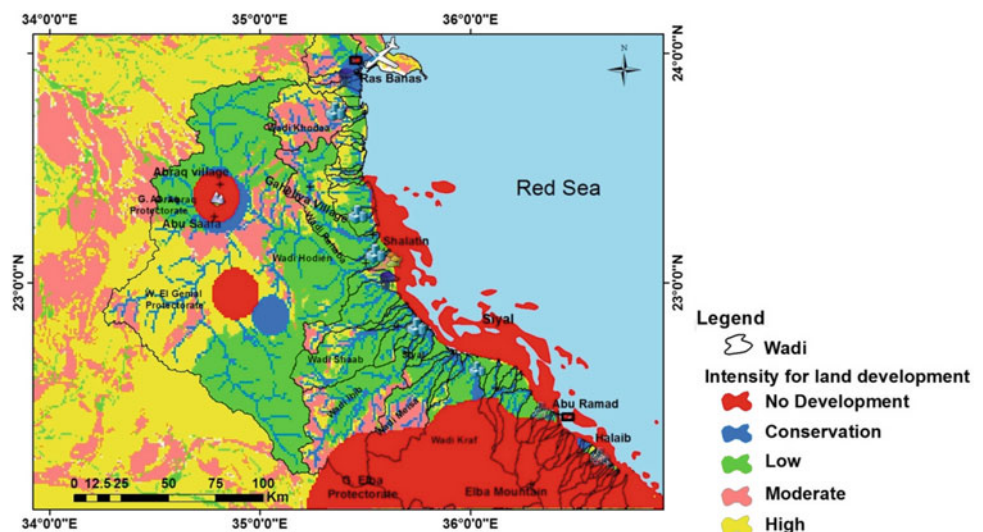


Fig. 55 Land suitability map of HS area



5.5 Land Suitability Map

This map (Fig. 55) combines the outcomes of the physical environment analysis and the results of the analysis of natural-heritage resources for economic activities and provides information on the suitable use of the territory in relation to its hazard and its resources. The map shows the areas of:

- No development: due to hazards, protected sites, natural sites, in this category are recommended no development;
- Conservation: due to the presence of heritage sites, it allows the development of important activities for tourism like restoration and renewal of high sights and infrastructures development;

- Low intensity: related to the presence of limited existing agricultural and flood areas, in such areas the suggested predominant activity is agriculture, but such areas are also suitable for industrial processing of agricultural products.
- Moderate intensity: it refers to locations in the proximity of existing and planned mining sites, therefore suitable for mining activity, mix-use urban function, light industrial function.
- High intensity: it refers to locations along development corridors, around existing urban nodes and suitable for industrial, urban, logistic, and heavy infrastructures development.

5.6 Land Use Master Plan

This work aims to build an LMP. This LMP is to report the objectives and baseline data in one map. This map is a crosscutting approach that will identify issues that are essential to deliver an overall master plan (regional or semi-detailed scale). The HS Triangle has many different economies, which could be good drivers for country development strategies.

The activity integration means that all the components of development are available and ready for use. The governmental rules and private sector initiatives are of pivotal importance.

The definition and combination of activities in the HS Triangle are to maximize the efficiency of different sectors outputs through a combination of a series of actions taking place at different spatial levels of work implementation: *Sustainability*, *Multidisciplinary*, and *Private or Public*.

Integration of the three complementary divisions is to capture all the applications and aspects of LMP formulation, which could be applied on the ground.

This approach is formalized with an explanation of the three layers (divisions), as follows:

– Sustainability

The present work is underpinned by the principle that all activities should take place under the broad umbrella of sustainability, where NARSS has chosen to interpret it as the development of a **Green Economy**; this will rotate around three parameters:

- a. **People**: by being conscious that every aspect of the development plan must recognize the resource presented by the people resident in the HS Triangle, as well as those living in adjacent territories.

- b. **Economic activity**: This will mean targeting international and domestic investors prepared to share the HS Triangle's values and develop their businesses recognizing that water will be priced as a limited resource and that technology will be deployed to enable directly employed workers to be economically productive in different sectors.

- c. **The environment**: Just by being conscious of the environmental impacts of economic activity and the presence of urban communities in otherwise virgin lands. It should be taken into consideration the limited availability of natural resources (e.g., water, agricultural lands, mines areas outside protected areas), whereas solar energy is fully renewable.

– Multidisciplinary

Perhaps the area of integration that we all think about most is between the ranges of business units and the infrastructural projects that will need to be put in place to ensure the efficiency of the implementation of the master plan's economic driver sectors.

– Private or Public

This is the level of integration that allows private sector enterprises to manage the achievement of efficiency and the best creation of value, within a collection of enterprises within a sector. **Mining, ecotourism, trading, animal husbandry, trading, industry, agro-industry, fisheries, etc.** are being planned on a short-, medium-, and long-term bases. This means the development of integrated activities on both a large, medium, and small scales; which would enable different classes of investors to participate in activities development.

5.6.1 The Strategy for Upgrading Land Use Master Plan

The report integrates all the previously discussed parameters of the present work, which has addressed more in detail the economic development of HS Triangle region.

The main objectives of the Master Plan are the following:

- The urban nodes for workers employed in mining, fisheries, industrial, and tourism sectors have been combined, to form a stronger cluster;
- The urban nodes for mining, tourism, fisheries, and industrial sectors have been located considering the linear urban development principle (development along connecting roads and infrastructures).
- The cities of Shalatin and Halaib participate in the urban growth associated to the economic development of

trading, mining, fisheries, tourism, and industrial sectors. This, because some industrial activities will be located in proximity of the two cities, due to technical and logistic requirements as expressed by specific sector strategies, as well as, the proximity of some mining sites to the two cities, than the creation of new urban nodes.

- The proposed new urban nodes at the deltas of main wadis to capture all planned or expected urban growths in future, and to overcome the demographic vacuum and to build man power for the planned developmental sectors.

In other words, the LMP of HS triangle region has been studied for each main area, that includes the following:

1. Proposed or current protected areas.
2. Conservation areas.
3. Agriculture (Green House or Medical Herbs).
4. Fisheries.
5. Energy production.
6. Tourism use.
7. Mining use.
8. Industrial use.
9. Logistics.
10. Ports.
11. Airports.
12. Development corridors.
13. Urban nodes—Existing.
14. Urban nodes—Proposed.

5.6.2 Developing the Master Plan

Reasons Behind the Construction of LMP

The reason behind the construction of LMP has been based on the following principles and objectives:

1. To promote integrated and sustainable development of HS Triangle.
2. To better exploit the physical characteristics and natural resources of HS Triangle.
3. To add value to the socioeconomic development of the country, in terms of attractiveness for population, employment created, attractiveness for public or private enterprises, and economic activities.
4. To better use the territory in a balanced and sustainable way, with long-term view.
5. To better sustaining an efficient and internal interconnectivity between land uses and urban nodes are existing and proposed.
6. To better planning for future land use parallel to urban and economic growth.

7. To create attractive urban nodes as clusters for the sustainable and integrated development for the region and the country.

Land Use Units

Based on the methodology outlined above, land use zones have been identified.

Each zone is defined by the following characteristics:

- Predominant use.
- Allowed use.

The identified land use units are the followings:

1. Proposed Protected Areas

These areas have been recognized as environmentally sensitive and they have been envisaged as future planned protected areas by the Egyptian Environmental Affairs Agency (EEAA). Intervention is subject to environmental impact assessment (EIA) and to the approval of a specific development project.

2. Conservation Areas

These are natural parks and wadies subject to conservation; aiming at forming a green natural vegetation belt between cities and productive areas, and flood water harvesting theater, ecotourism and safari tourism platform, nomadic use, and animal husbandry, etc.

- Predominant use: including the sustainability principles, are providing public natural zones to balance the industrial–urban development.
- Allowed use: tourism, ecotourism and infrastructures, subject to the approval of specific development project.

3. Agriculture-Intensive Use

This area is the main wadi deltas nearby urban nodes with adequate distances from the Red Sea; it is characterized by intensive agriculture on desalinized water mixed with urban villages (existing or proposed urban nodes), in detail:

- Predominant use is agriculture for sustaining principal crops to the residents and nomadic communities;
- Allowed uses are: tourism, mix-urban use (artisanal, commercial, offices, residential, services), urban (residential–public services).

4. Agriculture Minor Use

These areas include the wadi beds of the drainage basins and the mountainous desert areas, and between the Red Sea coast and the mountain areas; the area is suitable for agriculture extensive use, according to the strategy of the specific agriculture sector (i.e., medical herbs, green houses on groundwater in Abu Saafa), in details:

- Predominant use is agriculture;
- allowed uses are urban (residential–public services) and tourism.

5. Energy Production Use

Areas that are suitable for solar energy production.

- Predominant use: energy production;
- Allowed uses: Tourism, Urban Park, Infrastructure.

6. Tourism Use

These are the areas with peculiar environmental attractiveness for tourism use; they include the entire Red Sea coast, mountains, desert wadis, heritage areas within remote deserts and the existing urban centers (particularly Shalatin, Halaib, Abu Ramad, Abu Saafa, Gahelia, and Abra) and other heritage areas identified in the suitability analysis, in details:

- Predominant use: tourism;
- Allowed uses are urban (residential–public services) and agriculture;

7. Mining Use

These are the areas with a concentration of suitable mining sites in the mountains outside the environmentally protected areas, as emerged in the suitability analysis, in details:

- Predominant use is mining;
- Allowed uses are: tourism, infrastructures, facilities associated with the mining activity.

8. Industrial Use

These are the areas where products will be processed; products related to the following sectors:

- Fisheries (fishing, canning, exporting).
- Mining sector.

- Agriculture sector (Medical herbs preparation, drying, and canning).
- Construction sector.
- Energy.
- Other industrial sectors:
- The areas are confined along development corridors, in proximity of:
 - Available human resources–work force;
 - Available water resource;
 - Available infrastructure–road–transport network.

These land use units are also in proximity of urban centers, in order to reduce the commuting time and costs, planned in a way not to affect the urban center with pollution. Accordingly, a set of mitigation measures should be taken into consideration, among which we mention: maintain a minimum distance of 5–10 km between urban and industrial sites; study of the local microclimate in particular wind directions; introducing a “green belt-urban park” as a buffer between the urban area and industrial one. In details:

- Predominant: industrial use;
- allowed use: Logistics, infrastructures, support services, public services;

9. Logistics

These are the areas with logistic value, as per specific sector plan. They include dry ports. In details:

- Predominant use is logistic;
- Allowed uses are industrial, port, infrastructures, public services;

10. Ports

These are the areas with port use, as per specific Sector Strategy.

- Predominant use is port;
- Allowed use is logistics, infrastructures, public services.

11. Development Corridors—Mix-Urban Use

These are the areas with a vocation for mix use, which includes handicraft, commercial, offices, residential, services. Consequently, they are located along development corridors-connecting roads, to link/complement urban areas with economic development zones. In details:

- Predominant use is a mix use (handicraft, commercial, offices, residential, services);
- Allowed use: tourism, infrastructures, public services.

12. Urban Use Existing

These are the existing urban centers in Shalatin, Abu Ramad, and Halaib, plus minor centers in Abraaq, Abu Saafa, and Gahelia villages along connecting roads. In details:

- Predominant uses are residential, commercial, retail, offices, public services, tourism;
- Allowed uses are tourism, handicrafts, and agriculture;

13. Urban Use Proposed

Areas that are planned urban centers or nodes at the peripheries of main wadis deltas in W. Shaab, W. Meisah, W. Kraf, etc. These proposed urban nodes could be used as

attractive areas for new residents, especially with the expansion of economic projects in all sectors.

As a final product for the previous discussed peculiar maps, the final land/use master plan for HS region was constructed successfully (Fig. 56). Units of the proposed land use unit were calculated and listed in Table 14.

6 Summary and Conclusions

HS area is considered to be a promising region for different developmental activities as tourism and mining. The present work presented an overview of the optimum use for the natural resources in HS area.

The topography of the area ranges from gently sloping coastal plains to rugged mountainous and hilly lands. Geologically, the basement rocks occupy the area completely (except the area of Gebel Abraaq and the upstream portion of W. Hodein), that covers vast areas forming high to medium topographic reliefs. The sedimentary rocks cover a relatively smaller area forming moderately weathered-bedded hills.

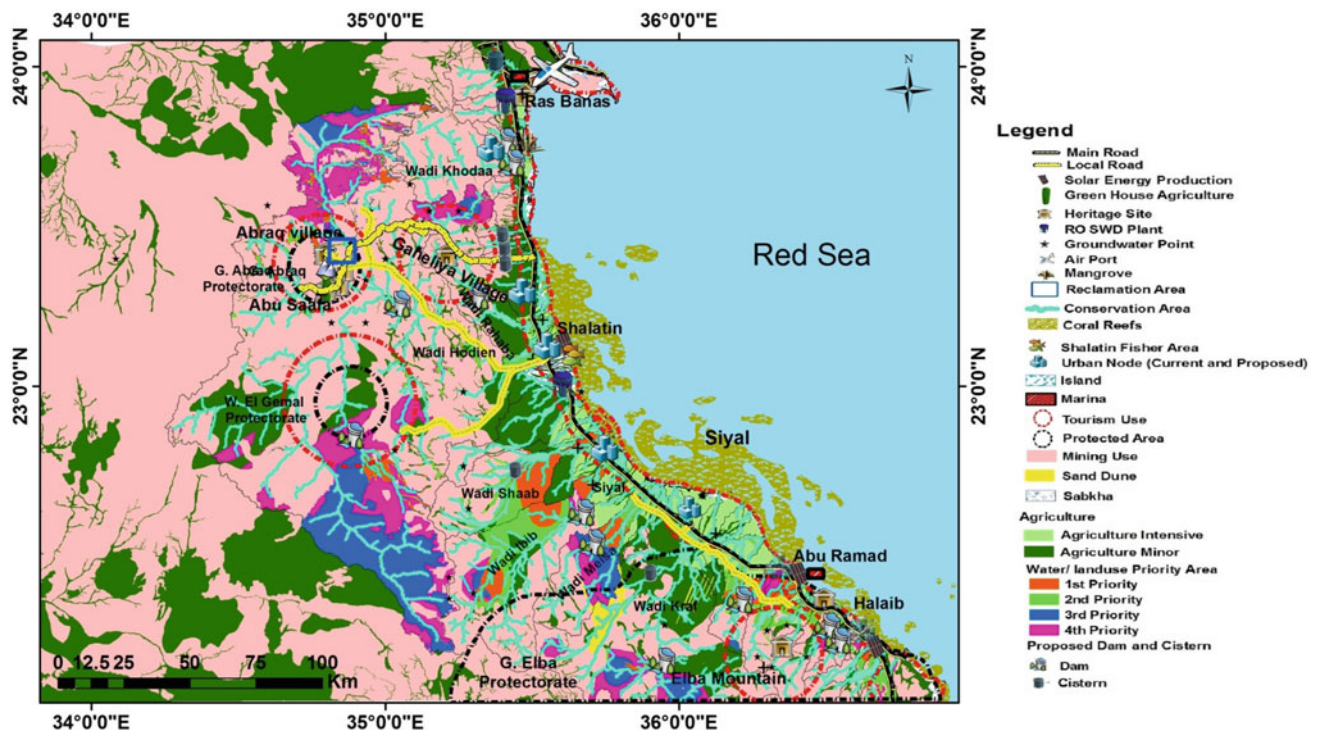


Fig. 56 Map of Land use master plan of HS area

Table 14 Land use units of HS area

Land use unit	Area (km ²)
1st priority area for water/land use	1164.6
2nd priority area for water/land use	1293.5
3rd priority area for water/land use	1792.7
4th priority area for water/land use	2231.7
Agriculture intensive	1582.6
Agriculture minor	10489.7
Mining use	35681.6
Conservation area	5031.0
Tourism area	7638.2
Protected area	7030.2
Sand dunes	407.1

Quaternary deposits are present mainly along the Red Sea coast and partially cover the sedimentary and Precambrian rock units.

Drainage net map and hydromorphometric parameters are introduced in details for all HS watersheds through the present work.

RS, watershed modeling, and GIS techniques are modern research tools that proved to be highly effective in mapping, investigation, and modeling the runoff processes and optimization the RWH. In the present work, these tools were used to determine the potential sites or areas suitable for the RWH in HS area (South Eastern Desert).

The RWH potential areas were determined by spatially integrating eight thematic layers, which represent the most important hydrographic and hydromorphometric parameters or criteria for determining the RWH potentiality. These thematic layers, which represent the weighted spatial probability modeling (WSPM) inputs, include: average OFD, VAF, BS, Dd, BL, BA, IF, and MFD. The performed WSPMs segregated these watersheds into five potential classes for the RWH potentiality, which are graded from the very low to very high. WSPM is a very effective method for determining the potential sites for RWH, especially based on justified weights by sensitivity analysis.

The performed WSPM which is based on justified weights elucidated that the area of high and very high potentiality for RWH is occupying about 47% of total HS study area (7493.48 and 4495.276 km², respectively). High and very high RWH classes are occupied by the upstream parts of the larger watersheds (i.e., Hodein, Kraf, Ibib, El-Rahaba, and Shaab) decreased to low and very classes in the downstream parts. A LMP was developed by the present work to foster the sustainable development of HS area.

Acknowledgment The authors wish to express their deep gratitude for the National Authority for Remote Sensing & Space Sciences (NARSS) for funding the project entitled “Planning for the Sustainable Development of Halaib-Shalatin Area, South Eastern Desert, Using RS, GIS, and other Techniques,” where the present work was performed.

References

- Abdel Razik, T. M. (1972). Comparative studies on the upper cretaceous-early Paleocene sediments of the Red Sea coast, Nile Valley and Western Desert, Egypt. In *8th Arab. Petroleum Congress, Algiers*, 23p.
- Adiga, S., & Krishna Murthy, Y. V. N. (2000). Integrated sustainable development of land and water resources using space technology inputs. *Space Forum*, 5, 179–202.
- Akkad, M. K., El-Ramly, M. F. (1960). Geological history and classification of the basement rocks of the Central Eastern Desert of Egypt. *Geological Survey of Egypt*, 24p.
- Anon. (1975). Munsell soil color charts Macbeth Division of Kollmorgen Corporation. 2441 North Cavert Street, Baltimore, Maryland, USA.
- AQUAVEO. (2008). Water modeling solutions. Support forum for sub-watershed modeling system software (WMS). www.aquaveo.com.
- Bruins, J. H., Guedj, H. B., & Svoray, T. (2019). GIS-based hydrological modelling to assess runoff yields in ancient-agricultural terraced wadi fields (central Negev desert). *Journal of Arid Environments*, 166, 91–107.
- Butzer, K. W. (1959). Environment and human ecology in Egypt during pre-dynastic and early dynastic times. *Bulletin of the Society Geographical Egyptian*, 32, 42–88.
- CONOCO. (1987). Geological map of Egypt, scale 1:5000,000. EGPC, Cairo, Egypt.
- Davis, G. H. (1965). Groundwater networks in United States. *International Association of Scientific Hydrology*, Publ. no. 68, 433p.
- Desert Research Institute. (1998). *Meteorological Data Recorded at Shalatin station*. Cairo, Egypt: Installed by Desert Research Institute.

- EGACS. (1989). Egyptian general authority for civil survey. Topographic sheets, scales 1:500000–1:250000.
- Elewa, H. H., Qaddah, A. A. (2011). Groundwater potentiality mapping in Sinai Peninsula, Egypt, using remote sensing and GIS-watershed-based modeling. *Hydrogeology Journal*, (Springer, Heidelberg, Berlin), 19, 613–628. <https://doi.org/10.1007/s10040-011-0703-8>.
- Elewa, H. H., Qaddah, A. A., & El-Feel, A. A. (2012). Determining potential sites for runoff water harvesting using remote sensing and geographic information systems-based modeling in Sinai. *American Journal of Environmental Sciences*, 8, 42–55. (Science Publications, USA).
- Elewa, H. H., Ramadan, E. M., El-Feel, A. A., Abu El Ella, E. A., & Nosair, A. M. (2013). runoff water harvesting optimization by using RS, GIS and watershed modelling in Wadi El-Arish, Sinai. *International Journal of Engineering Research & Technology (IJERT)*, 2, 1635–1648.
- Elewa, H. H., Ramadan, E. M., El Feel, A. A., Abu El Ella, E. A., & Nosair, A. M. (2014). Runoff water harvesting optimization by using RS, GIS and watershed modelling in Wadi El-Arish, Sinai. *International Journal of Engineering Research & Technology (IJERT)*, 2, 1635–1648.
- Elewa, H. H., Ramadan, E. M., Nosair, A. M. (2016). Spatial-based hydro-morphometric watershed modeling for the assessment of flooding potentialities. *Environmental Earth Sciences*, 75, 927.
- El-Naggar, Z. R. M. (1970). On a proposed lithostratigraphic subdivisions for the late cretaceous-early paleogene succession in the Nile Valley, Egypt. In *7th Arab Petroleum Congress*, Kuwait.
- El-Ramly, M. F. (1972). A new geological map for the basement rocks in the eastern and south western deserts of Egypt, scale 1: 1000,000. *Annals of the Geological Survey of Egypt*, 2, 1–18.
- Endriszewitz, M. (1988). Gliederung der Nubischen Serie in Südost-ägypten. Auswertung von Gelände-Und Fernerkundungsdaten-Berliner geowiss. Berlin, Ah. A, 79, 141p.
- ERDAS Field Guide. (2005). Geospatial imaging, LLC Norcross, Georgia, United States of America.
- ESRI. (2007). ArcGIS 9.2[®] Software and user manual. *Environmental Systems Research Institute*, Redlands, California 92373-8100, USA. <http://www.esri.com>.
- Faniran, A. (1968). The index of drainage intensity—A provisional new drainage factor. *Australian Journal of Science*, 31, 328–330.
- Feizizadeh, B., Jankowski, P., & Blaschke, T. (2004). A GIS based spatially-explicate sensitivity analysis approach for multi-criteria decision analysis. *Computers Geosciences*, 64, 81–95.
- Finkel, H. H. (1979). Water resources in arid zone settlement, a case study in arid zone settlement. In G. Colany (ed.), *The Israeli Experience*, Pergamon.
- Garbrecht, J., Martz, L. W. (1997). TOPAZ: An automated digital landscape analysis tool for topographic evaluation, drainage identification, sub-watershed segmentation and sub catchment parameterization; TOPAZ Overview, U.S. Department of Agriculture, Agricultural Research Service, Grazing lands Research Laboratory, El Reno, OK, USA, ARS Publication No. GRL 97-3.
- Gregory, K. J., & Walling, D. E. (1973). *Drainage Basin form and process: A geomorphological approach* (p. 456p). London: Edward Arnold.
- Greimann, B. (1987). Design of small dams, (3rd edn), United States Department of the Interior, Bureau of Reclamation, a water resources technical publication, (pp. 287–312).
- Ha, W., Lu, Z., Wei, P., Feng, J., & Wang, B. (2012). A new method on ANN for variance based importance measure analysis of correlated input variables. *Structural Safety*, 38, 56–63.
- Hendricks, F., & Luger, P. (1987). The Rakhayat formation of the Gebel Qreiya area: Evidence of middle campanian to Early Maastrichtian syn-sedimentary tectonism-Berliner geowiss. *Abh. A.*, 75, 83–96.
- Horton, R. E. (1945). Erosional development of stream and their drainage basins; hydrophysical approach to quantitative morphology. *Geological Society of America Bulletin*, 56, 275–370.
- Ismail, H. A., Bahnassy, M. H., Abd El-Kawy, O. R. (2005). Integrating GIS and modelling for agricultural land suitability evaluation at East Wadi El-Natron, Egypt. *Egyptian Journal of Soil Science*, 45, 297–322.
- Jain, V., & Sinha, R. (2003). Evaluation of geomorphic control on flood hazard through geomorphic instantaneous unit hydrograph. *Current Science*, 85, 26–32.
- Javed, A., Khanday, M. Y., & Ahmed, R. (2009). Prioritization of sub-watersheds based on morphometric and land use analysis using remote sensing and GIS techniques. *Journal of Indian Society of Remote Sensing*, 37, 261–274.
- Jenson, S. K., & Domingue, J. O. (1988). Extracting topographic structure from digital elevation data for geographical information system analysis. *Photogrammetric Engineering and Remote Sensing*, 54, 1593–1600.
- Jones, J. A. A. (1999). *Global hydrology: Processes* (p. 399p). Resources and Environmental Management: Longman.
- Klitzsch, E., List, F. K., Pohlmann, G. Handley, R., Hermina, M., Meissner, B. (1986). Geological map of Egypt, scale 1:500,000, 20 sheets, Cairo (Conoco/EGPC).
- Kunitomo, N. (2000). *Design and construction of embankment dams* (pp. 2–5). Aichi Institute of Technology: Department of Civil Engineering.
- Leopold, L. B., Maddock, T. (1953). The hydraulic geometry of stream channels and some physiographic implications: U.S. Geological Survey Professional Paper 252, 52p.
- Ligmann-Zielinska, A. (2013). Spatially-explicit sensitivity analysis of an agent-based model of land use change. *International Journal of Geographical Information Science*, 27, 1764–1781. <https://doi.org/10.1080/13658816.2013.782613>.
- Malczewski, J. (1996). A GIS-based approach to multiple criteria group decision-making. *International Journal of Geographic Information Science*, 10, 955–971.
- Malczewski, J. (2006). GIS-based multi criteria decision analysis: A survey of the literature. *International Journal of Geographic Information Science*, 20, 703–726.
- Leica Geosystems GIS & Mapping, LLC. (2008). *ERDAS field guide* (Vol. 1), Norcross, GA: Leica Geosystems Geospatial Imaging, LLC.
- Mark, D. M. (1984). Automatic detection of drainage networks from digital elevation models. *Cartographica*, 21, 168–178.
- Martz, L. W., & Garbrecht, J. (1992). Numerical definition of drainage network and Sub-catchment areas from digital elevation models. *Computers & Geosciences*, 18, 747–761.
- Mcmahon, J. R. (2004). *General design and construction considerations for earth and rock-fill dams*, Department of the Army (pp. 2–8). Washington: U.S. Army Corps of Engineers.
- Montgomery, D. R., & Dietrich, W. E. (1989). Source areas, drainage density, and channel initiation. *Water Resources Research*, 25, 1907–1918.
- Moore, I. D., Grayson, R. B., & Ladson, A. R. (1991). Digital Terrain modeling: A review of hydrological, geomorphological and biological applications. *Hydrological Processes*, 5, 3–30.
- Morisawa, M. E. (1959). Relation of morphometric properties to runoff in the Little Mill Creek, Ohio Drainage Basin, (Columbia University, Department of Geology), Technical Report, 17, office of Naval Research, Project NR 389-042.
- Nuweir, A. M., & El-Sharkawi, M. A. (1978). The Um Had-Um Effein metamorphic aureole, Central Eastern Desert, Egypt. *Bulletin, Faculty of Science*, 51, 285–301. Cairo University.
- Ponce, V. M., & Hawkins, R. H. (1996). Runoff curve number: Has it reached maturity? *Hydrologic Engineering*, 1, 11–19.

- Rabus, B., Eineder, M., Roth, A., & Bamler, R. (2003). The shuttle radar topography mission- a new class of digital elevation models acquired by space-borne radar. *Journal of Photogrammetry and Remote Sensing*, 57, 241–262.
- Sabet, A. H. (1972). On the stratigraphy of the basement rocks of Egypt. *Annals of Geological Survey of Egypt*, 2, 79–101.
- Said, R. (1990). *The geology of Egypt* (p. 734p). Rotterdam: A.A. Balkema.
- Saisana, A., Saltelli, A., & Tarantola, S. (2005). Uncertainty and sensitivity analysis techniques as tools for the quality assessment of composite indicators. *Journal of Royal Statistical Society*, 168, 307–323.
- Saltelli, A., Chan, K., & Scott, E. M. (2000). *Sensitivity analysis*. New York: Wiley.
- Sepehri, M., Malekinezhad, H., Ilderomi, A. R., Talebi, A., & Hosseini, S. Z. (2018). Studying the effect of rain water harvesting from roof surfaces on runoff and household consumption reduction. *Sustainable Cities and Society*, 43, 317–324.
- Summerfield, M. A. (1991). *Global geomorphology. An introduction to the study of landforms*. xxii + 537 pp. Harlow: Longman; New York: John Wiley Inc. Price £17.99 (paperback). ISBN 0 582 30156 4 (Longman), 0 470 21666 2 (Wiley).
- Tribe, A. (1992). Automated recognition of valley heads from digital elevation models. *Earth Surface Processes and Landforms*, 16, 33–49.
- Van Griensven, A., Meixner, T., Grunwald, S., Bishop, T., Diluzio, M., & Srinivasan, R. (2006). A global sensitivity analysis tool for the parameters of multi-variable catchment models. *Journal of Hydrology*, 324, 10–23. <https://doi.org/10.1016/j.jhydrol.2005.09.008>.
- Verstappen, H. (1983). *The applied geomorphology*, International Institute for Aerial Survey and Earth Science (I.T.C.), Enschede, Netherlands, Amsterdam, Oxford, New York.